PFC/RR-84-9 DOE/ET/51013-123

METHODS OF FIRST WALL STRUCTURAL ANALYSIS WITH APPLICATIONS TO THE LONG PULSE COMMERCIAL TOKAMAK REACTOR DESIGN

by

RENE JOSEPH LECLAIRE, JR.

Massachusetts Institute of Technology
Plasma Fusion Center
Department of Nuclear Engineering
Cambridge, MA 02139

May 1984

METHODS OF FIRST WALL STRUCTURAL ANALYSIS WITH APPLICATIONS TO THE LONG PULSE COMMERCIAL TOKAMAK REACTOR DESIGN

by

RENE JOSEPH LECLAIRE, JR.

B.S., M.S., University of Lowell

1980

Submitted to the Department of
Nuclear Engineering
in Partial Fulfillment of the
Requirements for the Degrees of

MASTER OF SCIENCE
and
NUCLEAR ENGINEER

at the
MASSACHUSETTS INSTITUTE OF TECHNOLOGY
MAY 1984

© Massachusetts Institute of Technology, 1984

Signature of Author _____
Department of Nuclear Engineering, May 11, 1984

Certified by _____
John E. Meyer
Thesis Supervisor

Accepted by _____
Allan F. Henry
Chairman, Departmental Graduate Committee

METHODS OF FIRST WALL STRUCTURAL ANALYSIS WITH APPLICATIONS TO THE LONG PULSE COMMERCIAL TOKAMAK REACTOR DESIGN

by

RENE JOSEPH LECLAIRE, JR.

Submitted to the Department of Nuclear Engineering
on May 11, 1984 in Partial Fulfillment of the
Requirements for the Degrees of
Master of Science and Nuclear Engineer

ABSTRACT

Methods of analysis for fusion first wall design are developed. Several design limits have been evaluated and combined to present trade-offs in the form of design windows. These considerations include limits related to thermal fatigue, primary membrane strength, displacement under loading, ratcheting, radiation damage, and plasma-wall interactions. Special emphasis is placed on the investigation of thermal fatigue using a two dimensional treatment of a tubular first wall configuration. The work is motivated by the proposal of the Ultra Long Pulse Commercial Reactor (ULTR), a machine capable of delivering plasma burn pulses of up to 24 hours in length.

The present work looks in detail at the impact of pertinent characteristics of the ULTR design such as pulse length, coolant pressure, first wall thickness and first wall lifetime on the structural effects considered. Computer programs are developed and consider several major structural effects on a cylindrical first wall element for both 316 Stainless Steel and Vanadium alloy.

Results indicate that short pulse lengths (greater than a few minutes) can be tolerated in tokamak operation. For Stainless Steel this is true for heat depositions up to $1 MW/m^2$ while Vanadium can tolerate heat depositions as high as $2 MW/m^2$. Long pulse operation can be used to increase modestly the allowable heat deposition or to increase useful wall thickness by one to two millimeters. It appears that irradiation swelling and embrittlement, not fatigue, ultimately limits the first wall design.

Thesis Supervisor: Dr. John E. Meyer
Title: Professor of Nuclear Engineering

ACKNOWLEDGMENTS

The author would like to thank Professor John Meyer for his guidance throughout the development of this work. I benefited a great deal from his knowledge and experience. Many thanks are also due Dr. Daniel Cohn of the MIT Plasma Fusion Center for his input into this work and his financial support in the form of a Research Assistantship. A graduate student couldn't ask for two greater bosses.

Special thanks go to my wife, Cathy, for marrying me, for the support she gave me despite my neglect of her, and for her work on many of the figures.

I have benefited tremendously from interaction with the many friends I have made at MIT, both student and staff. In particular, I wish to thank Leslie Bromberg (Dr. B.) for his guidance in subjects ranging from MACSYMA programming to the philosophy of fusion.

My thanks also go to Linda Denning who did alot of work on the figures on short notice.

Finally, I would like to acknowledge the support of my family, especially my parents. They are truly the unsung heroes behind whatever success I might achieve.

TABLE OF CONTENTS

LIST OF FIGURES

LIST OF TABLES

Page

1. INTRODUCTION

One of the major criticisms of most tokamak concepts for use as commercial fusion power reactors has been the pulsed nature of their operation. A major concern has been in the area of thermal fatigue of the first wall both because of a direct thermal loading from the pulsed plasma and because of the vulnerability of reactor operation to even very small first wall leaks. Also, there exist several other potential problems associated with pulsed tokamak operation such as mechanical fatigue in the toroidal field (TF) coils. In addition, some provision must be made for the dwell time when the fusion power will be unavailable to the electric utility.

Various forms of current drive have been proposed and are being investigated experimentally that may eventually make a tokamak operating in the steady state possible. However, it seems prudent in light of the uncertainties associated with the application of current drive in future tokamak designs [1] to explore the potential of an entirely ohmically driven design. It is in this spirit that the Ultra Long Pulse Commercial Reactor (ULTR) has been proposed, a machine capable of delivering pulses of up to 24 hours in length [2].

An artist's conception of ULTR is shown in figure 1.1. Long pulse operation is obtained with a large major radius design, taking advantage of the rapidly increasing capability of the ohmic transformer with increasing major radius. Illustrative parameters for an ULTR device with a 24 hour pulse length are found in Table 1.1. The magnet system is optimized for long pulse operation and is completely modularized with the TF coils in individual dewars.

The present work began in an effort to identify the possible advantages of long pulse operation for the design of the first wall, especially in regard to thermal fatigue. Early results indicated that there were gains associated with longer pulses but only up to pulse lengths between one half and two hours. Since then, a more

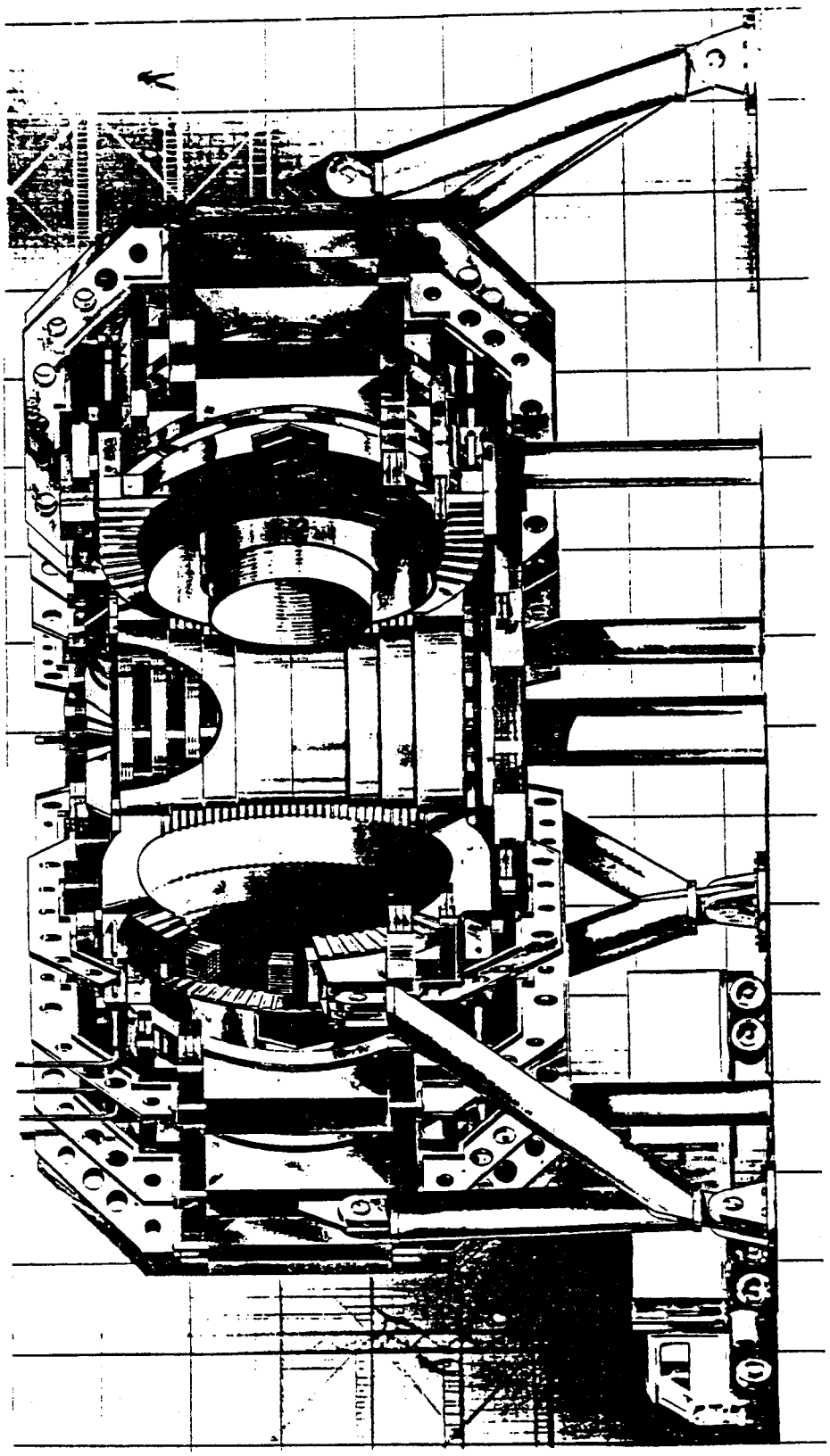

FIG. 1.1 Perspective View of ULTR

Table 1.1

ULTR Parameters

Major Radius (m)	9.7
Minor Radius (m)	2.0
Plasma Elongation	1.5
Toroidal Beta	0.036
Magnetic Field on Axis (T)	6.0
Plasma Current (MA)	9.7
Peak Electron Temperature (keV)	35
Average Neutron Wall Loading (MW/m^2)	2.3
Fusion Power (MW)	3200
Superconductor	Nb_3Sn
Voltsecond Capability of OH Transformer($V \cdot s$)	1100
Peak Field in OH Transformer(T)	10.5
Pulse Length(hours)	24

accurate description of the stress state and boundary conditions for the first wall has been included. Several other design limits in addition to thermal fatigue have been evaluated and combined to present trade-offs among these limits in the form of design windows. These considerations include limits related to primary membrane strength, displacement under loading, ratcheting, radiation damage, and plasma-wall interactions.

A 1978 paper by J.E. Meyer [3], which evaluated the impact of pulse length on thermal fatigue effects using design curves in the ASME Boiler Code Case N-47-17 [4], indicated a significant advantage for long pulse operation in terms of allowable wall loading and first wall lifetime. A design window methodology was developed by Chan [5] in the form of an existing computer code which builds on earlier work by Smith et. al. [6], and Yu [7]. This methodology evaluates thermal fatigue and creep effects in the context of a Bree Diagram [8]. The present work extends the latter results by modifying the Bree diagram to increase its usefulness for examining design trade-offs and extends the early work by Meyer in thermal fatigue.

The present work looks in detail at the impact of pertinent characteristics of the Long Pulse design such as pulse length, coolant pressure, first wall thickness and first wall lifetime, on the structural effects considered. Computer programs are developed and consider several major structural effects on a cylindrical first wall element for both 316 Stainless Steel and Vanadium alloy. Effects leading to rupture caused by excessive primary stresses are limited by the application of maximum allowable stresses (S_{mt}) from the ASME code. Analysis of cyclic deformation due to primary stresses and cyclic secondary stresses is provided in the form of two modified Bree Diagrams. Standard Bree diagrams identify the elastic, shakedown (plastic deformation relaxing to elastic behavior after a few cycles), plastic (plastic deformation limited by material hardening), and ratcheting (progressive plastic deformation) regions in a plot of secondary versus primary stresses. The Bree

diagram can be modified to incorporate a simple model for a cylindrical first wall which translates the plot into either surface heat load or wall inner radius versus first wall thickness. The effect of cyclic creep is included in the analysis by limiting the creep strain according to the method of O'Donnell and Porowski [9].

Design curves for Stainless Steel as used in the ASME code are employed to limit the cumulative damage due to the creep-fatigue interaction. This analysis is based on the allowable strain range as a function of the number of cycles to failure, and an allowable stress based on the time to material rupture. Also, the effects of irradiation induced swelling and embrittlement are evaluated and integrated into the design windows. Although multiple efects are included and form valid limits, effects of irradiation on ASME design curves are not included and may prove to be significant.

Work performed for the INTOR study [10], indicates erosion of the first wall due to physical sputtering and disruptions can be quite severe (several mm/yr for moderate particle fluxes to the first wall). This may have significant impact on the structural analysis if it is necessary to accommodate erosion with thicker first walls (in conflict with fatigue requirements for thinner dimensions.) Therefore, a reasonable effort is made to understand the processes involved and the possible advantages of incorporating a low Z coating such as beryllium are considered. Still, it is clear that a great deal more experimental and theoretical work in plasma wall interactions is needed. Thus, it is difficult to directly incorporate erosion in the design trade-offs with confidence.

Chapter two considers each of the design limits mentioned above and summarizes their development and impact on design. The geometry and stress analysis is detailed in chapter three with symmetric thin shell and two dimensional treatments of the first wall tubular geometry. The results of the fatigue evaluations using the development in chapter three appear in chapter four. Also included in chapter

four are the methodology and results from the design window analysis. Summary and conclusions appear in chapter five.

2. DESIGN LIMITS

2.1 Introduction

There are many effects that may be considered in designing a first wall. These effects are generally associated with the heat deposition on the first wall plasma side, heat removal, pressure, corrosion on the coolant side, or from neutron irradiation effects.

Surface heat deposition and internal heat generation will lead to thermal stresses within the structural material which may result in short term displacements, creep, radiation damage in the form of swelling and loss of ductility, fatigue damage, and erosion of the first wall surface from sputtering and melting.

The coolant will generally be under substantial pressure (e.g. 1 MPa for lithium, 15 MPa for water) with a wall pressure difference caused by near vacuum on the plasma side of the wall. This will impose strength requirements on the first wall. Coolant-wall interactions (corrosion) are a concern but will not be addressed directly in this work. However, there is much information available on these compatibility considerations from the literature. See, for example, Piet [11] and Yu [7].

The ASME code case 1592 (N-47-17) for Class I components in elevated temperature service forms the basis for much of the analysis and failure criteria considered. This code case provides well documented procedures for evaluation of the following seven failure mechanisms:

- Ductile rupture from short term loadings
- Creep rupture from long term loadings

- Creep-fatigue failure
- Ratcheting
- Excessive deformation
- Buckling with short term loadings
- Creep buckling with long term loadings

Since the code case covers a variety of conditions and configurations, the design criteria are conservative in general, although compatibility effects and irradiation effects are not accounted for. Note that in this study, the code case guidelines for a completely elastic analysis are used. This approach is, in general, conservative in design and appropriate for this type of parametric study. However, when a specific design is converged upon, a more detailed analysis may be used to eliminate some of the conservatism and identify any hidden effects which may be non-conservative.

2.2 Strength

The ASME code case N-47-17 provides design guidelines for load controlled quantities (primary stresses), the pertinent example in this work being the stresses set up as a result of the pressure difference across the wall. Primary stresses are limited by S_{mt}, which is the smaller of the time-independent stress intensity limit, S_m, and the time-dependent stress intensity limit S_t.

For ferritic steels and non-ferrous metals and alloys, S_m is defined as the lowest of: $1/3\ \sigma_u$ at room temperature, $1/3\ \sigma_u$ at design temperature, $2/3\ \sigma_y$ at room temperature, and $2/3\ \sigma_y$ ($0.9\sigma_y$ for austinetic steels) at design temperature, where

σ_u is the ultimate strength and σ_y is the yield stress. S_t is defined as the lowest of: 2/3 of the minimum stress for creep rupture in time t, eighty percent of the minimum stress to cause the onset of tertiary creep in time t, and the minimum stress to produce one percent total strain in time t. For safe operation the limit for primary stresses is then:

$$\sigma_p \leq S_{mt},$$

where σ_p is the primary membrane stress of interest. Values of S_{mt} for several materials are available in tabular or graphic form in the code as a function of temperature and time. The data for 316 Stainless Steel and Vanadium (from [6]) are given in appendix A.

2.3 Displacement

It is important in the design of the first wall to keep track of the displacements that the material undergoes during operation. First wall sectors must remain compatible with the surrounding structure and environment. For example, in the case of a tubular first wall section which tends to bend under non-uniform thermal stresses, the tube must be restrained from interfering with adjacent tubes or from bowing out too far into the plasma chamber and being damaged by excessive plasma-wall interaction.

Under the influence of stresses, both mechanical and thermal, the material will undergo strains (and thus displacement) according to the well known Hooke's Law as long as the material remains in the elastic regime. When stresses exceed yield, depending on the combination of primary membrane stresses and cyclic thermal stresses, the material may either shakedown to elastic behavior after a few

cycles, exhibit plastic behavior limited by strain hardening, or undergo progressive deformation (ratcheting). This information can be conveniently presented in the form of a Bree diagram [8]. In addition, at elevated temperature, creep effects become important in deformation evaluation. A method for including creep effects in ratcheting behavior is available from O'Donnell and Porowski [9].

The ASME code provides for a procedure to limit accumulated strains in materials exposed to constant primary and cyclic thermal stresses with the use of a Bree diagram. This diagram demarcates the primary stress-secondary stress plane into regions of elastic, shakedown, plastic, and ratcheting behavior, using an axisymmetric model for an elastic-perfectly plastic material, as shown in figure 2.1. The elastic regime is the only section where the material is ratchet-free, however, it is very difficult in a typical fusion environment to keep all elastically calculated stresses within yield. Fortunately, plasticity and creep deformation can be permitted within prescribed limits.

Specifically, if the inequality;

$$\sigma_p + \sigma_t \leq \sigma_y$$

is satisfied, where the subscripts p, t, and y stand for primary, secondary (or thermal), and yield stresses, then there will be no plastic ratcheting. Further, if the average wall temperature is below the creep regime for each stress extreme during a cycle, then creep ratcheting will not occur. The onset of the creep regime is defined in the code as the temperature at which S_m equals S_t for 10^5 hours. Once outside the elastic regime, the shakedown and plastic regimes are allowable (as long as creep ratcheting is precluded) but the ratcheting regime is not design allowable since progressive deformation will occur.

FIG. 2.1 Bree Digaram [8]

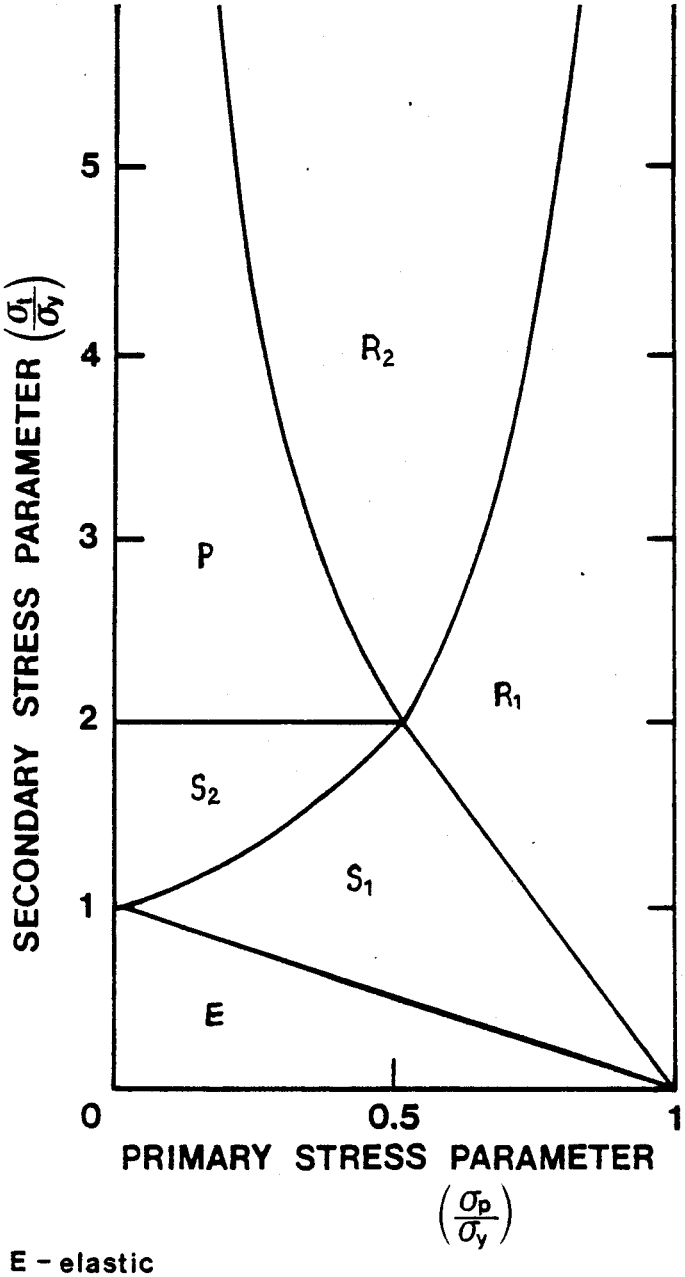

E - elastic
S - shakedown to elastic
P - plastic
R - ratcheting σ_y = yield stress

An entirely elastic approach to the analysis is being used here such that once outside the elastic regime, exact strains are not calculated (this would require detailed inelastic analysis.) Rather, the total accumulated strain is limited to less than one percent. This upper bound approach is conservative relative to the inelastic analysis. Reference [12] presents experimental results from cyclic ratcheting of pressurized cylinders which verifies the various regions of the Bree diagram. In addition, Reference [13] compares the upper bound method to the results of a rigorous inelastic analysis and finds the upper bound approach to be conservative.

Continuing with the discussion of the elastic analysis guidelines, excessive strains due to creep ratcheting are limited as recommended in the ASME code and formulated by O'Donnell and Porowski. In this method, elastically calculated stresses are used to define an effective creep stress which is entered on an isochronous stress-strain curve. (See appendix A for a sample.) Combined with a one percent strain limit, a material lifetime can be read directly from the isochronous stress-strain curve. Alternatively, the effective creep stress can be limited to some fraction of the yield stress to attain a desired lifetime. Note that this procedure is required only when the effective creep stress is less than yield.

The Bree diagram can be useful when converted to a design window approach in conjunction with a symmetric thin shell cylindrical first wall model. Smith et. al. [6] used this approach to obtain a Modified Bree diagram which depicts the Bree diagram in a plane of heat deposition versus first wall thickness. This approach, as well as another modification worked out in this study, is presented in detail in chapter 4.

2.4 Cyclic Damage

An important effect to be considered in first wall design is the fatigue damage

associated with thermal cycling. The analysis used in this study is a fatigue usage factor, U_f, approach outlined in the ASME code case N-47-17, where;

$$U_f = \sum_{i=1}^{I} (\frac{N_i}{N_{di}}),$$

and N_i is the total number of type i cycles and N_{di} is the number of type i cycles allowed for fatigue. Here, the "linear damage rule" for small creep effects is used such that;

$$U_f \leq 1$$

Only one cycle type is used in this work consisting of alternation between hot-zero power and hot-full power operation. Thus, the subscript i in the definition above can be omitted and N_i simply becomes the number of burn cycles in the life of the machine.

N_{di}, (or just N_d), is determined from a fatigue curve which plots the strain range, ϵ_t, versus N_d for a given material and maximum metal temperature during the cycle. Such a fatigue design curve is available for 316 Stainless Steel from the ASME code case. The curve used in this work (Fig. T-1430 in N-47) includes the effect of hold times and slow strain rates and is recommended for elastic analysis. The curve is constructed by reducing the best-fit curve of continuous cycling fatigue data by a factor of 20 on cycles or a factor of 2 on total strain range, depending on which is more conservative. A similar fatigue curve was used for Vanadium obtained from Reference [6]. This curve does not have temperature effects in it and may not be as conservative as the Stainless Steel curve.

The procedure to obtain fatigue limits for a cylindrical first wall element for a given material, heat deposition, bulk coolant temperature, and tube size is to :

- 1. Determine the temperature distribution.

- 2. Determine the stress distribution and the corrosponding strain tensor.

- 3. Calculate an equivalent strain range, $\Delta\epsilon_{equiv}$.

- 4. Obtain the allowable number of cycles, N_d, from the fatigue design curve.

Repeating this procedure using first wall thickness as a parameter leads to a plot of minimum required pulse length for fatigue versus first wall thickness (lifetime is fixed.) Results of this type of analysis are presented in chapter 4. Steps one and two above are detailed in chapter 3.

An equivalent strain range is used to obtain the strain range for a multi-axial stress state. For cylindrical geometry, the three strain ranges, $\Delta\epsilon_r$, $\Delta\epsilon_\theta$, and $\Delta\epsilon_z$ are defined for present purposes as;

$$\Delta\epsilon_r = \epsilon_r(during\ burn) - \epsilon_r(during\ rejuvenation)$$

with similar definitions for $\Delta\epsilon_\theta$ and $\Delta\epsilon_z$. Then, the equivalent strain range [4] is defined as (based on a Von Mises relation and a poisson's ratio of 0.5):

$$\Delta\epsilon_{equiv} = \frac{\sqrt{2}}{3}\left\{(\Delta\epsilon_r - \Delta\epsilon_\theta)^2 + (\Delta\epsilon_\theta - \Delta\epsilon_z)^2 + (\Delta\epsilon_z - \Delta\epsilon_r)^2\right\}^{\frac{1}{2}}$$

At elevated temperature, creep damage may contribute to fatigue and lead to a situation where the simple linear damage rule above is inadequate. For this purpose, the ASME code provides the following creep and fatigue damage rule;

$$U_f + U_c \leq D$$

where;

$$U_c = \sum_{k=1}^{J}(\frac{\Delta T_k}{T_{d,k}})$$

and J is the number of time intervals, ΔT_k is the duration of the time interval k, and $T_{d,k}$ is the allowable time to rupture during the time interval k. This reduces for our simplified burn cycle to:

$$\frac{N}{N_d} + \frac{\Delta t}{T_d} \leq D$$

where N is the number of applied cycles. N_d is the number of design allowable cycles obtained from the appropriate design curve as discussed above, t is the duration of the load. and T_d is the time to rupture at a reference stress σ_R, where σ_R is the smaller of;

$$\frac{\sigma_p + \sigma_t}{k}$$

and;

$$\frac{1.25\sigma_y}{k}.$$

The constant, k, is typically 0.9. The total creep-fatigue damage, D, is taken equal to one for elastic analysis. The time to rupture, T_d, is determined from a stress-to-rupture curve (stress versus time-to-rupture) which is available in the ASME code for several materials. The stress to rupture curve for 316 Stainless Steel is included in appendix A for reference.

2.5 Irradiation Embrittlement and Swelling

The major effects of irradiation; embrittlement (loss of ductility) and swelling, are of primary concern to fusion first wall integrity since they can lead to mechanical property degradation and component failure in a number of ways. These effects are unique among the structural considerations under investigation here in that they are relatively insensitive to the specific design geometry being considered.

Unfortunately, there are insufficient data available to model these effects accurately in the environment expected in present fusion reactor designs. The present exposure goal in the U.S. Fusion Reactor Materials Program is $40 MW \cdot yr/m^2$ [14] or, for example, a neutron wall loading of $4 MW/m^2$ for a 10 year lifetime. For Stainless Steel and Vanadium, this corresponds to roughly 440 displacements per atom (dpa) of radiation exposure, which is well beyond that obtained in LMFBR (Liquid Metal Fast Breeder Reactor) or HFIR (High Flux Isotope Reactor) irradiations to date.

Care must be taken in applying fission reactor data since the neutron spectra in the fusion environment, with source neutrons at $\approx 14MeV$, is significantly greater than source energies encountered in fission reactors ($\approx 1.0MeV$). There is evidence [15] that a greater amount of damage occurs within the fusion irradiation environment although no new damage effects are expected. The higher energy spectrum in fusion is particularly important since many of the thresholds for (n, α) transmutation reactions occur at energies $> 10MeV$ The presence of helium filled cavities is known to have strong effects on the mechanical properties and swelling characteristics of the candidate materials.

Due to the importance of helium effects, the helium/dpa ratio is a useful parameter in comparing the fusion and fission irradiation environments. This ratio is expected to be ≈ 25 in fusion first walls compared to 0.4 obtained in EBR-II. The HFIR has approximated these He/dpa ratios but only out to ≈ 60 dpa in the best characterized material, Stainless Steel. These data indicate that the fusion environment is indeed more severe than fission in terms of the degradation of mechanical properties. Although presently available data is inadequate for precise engineering evaluations at conditions of fusion interest, the present U.S. fusion materials development program is continuing efforts to increase the data base. Data should be available for irradiations to 100 dpa ($\approx 10MW \cdot yr/m^2$) within a year or two [16]. At the same time, extrapolations are being made of the presently available data to fusion relevant fluences [17].

In the following subsections, a brief discussion is made of the mechanisms of, and data available for, irradiation embrittlement and irradiation swelling. These effects are characterized in terms of fluence and irradiation temperature which allows use of the limited data available for design purposes.

2.5.1 Embrittlement

Neutron damage occurs in a material lattice in the form of the displacement of the lattice atoms from their equilibrium positions. The damage is propagated by the displaced atom which receives energy from the neutron and displaces many other atoms. The amount of damage incurred depends on the neutron energy and the temperature and stress state of the material.

The displaced atom, or interstitial, and the resulting empty lattice site, or vacancy, agglomerate into defect zones consisting of dislocation loops (two dimensional defects) and voids (three dimensional defects). The formation of these larger defects occurs at elevated temperature where the point defects are sufficiently mobile to agglomerate. For Stainless Steel this occurs at temperature above $\approx 350°C$.

The large defects have the effect of impeding further motion of dislocations in the process known as irradiation hardening. Irradiation hardening tends to increase the yield strength of the material. For temperatures less than half of the melting temperature ($1/2T_m = 550 - 600°C$ for Stainless Steel), this increase in yield stress causes an early onset of plastic instability (necking in a tensile test) which is manifested as a loss of ductility of the material. At $T > 1/2T_m$, the increase in yield strength does not persist due to the annealing out of damage zones. However, loss of ductility continues due to the migration and agglomeration of helium. These principles are illustrated in figure 2.2 for a face-centered-cubic structure (e.g. 316 Stainless Steel) and a body-centered-cubic structure (e.g. Vanadium).

The generation of helium in materials may lead to embrittlement in a similar manner to voids. Helium effects tend to dominate embrittlement at high temperatures ($> 1/2T_m$) where it is sufficiently mobile to agglomerate on grain boundaries and cause failure while other defect zones are annealing out.

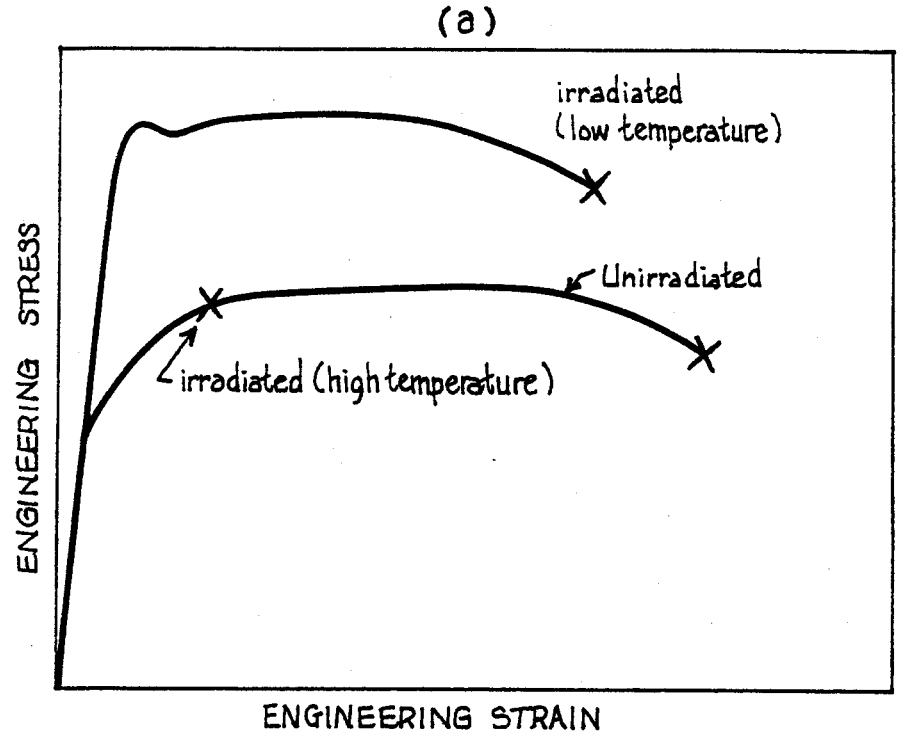

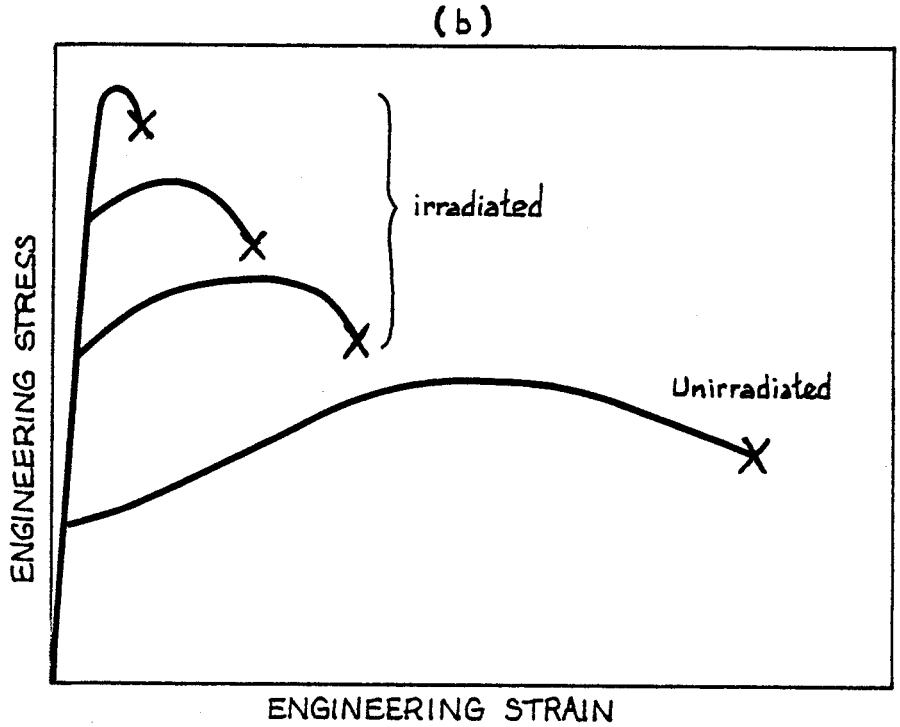

FIG. 2.2 Irradiation Hardening Effects on (a) FCC and (b) BCC Metals [20]

Thus, irradiation embrittlement will increase monotonically with fluence as the number of damage zones increases. The effect of irradiation temperature is more complex and is illustrated in figure 2.3 for 316 Stainless Steel. At low temperatures, the increase in yield strength leads to loss of ductility. As temperature is increased, the dislocations anneal out and the material recovers some of its ductility until the migration of helium to grain boundaries occurs and helium embrittlement drastically reduces ductility. Note that at high temperature, a moderate increase in ductility is observed due to plastic flow of the material which is eventually dominated by the effects of helium.

Figure 2.4 is a plot of the tensile properties of 316 Stainless Steel after irradiation in HFIR at temperatures from 350 - 700$^{\circ}C$ to 50 dpa and 4000 atomic particles per million (ppm) helium. Notice that there is significant reduction in both yield stress and ductility, measured in total elongation to fracture. According to this information, operation of Stainless Steel at these fluences limits the temperature to less than 500$^{\circ}C$ so that a 1 percent strain criterion, as recommended in the ASME code case N47, is not exceeded.

A modification to 316 Stainless Steel, achieved with the addition of $\approx$ 0.2 wt percent Ti (known as Prime Candidate Alloy (PCA) in STARFIRE [18]), exhibits improved irradiation embrittlement performance. This is also illustrated in figure 2.4. The data indicates that to these fluence levels, operation to 650$^{\circ}C$ is acceptable. The improvement of the titanium modified Stainless Steel is attributed to the formation of a TiC precipitate which accommodates the helium in smaller defect zones than would otherwise occur without the precipitate.

Irradiation embrittlement of Vanadium alloys occurs in two distinct temperature regions centered about 350$^{\circ}C$. Severe embrittlement is encountered at low temperature in this BCC metal due to the onset of plastic instability as described above. In fact, in order to satisfy the 1 percent strain criterion, operation at

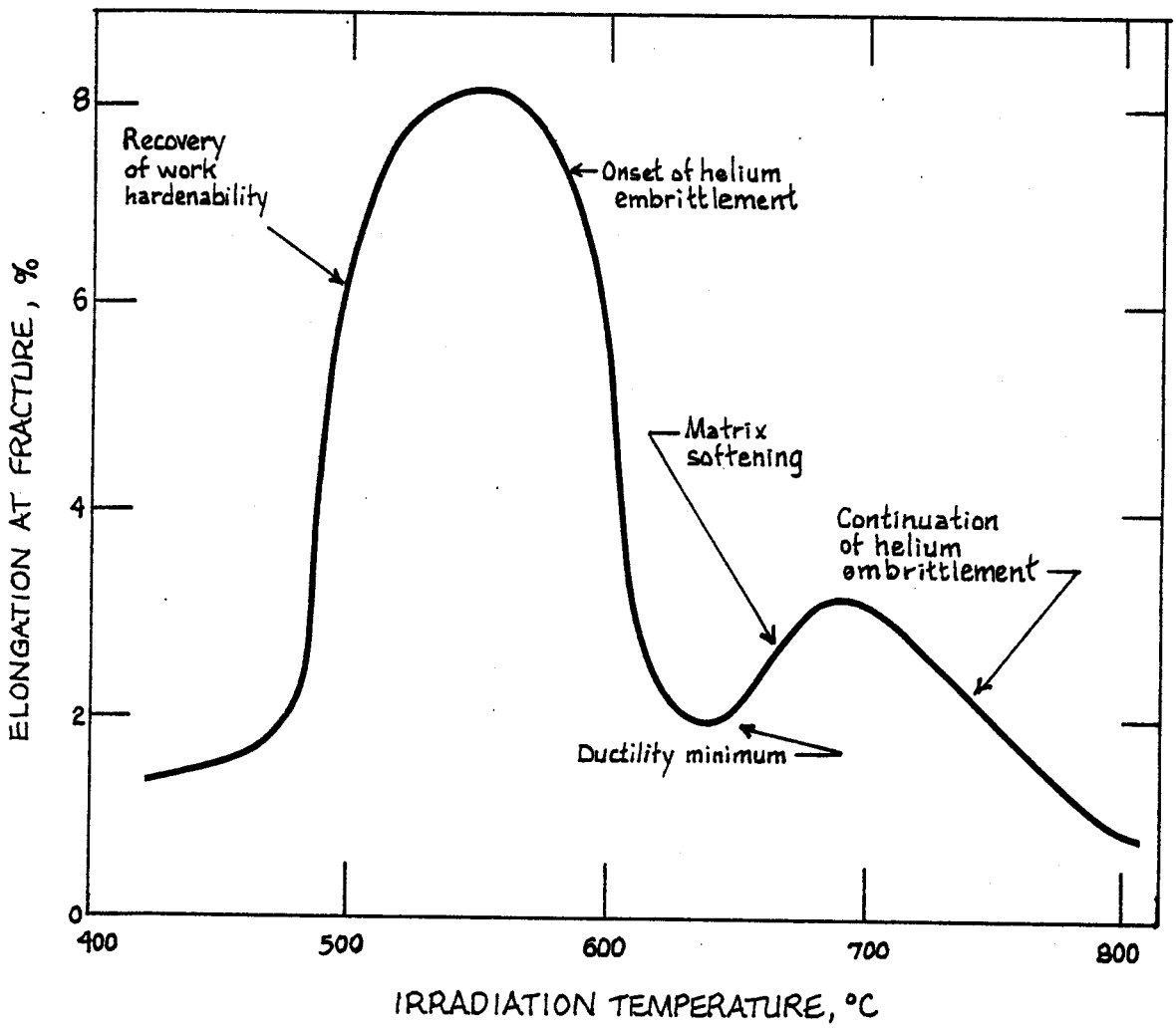

FIG. 2.3 Effect of Irradiation Temperature on Embrittlement [20]

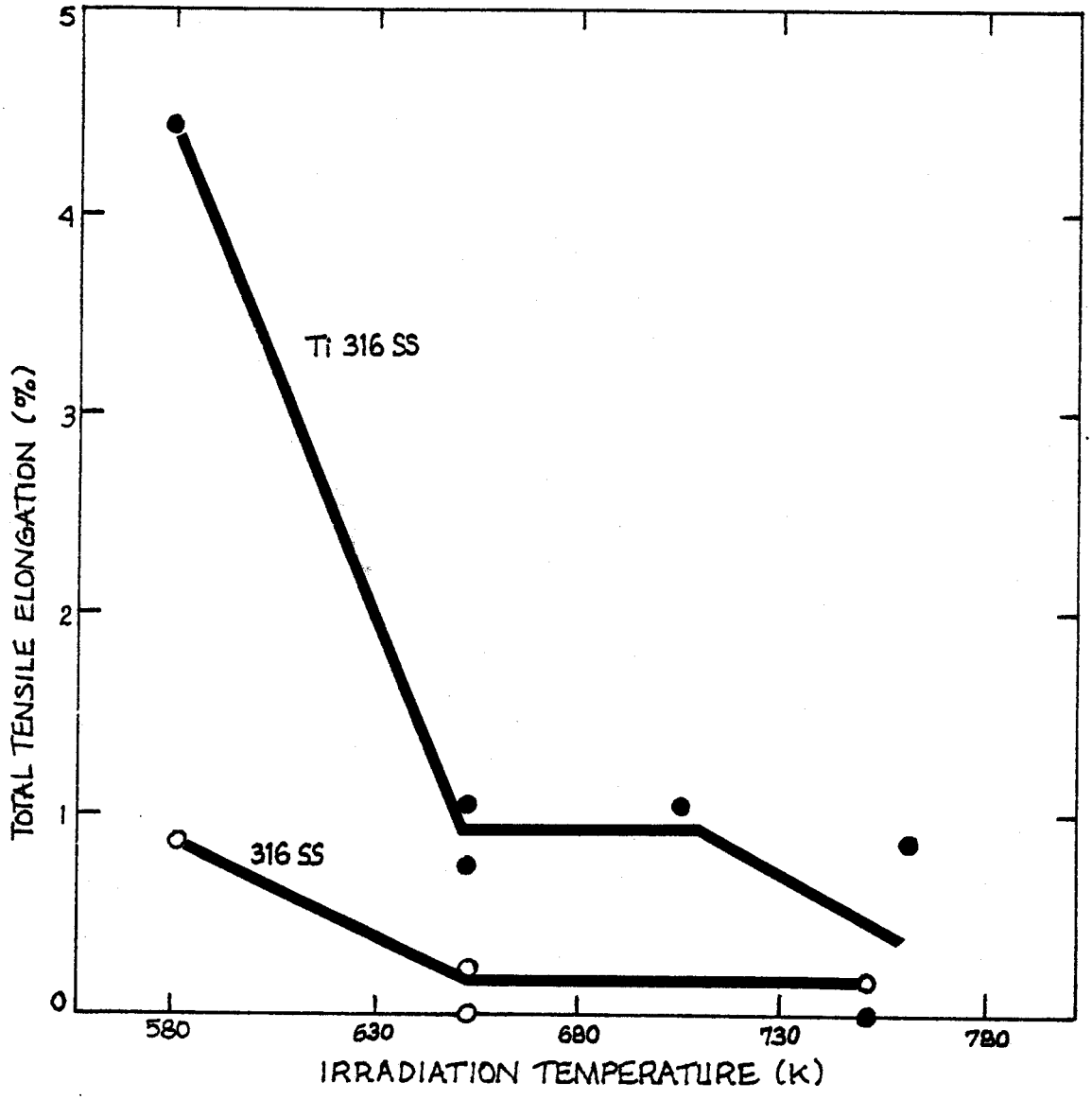

FIG. 2.4. Embrittlement of 316 Stainless Steel and Ti-316 (PCA) [15] (HFIR data at 50 dpa and 4000 ppm Helium, 350-700 C)

temperature greater than $300°C$ is recommended. Since Vanadium has a BCC structure, there is a well defined ductile to brittle transition temperature (DBTT) but this is expected to remain at or below room temperature even after irradiation at elevated temperature [10].

At temperatures greater than $300°C$, uniform elongation in Vanadium alloys is significantly improved. Irradiation tests have been performed for fluences to 17-36 dpa with 25-200 ppm helium contents in V-20Ti and V-15Cr-5Ti alloys [10]. The data shows that uniform elongation was reduced to not less than 1 percent due to loss of ductility for test temperatures up to $900°C$.

2.5.2 Swelling

Swelling of structural components of the first wall in fusion reactors can lead to flow restrictions, other dimensional changes not easily handled during design, and stress concentrations at points of support. Thus, it is important that the amount of swelling be restricted in design. Typically, swelling levels of $3 - 5$ percent fractional volume increase, $\frac{\Delta v}{v}$, are considered acceptable for fusion first wall applications [6], [7].

Swelling due to neutron irradiation is a result of the creation of defects in solids in the form of vacancy-interstitial pairs as discussed earlier. Interstitial atoms tend to migrate into loops (two dimensional defects) and form extra planes in the lattice. The resulting increase in solid volume caused by the formation of these interstitial loops is not offset by the presence of vacancies because the vacancies agglomerate into voids (three dimensional defects) which do not result in a volume decrease which could offset the effect of interstitial loops. The presence of trace gases such as helium tends to stabilize void formation and prevent collapse of the voids to vacancy loops, although helium is not absolutely necessary to the void growth process.

The amount of swelling, expressed in terms of percent change in volume, can be scaled with fluence as

$$\frac{\Delta v}{v} \alpha \phi t - (\phi t)_o$$

where $\frac{\Delta v}{v}$ is percent change in volume, ϕt is the fluence, and $(\phi t)_o$ is a reference fluence below which swelling is not observed. This incubation dose is probably due to a lack of significant generation of dislocations and helium for stabilization of the voids and to micro-chemistry effects [19].

Swelling is also a strong function of temperature since higher temperature promotes migration of the defects necessary for interstitial loop and void formation. Significant swelling usually occurs for a given material at temperatures between 0.3 and 0.5 T_m. At $T < 0.3T_m$, the rates of migration of interstitials and vacancies is too low for loop and void formation. For $T > 0.5T_m$, the migration rates are so high that annealing occurs, where rapid annilation (recombination of interstitials and vacancies) and access to defect sinks in the material leads to reduced swelling. Thus, the volumetric swelling versus temperature is typically a bell shaped curve peaked near 0.5 T_m.

Empirical relations have been developed for various materials which describe the influence of fluence and temperature. Such a relation for 20 percent cw Stainless Steel is [19]:

$$\frac{\Delta v}{v} = 9.0 \times 10^{-35}(\phi t)^{1.5}(4.028 - 3.712 \times 10^{-2}(T)$$

$$-1.0145 \times 10^{-4}(T)^2 - 7.879 \times 10^{-8}(T)^3)$$

where T is in C.

Some of the presently available swelling data for 316 Stainless Steel and PCA is shown in figure 2.5. Note that to these fluences (60 dpa), operation of 316 Stainless Steel at greater than $\approx 550°C$ is not advisable. However, figure 2.5 indicates an improvement in swelling behavior for PCA. At the same fluences, PCA can be reasonably operated to $\approx 650°C$.

A review of the presently available swelling data for Vanadium alloys is available from the INTOR study [10]. Due to the BCC structure of Vanadium and the addition of titanium in the alloys, it appears that under irradiations to date (less than 35 dpa), very little swelling occurs at any temperature.

As part of a recent blanket evaluation study at Argonne [17], extrapolations of the presently available swelling data were made for several materials. The swelling response of PCA and Vanadium in particular were approximated with a bi-linear swelling curve of $\frac{\Delta v}{v}$ versus fluence. The result is shown in figure 2.6. For PCA in the temperature range $450°C < T < 550°C$, a swelling rate of 0.02 percent/dpa is predicted for fluences less than 100 dpa with a huge increase in swelling rate above 100 dpa (0.5 percent/dpa). Thus, according to these extrapolations, the use of Stainless Steel is restricted to fluences of less than $10 MW \cdot yr/m^2$.

Similar predictions for Vanadium indicate that it may be used to fluences of 200 dpa although the data for Vanadium is considerably more limited than that of Stainless Steel. At best, these predictions for PCA and Vanadium can only provide a rough guide for engineering calculations since many questions remain about the

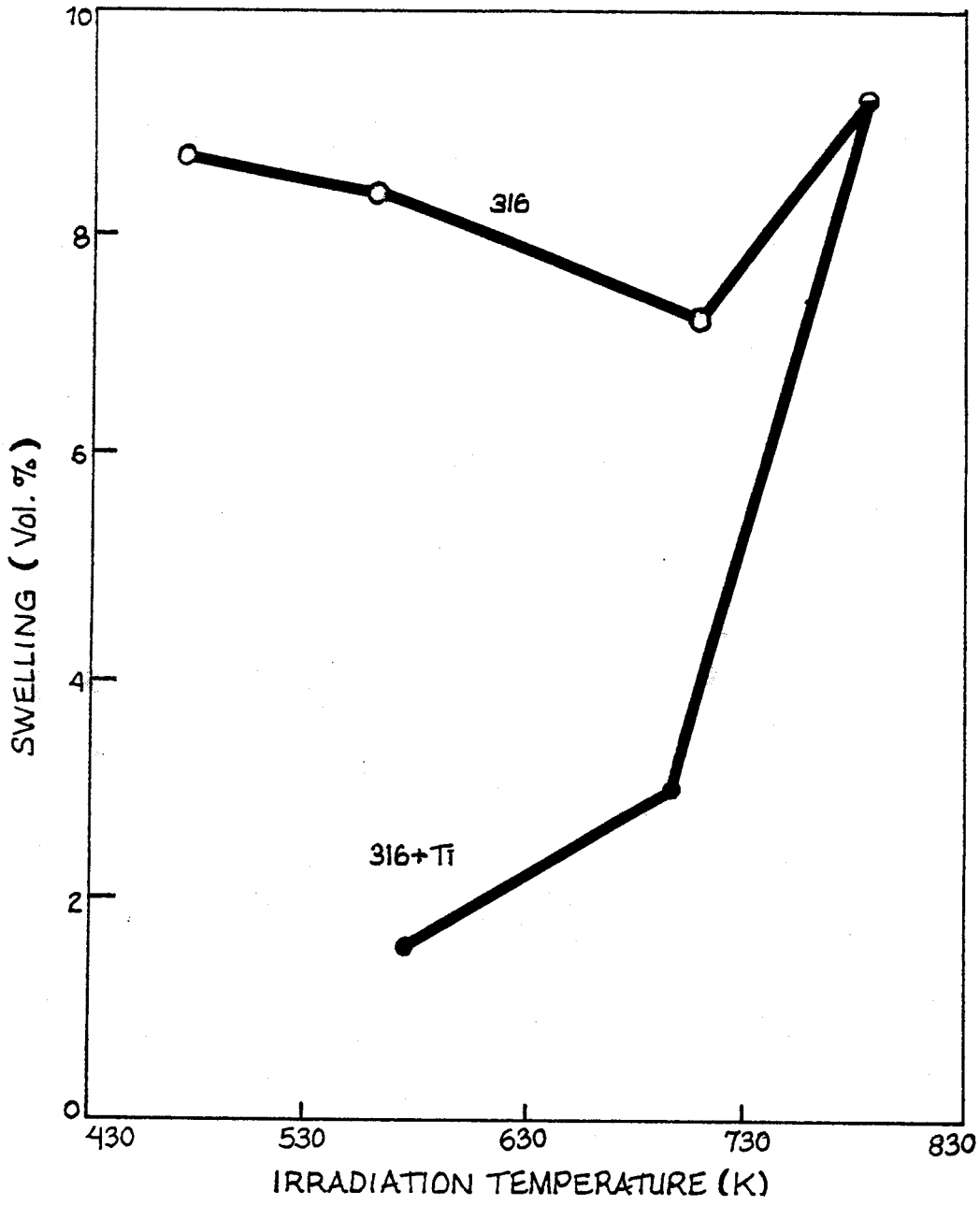

FIG. 2.5 Swelling Data for 316 Stainless Steel and Ti-316 (PCA) [15]
(HFIR data at 50 dpa and 4000 ppm Helium, 350-700 C)

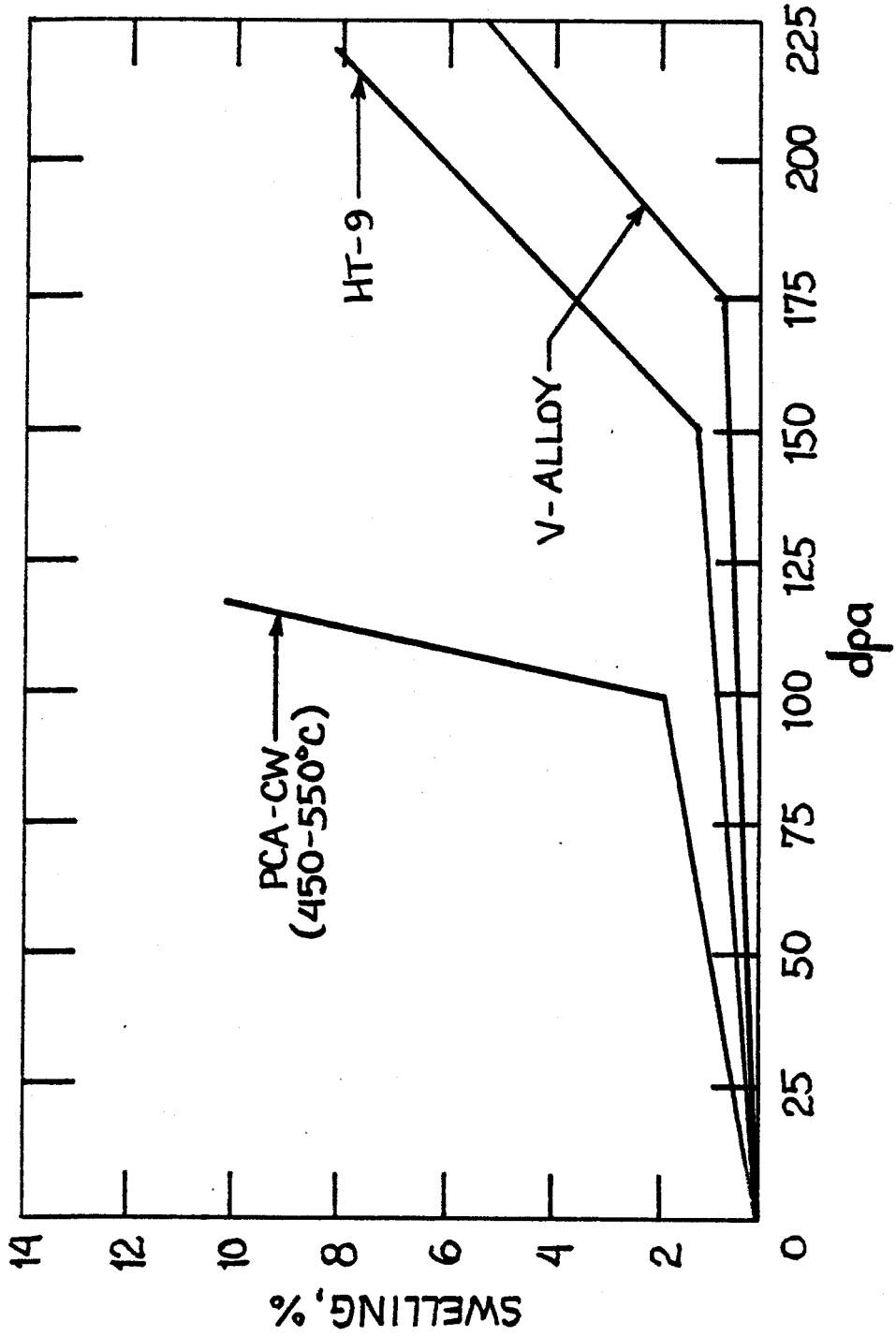

FIG. 2.6 Extrapolated Swelling Behavior for PCA and Vanadium [17]

effects of helium, high fluences, and the addition of alloying elements such as titanium.

2.6 Plasma-Wall Interactions

In recent years, plasma-wall interactions have become one of the most critical issues in fusion reactor design. This concern is to a large degree attributable to studies done at ANL (Argonne National Laboratory) and as a part of the INTOR (International Tokamak Reactor) project. These studies indicate that physical sputtering and erosion due to plasma disruption may lead to excessive ($\approx$ tens of mm/yr) erosion of the limiter, divertor plates, and first wall.

At first glance, this topic may seem to be on the periphery of the scope of this work but the implications of even the relatively low erosion rates now being predicted for the majority of the first wall ($\approx 1mm/yr$) must be evaluated. Any allowance for added wall thickness necessary for erosion will also impact the fatigue behavior of the first wall. This is discussed in more detail in chapter four.

In the following, physical sputtering and plasma disruptions are discussed separately. The major issues are outlined and calculations done as part of this work are shown. The result is not a detailed evaluation for the ULTR design since there is a great deal still unknown about erosion, especially in regard to the redeposition of the sputtered material and the frequency and distribution of plasma disruptions. Rather, an awareness of the issues regarding erosion is sought and qualitative and semi-quantitative design guidelines are outlined.

2.6.1 Physical Sputtering

Physical sputtering is a momentum transfer process by which a lattice atom from

a material surface facing the plasma is ejected into the plasma region as the result of a collision (either direct or indirect) with a plasma particle (usually hydrogen-H, deuterium-D, tritium-T, and helium-He). This form of first wall erosion is the dominant erosion mechanism under expected fusion conditions.

An energetic ion or neutral atom incident on the wall material produces a cascade of atomic displacements which can lead to a sputtered atom if a surface atom receives enough energy to exceed its binding energy. The number of sputtered atoms per incident ion (or neutral) is called the sputtering yield. Theoretical investigations of the dependence of sputtering yield on incident energy and angle, and the nature of the wall material have been performed [20]. The theory does not fit the experimental data accurately, but does yield the correct general scaling for yield dependence on incident energy.

One of the most recent sputtering models based on experimental data is available from D.L. Smith [21],[22]. The model incorporates recent data on physical sputtering into an analytical expression of sputtering yields for various materials as a function of incident energy and angle of typical plasma ions. This expression is in the form;

$$S(E,\theta) = S(E)S(\theta)$$

where;

$$S(E) = \frac{C}{U_0} {Z_1}^{0.75} (Z_2 - 1.8)^2 (\frac{M_1 - 0.8}{M_2})^{1.5} \frac{(E - E_{th})}{(E - E_{th} + 50 {Z_1}^{0.75} Z_2)^2}$$

and:

$$S(\theta) = (cos(\theta))^{-f}$$

where;

$$f = \frac{1}{(20Z_1)^{0.5}}(\frac{M_2}{M_1})^{0.25}(E - 4E_{th})^{0.25}(1 - \frac{\theta}{90})^{0.5}$$

and;

$$E_{th} = \frac{(4M_1 + M_2)^2}{4M_1M_2}U_0$$

The following definitions apply:

C = 2000 for incident hydrogen

= 400 for all other incident particles

U_0 = binding energy of wall material, eV

Z_1 = atomic number of incident particle

Z_2 = atomic number of wall material

M_1 = mass number of incident particle

M_2 = mass number of wall material

E = energy of incident particle, eV

E_{th} = threshold energy for sputtering

The energy dependent yield, S(E), is plotted in figure 2.7 for several light ions incident on a Beryllium target (representative of a first wall coating.) Note that the curve exhibits a threshold with a nearly linearly increasing energy dependence at low energies. At high energies, the profile falls off as $\frac{1}{E}$.

Physically, a threshold for sputtering is expected since the ejected atom must acquire at least its binding energy. This leads to a direct dependence of yield on incident energy and inverse dependence on binding energy of the wall material. The decrease of the yield at high incident particle energy is explained by the energy of the incident particle being deposited further into the wall material away from the surface.

Figure 2.8 is a plot of the angular dependent function $S(\theta)$, for a 1.0 keV ions incident on iron. The yield is enhanced considerably at large values of theta (close to grazing incidence) where theta is defined as zero at normal incidence. Relatively little work has been done on the angular dependence of the sputtering yield but the increase may be explained by an increased probability of the incident ions being backscattered normal to the surface of the material [22].

The calculations done by Smith at ANL using these correlations and those by Abdou *et al.* in the INTOR study using these or similar correlations were performed by using a transport code to follow plasma particles as they interact with material surfaces. As part of the present work, a simpler approach to the use of these correlations for erosion evaluation was used. To circumvent the need for a transport calculation, integration over an assumed energy and angular distribution of the incident particles was performed and reasonable agreement with the above work

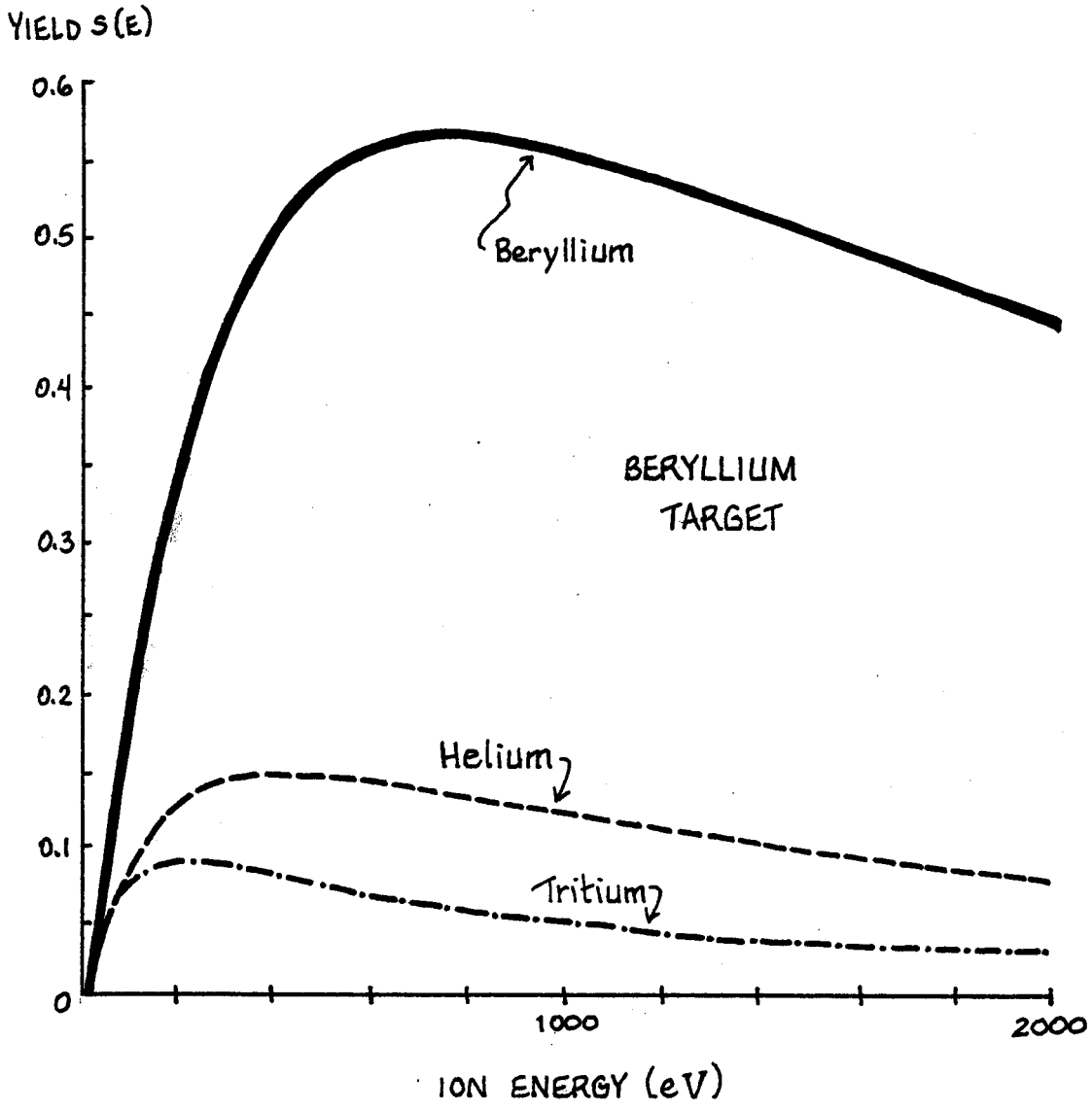

FIG. 2.7 Energy Dependent Sputtering Yield

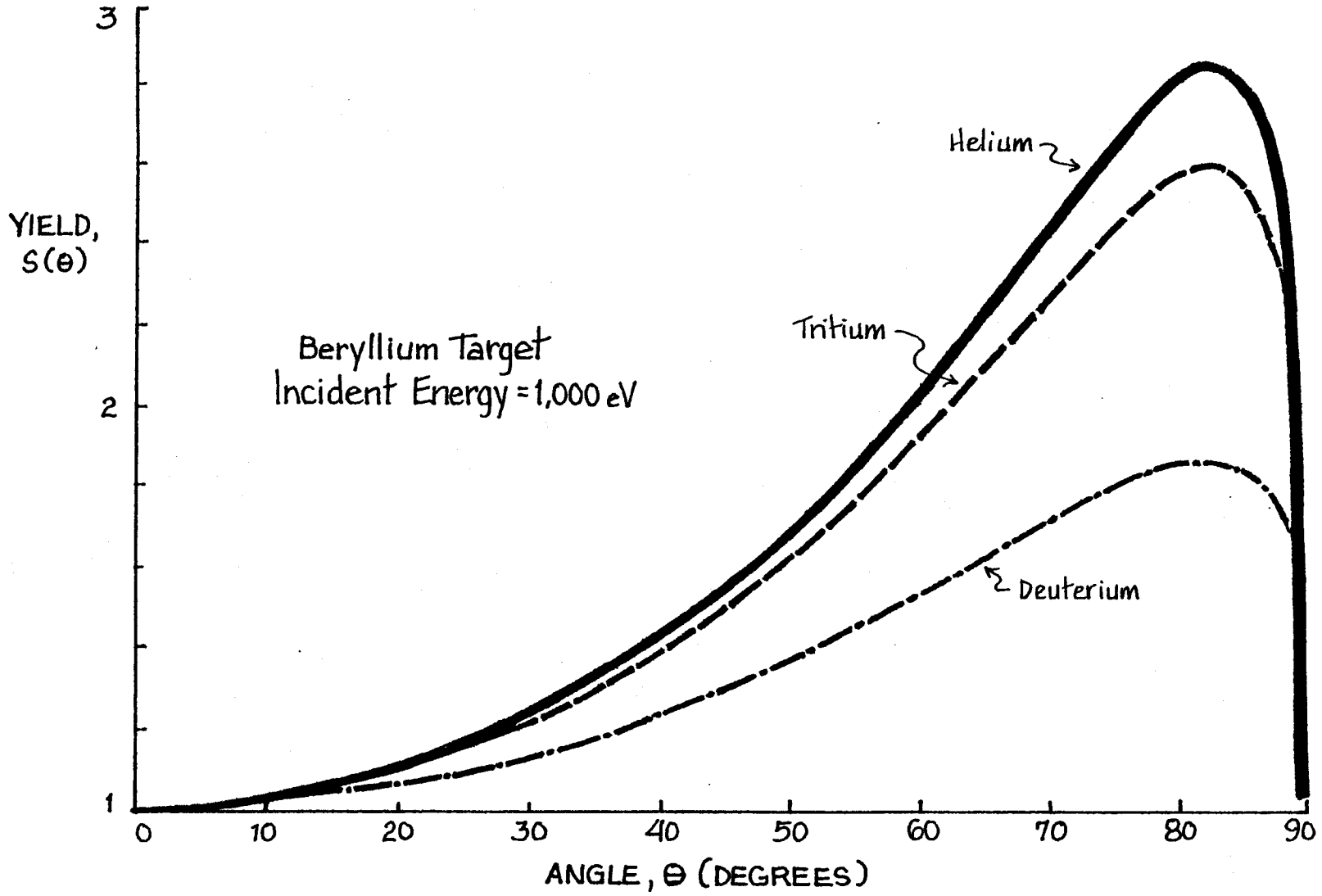

FIG. 2.8 Angular Dependent Sputtering Yield

was obtained. Details of this calculation, which served to illustrate the principles and trade-offs with various plasma conditions and first wall materials, may be found in appendix B. The code SPUT, used for these calculations, was written with the program MACSYMA which is a language within a program (written in LISP language) that is quite similar to FORTRAN in many respects. Helpful hints on this language are provided in the appendix so that it is possible for the reader to interpret the code and rewrite it in FORTRAN if desired.

Each of these studies has been valuable in evaluating the erosion characteristics of various sputtered particles, plasma particles, and first wall and limiter/divertor materials. The major results will be summarized here to illustrate the trade-offs within the sputtering question in regard to viable wall materials, the effects of the plasma sheath potential, and the impact of self sputtering.

Since most of the sputtered atoms are expected to be ionized and returned along the magnetic field lines, self sputtering, where a sputtered atom causes further sputtering damage, is a concern. In particular, self sputtering yields may exceed unity which could lead to an unstable or runaway erosion condition. There are few data available on self sputtering yields but they can be estimated from the sputtering data of an inert gas with a similar mass to the atom in question. In general, low-Z materials have a self-sputtering yield less than one at all incident energies but medium and high-Z materials may have a self-sputtering yield exceeding unity at incident energies as low as 400 eV.

The existence of the sheath potential, an electric field set up on the order of a debye length from the wall surface facing the plasma, is a key feature in determining the energy of the ions incident on the wall. The ion is accelerated through this potential in proportion to its charge and the magnitude of the potential so that its energy is:

$$E = \frac{3}{2}KT_e + eZ\phi$$

where $\frac{3}{2}kT_e$ is the initial energy (edge temperature) of the ion (for a maxwellian distribution), Z is the charge state of the ion, and ϕ is the sheath potential. Typically, the sheath potential is $\approx 3\ T_e$ and the charge state is 2-3 for low Z materials and ≈ 4 for high Z materials. Thus, the peak ion energy incident on a limiter/divertor surface is $\approx 6 - 9\ T_e$ for low-Z materials and $\approx 12\ T_e$ at high-Z.

In the area of the first wall, a scrape-off region created by the protrusion of the limiter into the plasma exists. The temperature generally decreases exponentially through this scrapeoff region so that incident ion energies are characteristically lower. For this reason, and the fact that the limiter/divertor is designed to take the majority of the incident flux in the first place, the erosion problem for the majority of the first wall is significantly reduced from that of the limiter or divertor.

The importance of the plasma edge temperature in determining the incident ion energies and corresponding sputtering yields makes it convenient to characterize physical sputtering within three regimes of plasma edge temperature. At edge temperatures $T_e > 700eV$, the sputtering yield for low-Z materials is generally quite acceptable because of the $\frac{1}{E}$ dropoff of the yield at high temperatures. For high-Z materials this regime is unacceptable because the self-sputtering coefficient is generally greater than one. This edge temperature regime may be possible with pellet fuel injection but it does not appear to be viable due to increased pumping needs for the limiter divertor system and uncertainties in the amount of impurity radiation that could cool off the edge region.

The edge temperature regime $100eV < T_e < 400eV$ is the most likely regime for the expected fusion environment but, unfortunately, physical sputtering in

this temperature range appears to be a difficult problem for both low and high-Z materials. The sputtering yield for low-Z materials tends to peak in this regime while for high-Z materials, the self-sputtering coefficient remains unacceptable. The low edge temperature regime ($T_e < 50eV$) appears to be ideal for high-Z materials since the yields are quite low, however, this temperature range is also difficult to achieve. Enhancement of impurity radiation has been proposed [10] to achieve the low edge temperatures desired, however, there is still a great deal of uncertainty regarding this scheme since it has not been possible to verify the theoretical models experimentally.

The amount of erosion in mm/yr due to physical sputtering is calculated as follows from the sputtering yield:

$$Erosion = S\frac{\phi}{N}K$$

where S is the average sputtering yield in atoms per incident ion, ϕ is the flux of ions incident on the surface, N is the number density of the wall material, and K is a conversion constant to make the units compatible (see appendix B). Thus, to minimize the erosion rate, the yield and/or the incident flux must be lowered as much as possible.

To illustrate the magnitude of typical erosion rates, the results from an INTOR study are used. It is important to point out that the numbers here include the redeposition of the sputtered material and that questions still remain regarding the validity of this calculation. Specifically, the erosion and redeposition rates are so large that the net erosion rate (erosion - redeposition) may contain large relative error. In addition, there are questions remaining about the metallurgical character of the redeposited material compared to the original wall material. Despite these

questions, the calculations are state-of-the-art and illustrative of the expected erosion problem.

Typical erosion rates for INTOR limiter/divertor plates for low-Z materials vary from 8 mm/yr at T_e of 20 eV down to $\approx$ 3 mm/yr at T_e of 1200 eV. Thus, the erosion rate is limited to less than 10 mm/yr even in the worst (and most likely) edge temperature regime. As expected, high-Z materials are not viable at $T_e > 50eV$ due to self sputtering but the net erosion below 50 eV is generally less than 10 mm/yr except at the leading edges of the limiter, where higher fluxes can lead to net erosion more than an order of magnitude higher.

However, the region we are primarily concerned with in this study, the first wall, has significantly lower erosion rates for low-Z materials. Typically, erosion rates are on the order of 1 mm/yr, except in regions local to the limiter or divertor where erosion can be as high as tens of mm/yr. Special protective shielding will be required in these local areas but, in general, it will be assumed that an erosion rate on the order of one mm/yr will have to be contended with in the first wall design.

The selection of a low-Z material coating on the first wall seems to be the favorable choice for erosion resistance because of the intermediate edge temperature regime expected in fusion environments. Several materials have been proposed but beryllium is the prime candidate since other possible materials tend to be at a disadvantage relative to beryllium for a variety of reasons. In particular, erosion due to chemical interactions between hydrogen and/or oxygen and the coating material is a problem for graphite. Boron has poor fabrication and thermophysical properties and silicon carbide has both poor thermophysical properties and large self-sputtering yields.

2.6.2 Disruptions

A plasma disruption is a sudden loss of plasma confinement in a tokamak device which results in the elimination of the plasma burn and dumping of some or all of the plasma energy onto the first wall or limiter/divertor. The nature and origin of a disruption is not completely understood but it is clear that the deposition of several MJ/m^2 in the space of milliseconds, which typically accompanies a disruption, will have significant consequences in terms of melting and vaporization of the first wall.

A useful analysis of the disruption erosion problem is available from B.J. Merrill [23]. The details of the analysis will be avoided here but, simply put, the plasma disruption is modeled as a given energy density being deposited on a portion of the first wall (or limiter) surface. The energy that is dissipated at the surface (since some of the energy will be conducted or convected away) will result in rapid temperature rise and subsequent vaporization and melting of the surface material. An energy balance is used to keep track of the energy content at the wall and the vaporization and melting processes are modeled using equations of state for a variety of possible wall materials.

The results of the work by Merrill is in graphic form and is convenient for application to a range of conditions. The results available are peak surface temperature versus time of the disruption for several plasma energy densities, and vaporization and melt layer depth versus plasma energy density for several values of disruption duration. This data is used to model disruption erosion for ULTR, assuming a given disruption time and disruption frequency. These calculations indicate that disruption erosion rates for ULTR may be less than a millimeter per year.

All of these calculations indicate that beryllium is acceptable in terms of resistance to the effects of plasma disruption, superior to Stainless Steel, and is not as effective as carbon. For all three materials, the magnitude of erosion is less than that of physical sputtering as long as the melt layer on the wall surface remains stable and

is not stripped off. Much work is still needed in this area because the results are sensitive to several assumptions which must be verified. These include the length of the disruption, the frequency of disruption, the stability of the melt layer, and the area of the first wall subjected to the energy deposition.

2.7 Summary

The present study considers the following phenomena in the design of a fusion first wall:

- Strength
- Displacement
- Cyclic damage
- Irradiation embrittlement and swelling
- Plasma-wall interaction

A method of analysis for each of these design limits has been outlined. Procedures for the evaluation of strength, displacement, and cyclic fatigue limits are available in the ASME code. Methods of analysis for irradiation effects and plasma-wall interactions are more difficult to apply due to a lack of data and lack of a thorough understanding of the physical processes involved. However, these two important effects can be considered as shown here on the basis of our present understanding and the available data.

In chapter 4, the analysis methods presented here are used to examine thermal

fatigue in detail and establish design windows. However, first the stress analysis for a tubular first wall geometry is considered.

3. STRESS ANALYSIS

3.1 Introduction

This chapter is concerned with the calculation of the temperature distributions and stresses due to pressure and thermal loads encountered in tubular first wall designs. Most parametric studies in first wall fatigue previously have been based on tubular geometry and the thin shell approximation for combined pressure and thermal stresses with symmetric heat deposition. The choice of tubular geometry seems prudent since this is both a relatively simple problem to approach analytically and is representative of several of the first wall designs that have been considered to date.

However, in many cases of interest, the symmetric thin shell approximation does not accurately represent the stress state in a tubular first wall design. Thus, the major portion of this chapter will be concerned with an analytical, two dimensional treatment of the tube temperature distribution and stresses, including an asymmetric heat deposition and internal heat generation. The application of these calculations for both one dimensional (thin shell) and two dimensional treatments to fatigue calculations will be undertaken in chapter four.

3.2 Geometry and Conditions of Analysis

The geometry under consideration is depicted in figure 3.1. The tokamak is split into a number of sectors (there are 20 in the ULTR design), each of which consist of the plasma region, first wall, blanket/shield sector, and magnet. The first wall is the first material surface exposed to the plasma and is made of many right circular tubes running the length of the sector in the toroidal direction (perpendicular to the sector cross-section.) These tubes may be welded or brazed together or welded to a structural wall at the first wall/blanket boundary.

FIG. 3.1 ULTR First Wall Geometry

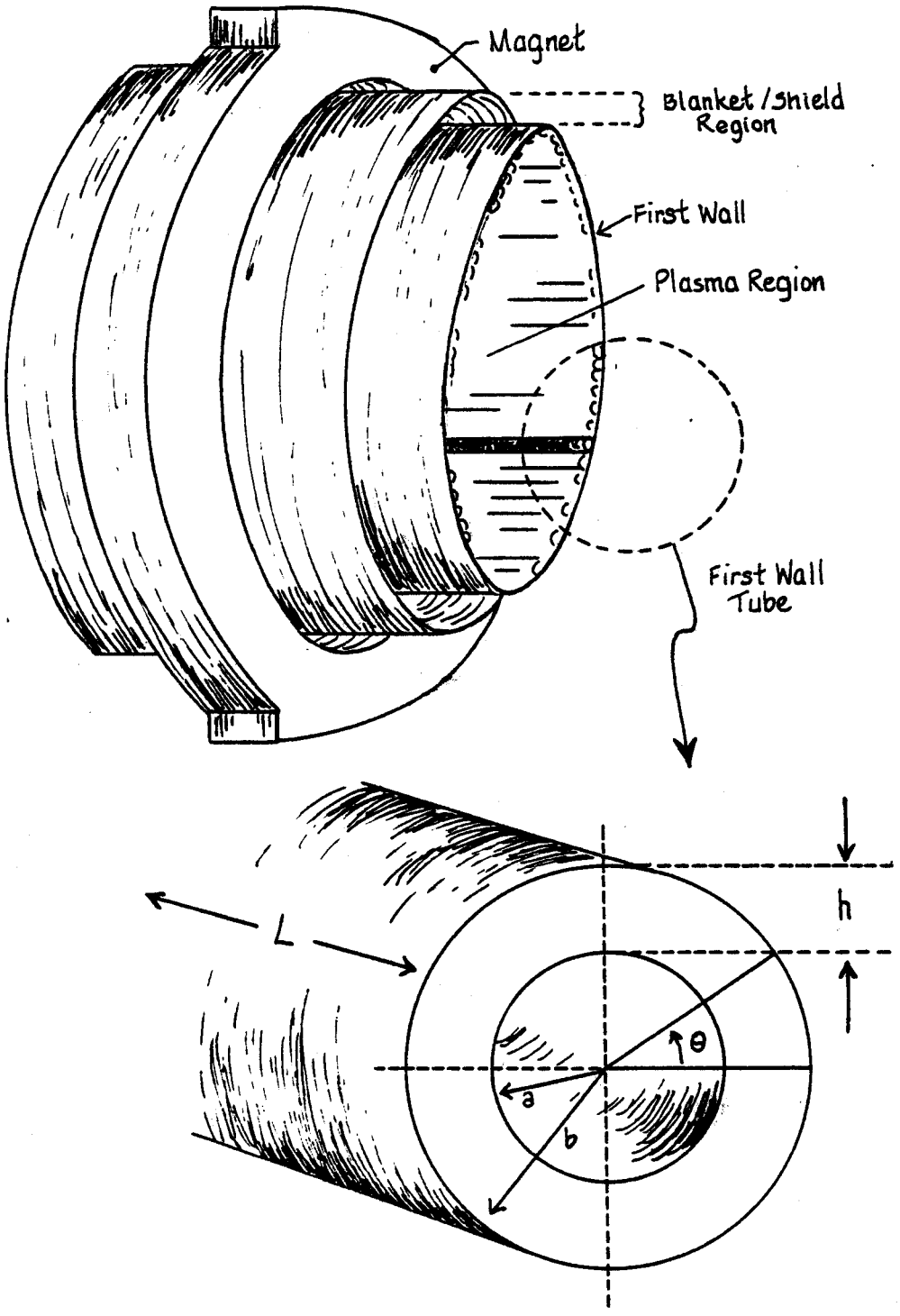

Each tube of inside radius a, outside radius, b, and length, L, will be exposed to an asymmetric heat flux (q'') from the charged particle and electromagnetic radiation flux from the plasma. The neutron flux, also emanating from the plasma, will produce internal volumetric heat generation (q''') within the material making up the first wall tubes. Coolant, at a pressure p, flows down the center of the tubes in the toroidal direction and removes the heat generated in the material from the surface and volumetric heat loads which are typically $2MW/m^2$ and $80MW/m^3$, respectively.

The stresses calculated here will be entirely elastic. These will not always be the actual stresses existing in the tube during operation if the stresses exceed yield stress or relax during operation. However, the ASME code provides design guidelines relevant to this work based on entirely elastically calculated stresses.

3.3 One Dimensional (Thin Shell) Treatment

The simplest model for the cylindrical first wall geometry under consideration is that of a long, thin shell with;

$$h = (b - a) \ll R \qquad 3.1$$

where R is the mean radius of the tube. We consider that the shell is subjected to an internal pressure p, zero external pressure, and a cylindrically symmetric heat flux incident on its outer surface. Under these conditions, a temperature drop which is approximately linear develops across the shell. This temperature drop will be cycled between ΔT (during the plasma burn) and zero (during the rejuvenation period). The temperature distribution is:

$$T = T_a + \Delta T(\frac{r-a}{h}) \qquad 3.2$$

where:

$$\Delta T = \frac{q''h}{k} \qquad 3.3$$

and r is radius varying through the tube thickness, T_a is the temperature at the inner radius a, and k is the thermal conductivity of the wall material.

Furthermore, we allow the cylinder to be axially unrestrained so that the principal mechanical stress of interest is:

$$\sigma_p = \frac{pR}{h} \qquad 3.4$$

which is a primary stress in the theta direction (see figure 3.1 for orientation of theta.) The maximum thermal stress in the tube is:

$$\sigma_t = \frac{\alpha E \Delta T}{2(1-\nu)} \qquad 3.5$$

where α is the thermal expansion coefficient, E is the modulus of elasticity, and ν is Poisson's ratio. Thus the total stress (during the burn) is:

$$\sigma_\theta = \sigma_p + \sigma_t(\frac{(2a+h)-2r}{h}). \qquad 3.6$$

Thus, for a given pressure, heat flux, and tube geometry, we can evaluate the temperature and stress distributions in the tube.

3.4 Two Dimensional Treatment

The mechanical stresses encountered in a thick annular section with internal pressure, p, and externally unrestrained in the axial direction are (from Rust [24]);

$$\sigma_r = -p(\frac{a^2}{b^2 - a^2})(\frac{b^2}{r^2} - 1) \qquad 3.7$$

$$\sigma_\theta = p(\frac{a^2}{b^2 - a^2})(\frac{b^2}{r^2} + 1) \qquad 3.8$$

$$\sigma_z = p(\frac{a^2}{b^2 - a^2}) \qquad 3.9$$

Evaluation of thermal stresses in tubes subjected to surface and volumetric heat loads has been treated by McManamy [25] This work was based on a general formulation in Boley [26] for elastic thermal stresses. Here, we begin by developing an expression for the temperature distribution under the conditions of interest. Then we present the general formulation for the primary stresses in the radial and theta directions in terms of integrals over the temperature distribution and establish the end conditions which will determine the axial stress component. The temperature distribution is encorporated into the stress formulations to obtain the equations for thermal stresses in the first wall which can be incorporated into a parametric computer code.

3.4.1 Temperature Distribution

With internal heat generation and asymmetric surface heat depositions on the first wall, the temperature will vary radially and in theta. Here, q''' is uniform in the tube but q'' is approximated as a cosine distribution on the side facing the plasma. The side away from the plasma is assumed to behave adiabatically. The solution of Laplace's equation for this case is sketched by McManamy.

Since the problem is linear, the contributions of q''' and q'' to the temperature distribution can be separated and the resulting solutions added to obtain their simultaneous contribution. The solution to Laplace's equation with $q''' = 0$ is symmetric about $\theta = 0$ (theta is defined in figure 3.1) and is;

$$T(r,\theta) = \sum_{n=0}^{\infty} F_n(r) cosn\theta \qquad 3.10$$

where

$$F_n(r) = \frac{C_n}{r^n} + D_n r^n; \qquad n \geq 1 \qquad 3.11$$

The following boundary conditions are applied; At $r = a$:

$$k\frac{\partial T}{\partial r} = H(T - T_b) \qquad 3.12$$

At $r = b$:

$$k\frac{\partial T}{\partial r} = q'' cos\theta; \qquad 0 \leq \theta \leq \frac{\pi}{2} \qquad 3.13$$

$$\frac{\partial T}{\partial r} = 0; \qquad \frac{\pi}{2} < \theta \leq \pi \tag{3.14}$$

That is, the heat flux impinges unidirectionally on the outer wall facing the plasma and there is no heat transfer across the boundary facing away from the plasma.

We have assumed that H, the heat transfer coefficient, is independent of theta and have adopted a fixed fluid bulk temperature, T_b. Expressing the boundary conditions at $r = b$ as a fourier cosine series, we can obtain the constants C_n and D_n in the solution, Equation 3.11. The result is;

$$C_1 = \frac{q''a^2b^2}{2k}\left[\frac{k - Ha}{k(b^2 - a^2) + Ha(a^2 + b^2)}\right] \tag{3.15}$$

$$D_1 = \frac{q''b^2}{2k}\left[\frac{k + Ha}{k(b^2 - a^2) + Ha(a^2 + b^2)}\right] \tag{3.16}$$

$$C_n = \frac{q''}{\pi km}\left[\frac{(-1)^{m+1}}{(2m)^2 - 1}\right]\left[\frac{b^{2m+1}(2mk - Ha)}{2mk((\frac{b}{a})^{4m} - 1) + Ha((\frac{b}{a})^{4m} + 1)}\right] \tag{3.17}$$

$$D_n = \frac{1}{a^{4m}}\left[\frac{2mk + Ha}{2mk - Ha}\right]C_n \tag{3.18}$$

Equations 3.17 and 3.18 are for $n > 1$, $n = 2m$. $m = 1, 2, ...$, and $C_n = D_n = 0$ for odd n. This is the complete solution for the temperature due to q''. The solution for q''' is obtained by solving Laplace's equation again for uniform volumetric heat generation. The solution is (including the zero order q'' contributions):

$$T(r,\theta) = \frac{b}{k}(\frac{q''}{\pi} + \frac{q'''b}{2})ln(\frac{r}{a}) - \frac{q'''}{4k}(r^2 - a^2) + \frac{\pi(b^2 - a^2)q''' + 2aq''}{2\pi bH} + T_b \quad 3.19$$

Thus, the total solution for the temperature distribution on the first wall is;

$$T(r,\theta) = \frac{b}{k}(\frac{q''}{\pi} + \frac{q'''b}{2})ln(\frac{r}{a}) - \frac{q'''}{4k}(r^2 - a^2) + \frac{\pi(b^2 - a^2)q''' + 2aq''}{2\pi bH}$$

$$+ \sum_{n=1}^{\infty}(\frac{C_n}{r^n} + D_n r^n)cosn\theta + T_b \quad 3.20$$

A plot of $T(r,\theta)$ in a typical Stainless Steel first wall tube with $q'' = 1MW/m^2$, $q''' = 40MW/m^3$, $T_b = 320C$ is shown in figure 3.2.

3.4.2 Thermal Stress Formulation

The general three dimensional problem of thermal stresses in the first wall involves the determination of the six thermal stress components, $\sigma_{rr}, \sigma_{\theta\theta}, \sigma_{zz}, \sigma_{r\theta}, \sigma_{\theta z}, \sigma_{rz}$, the six corrosponding strain components (ϵ_{ij}) and three displacement components, u, v, and w for a given temperature distribution. Using the equations of equilibrium, the stress-strain relations, the strain-displacement relations and the appropriate boundary conditions, this problem has a unique solution but can only be solved on a computer with the temperature distributions of interest here. This general formulation may be found in many structural mechanics texts, for example Reference [27].

A two dimensional treatment of the problem can be developed with the use of the so called generalized "plane strain" assumption for sections very long in comparison

FIG. 3.2 Temperature Contours in Stainless Steel First Wall Tube

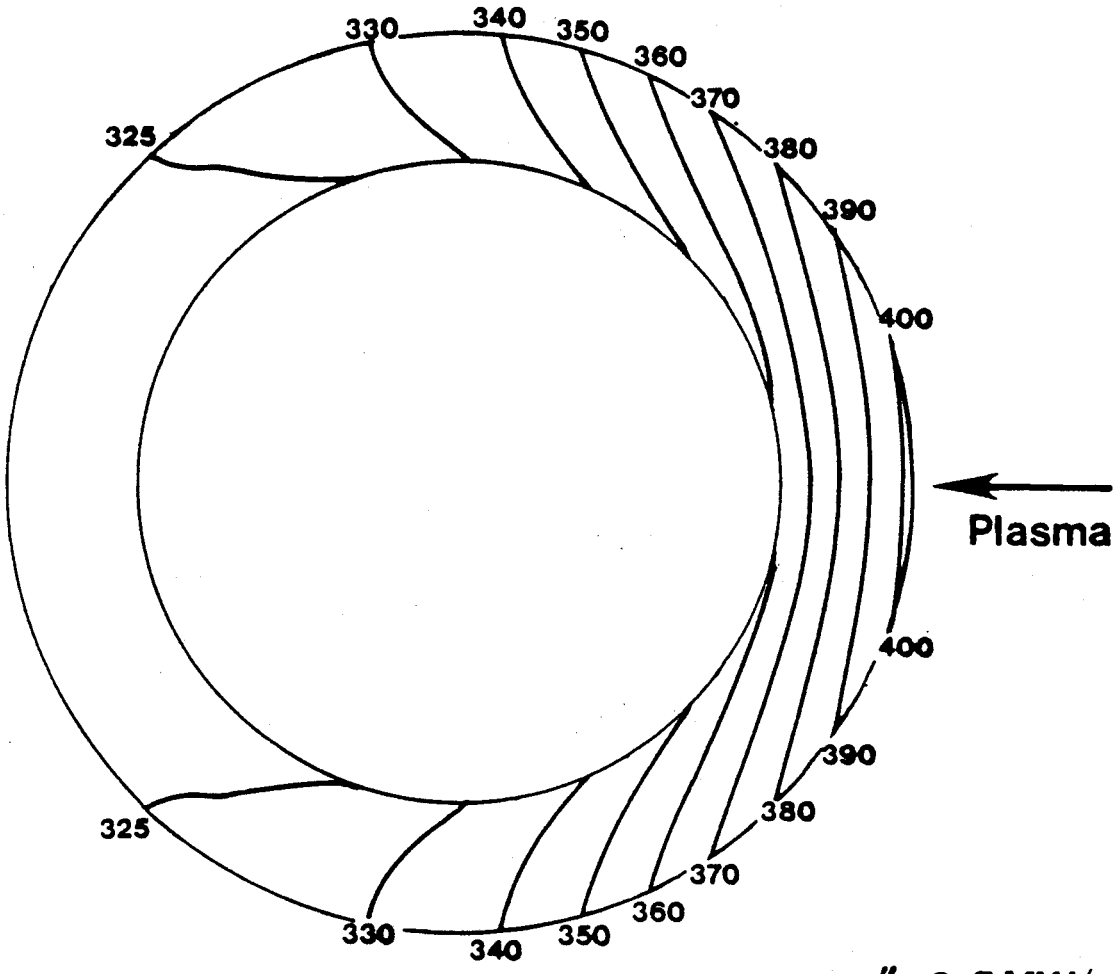

to their cross-section ($L \gg D$). Here, the displacement component in the axial direction, w, is constant and the remaining displacements are only a function of r, θ. Analytical solutions for the stresses with a temperature distribution varying in r, θ can be derived. The details of the formulation of the radial and theta stresses are available in Boley. Here we state only the results. The axial stresses, obtained later, will depend on the end conditions chosen.

If the temperature distribution is expressed in the form of a Fourier series as in section 3.4.1, Boley shows that the stresses due to the radial and theta components of the temperature distribution are separable and the solutions are derivable in terms of an integral over $T(r, \theta)$. The solutions for the temperature varying only in r are;

$$\sigma_{rr} = \frac{\alpha E}{(1-\nu)r^2}\left[\frac{(r^2-a^2)}{(b^2-a^2)}\int_a^b Trdr - \int_a^r Trdr\right] \qquad 3.21$$

$$\sigma_{\theta\theta} = \frac{\alpha E}{(1-\nu)r^2}\left[\frac{(r^2+a^2)}{(b^2-a^2)}\int_a^b Trdr - \int_a^r Trdr - Tr^2\right] \qquad 3.22$$

$$\sigma_{r\theta} = \sigma_{rz} = \sigma_{\theta z} = 0. \qquad 3.23$$

Since the temperature varies also in the theta co-ordinate, the following terms are added to the stresses:

$$\sigma_{rr} = \frac{\alpha E r}{2(1-\nu)(a^2+b^2)}(1-\frac{a^2}{r^2})(1-\frac{b^2}{r^2})C_1 cos\theta \qquad 3.24$$

$$\sigma_{\theta\theta} = \frac{\alpha E r}{2(1-\nu)(a^2+b^2)}(3 - \frac{a^2+b^2}{r^2} - \frac{a^2b^2}{r^2})C_1 cos\theta \qquad 3.25$$

$$\sigma_{r\theta} = \frac{\alpha E r}{2(1-\nu)(a^2+b^2)}(1 - \frac{a^2}{r^2})(1 - \frac{b^2}{r^2})C_1 sin\theta \qquad 3.26$$

The sum of the radial and theta temperature profile induced stresses is then the total thermal stress due to the profile. Now, using the results of section 3.4.1, the integrations can be performed to obtain σ_r and σ_θ as a function of the heat loads, the bulk temperature and the first wall geometry. The results are;

$$\sigma_r = \frac{q'''\alpha E b^2}{4k(1-\nu)}\left[(1 - \frac{a^2}{r^2})(\frac{ln(\frac{b}{a})}{(1-\frac{a^2}{b^2})} - \frac{a^2}{4b^2} - \frac{3}{4}) - ln(\frac{r}{a})\right.$$

$$\left. + \frac{1}{2} - \frac{a^2}{2r^2} + \frac{a^2}{4b^2}(\frac{r^2}{a^2} - \frac{a^2}{r^2})\right] + \frac{\alpha E T_o}{2(1-\nu)}\left[\frac{b^2}{r^2}(\frac{r^2-a^2}{b^2-a^2})ln(\frac{b}{a}) - ln(\frac{r}{a})\right]$$

$$+ \frac{\alpha E r}{2(1-\nu)(a^2+b^2)}(1 - \frac{a^2}{r^2})(1 - \frac{b^2}{r^2})C_1 cos(\theta) \qquad 3.27$$

$$\sigma_\theta = \frac{q'''\alpha E b^2}{4k(1-\nu)}\left[(1 + \frac{a^2}{r^2})(\frac{ln(\frac{b}{a})}{(1-\frac{a^2}{b^2})} - \frac{a^2}{4b^2} - \frac{3}{4}) - \frac{1}{2}\right.$$

$$\left. + \frac{a^2}{2r^2} - \frac{a^2}{4b^2}(\frac{3r^2}{a^2} + \frac{a^2}{r^2})\right] + \frac{\alpha E T_o}{2(1-\nu)}\left[\frac{b^2}{r^2}(\frac{r^2-a^2}{b^2-a^2})ln(\frac{b}{a}) - ln(\frac{r}{a}) - 1\right]$$

$$+ \frac{\alpha E r}{2(1-\nu)(a^2+b^2)}(3 - \frac{a^2+b^2}{r^2} - \frac{a^2b^2}{r^4})C_1 cos(\theta) \qquad 3.28$$

$$\sigma_{r\theta} = \frac{\alpha E r}{2(a^2+b^2)}(1-\frac{b^2}{r^2})(1-\frac{a^2}{r^2})C_1 sin(\theta) \qquad 3.29$$

As stated above, the stresses in the z direction will depend on the end conditions imposed. Here, we will derive the stresses for three cases;

- Case 1 : Ends totally restrained, tube not allowed to bend,
- Case 2 : Ends unrestrained, tube not allowed to bend,
- Case 3 : Ends unrestrained, tube allowed to bend

The axial stress, σ_z, is found from Hooke's law;

$$\sigma_z = E(\epsilon_z - \epsilon_T) + \nu(\sigma_r + \sigma_\theta) \qquad 3.30$$

where ϵ_T is the thermal strain and σ_r and σ_θ are found from the above discussion. We write an expression for the thermal strain, ϵ_T, as consisting of two terms; representing the thermal strain due to the average temperature of the rod and an additional strain taking into account the variation of the local temperature with the average temperature. Specifically;

$$\epsilon_T = \epsilon_{T,avg} + \alpha(\overline{T})(T - \overline{T}) \qquad 3.31$$

where;

$$\epsilon_{T,avg} = \int_{T_{ref}}^{\overline{T}} \alpha(T)dT \qquad 3.32$$

An expression for ϵ_z is now required for cases where bending of the rod may be allowed.

Beam theory will be used to derive the required result for the stress and strain in the z direction. General discussions of the principles of beam theory can be found in reference [27]. The major assumption is that sections of a beam originally lying in a plane will remain plane.

Figure 3.3.1 shows a side view of the first wall "beam." The strain (including any bending), ϵ_z, is measured at the beam centerline as the difference between the average z strain, $\overline{\epsilon_z}$, and the bending strain, ϵ_{bz}. The bending strain is a function of the coordinate designated x which is measured from the beam centerline as illustrated in figure 3.3.2. The coordinate x ranges from $x = -\frac{t}{2}$ to $x = +\frac{t}{2}$ where the beam thickness t is given by $t = 2b$. The bending strain at $x = +\frac{t}{2}$ is denoted by ϵ'_{bz}. Thus, at a general location:

$$\epsilon_z = \overline{\epsilon_z} - \epsilon_{bz} \qquad 3.33$$

and from similar triangles (figure 3.3.1) we have;

$$\frac{\epsilon_{bz}}{\epsilon'_{bz}} = \frac{x}{t/2} = \frac{2x}{t} \qquad 3.34$$

and equation 3.31 becomes;

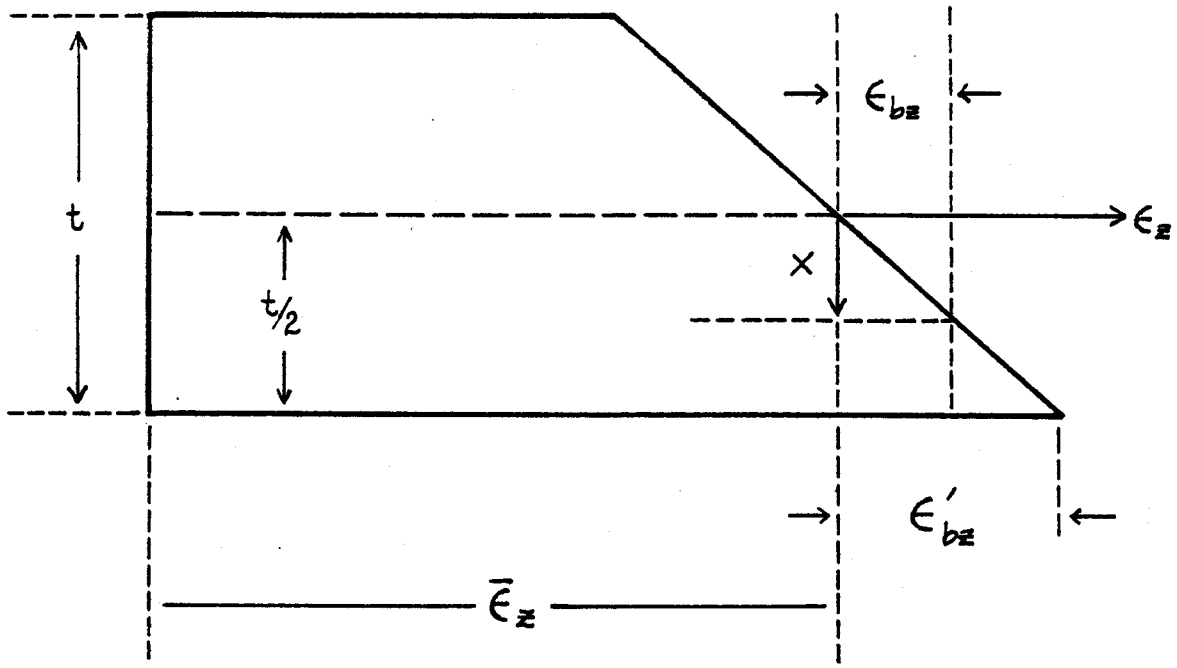

FIG. 3.3.1 Side View of First Wall Beam Representation for Bending Strain Definition

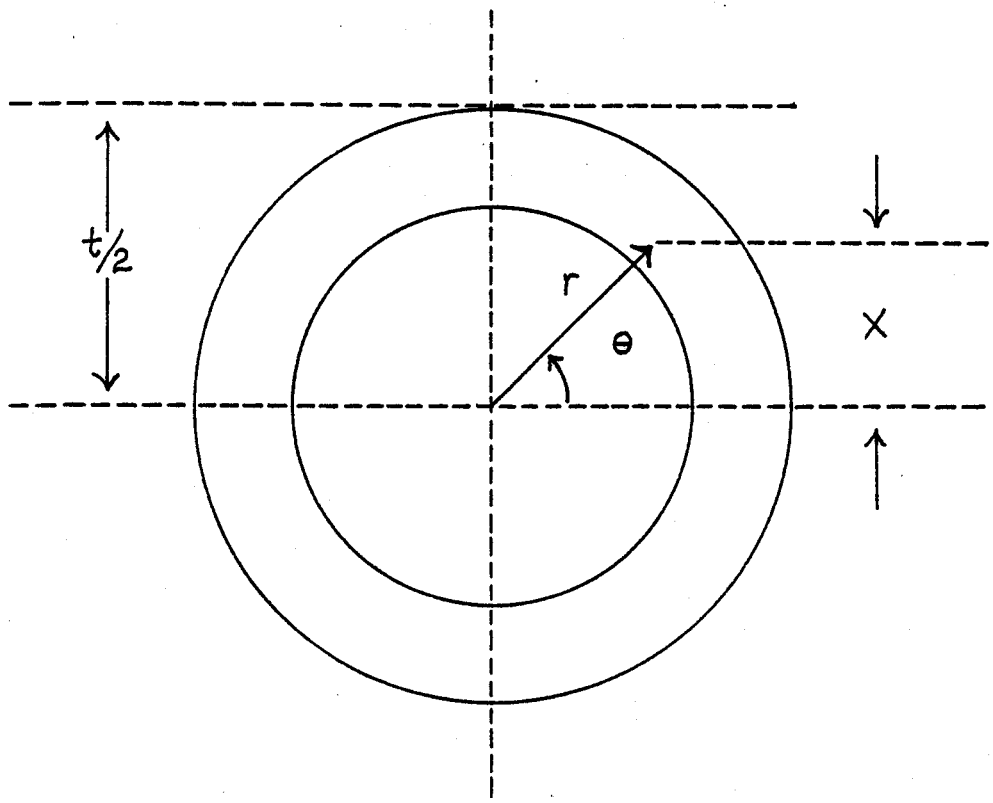

FIG. 3.3.2 Tube Cross-section showing x co-ordinate

$$\epsilon_z = \overline{\epsilon_z} - \epsilon'_{bz}(\frac{2x}{t}) \qquad 3.35$$

An expression for ϵ'_{bz} is found in terms of the radius of curvature, R_c, with the help of figure 3.3.3. Note that from similar triangles, the ratio of an increment in z, δz, to the radius of curvature is equal to the ratio of the corrosponding bending displacement to x. Thus, for ϵ'_{bz} $(x = \frac{t}{2})$,

$$\frac{\delta z}{R_c} = \frac{\epsilon'_{bz}\delta z}{t/2} \qquad 3.36$$

or;

$$\epsilon'_{bz} = \frac{t}{2R_c} \qquad 3.37$$

The radius of curvature is defined in terms of the displacement, w, with respect to the rod centerline as a result of bending:

$$R_c = -\frac{(1 + (\frac{\partial w}{\partial z})^2)^{\frac{3}{2}}}{\frac{\partial^2 w}{\partial z^2}} \qquad 3.38$$

Finally, for $\frac{\partial w}{\partial z} \ll 1$, we can combine 3.35, 3.37, and 3.38 to obtain for the z strain including bending;

$$\epsilon_z = \overline{\epsilon_z} - x\frac{\partial^2 w}{\partial z^2}. \qquad 3.39$$

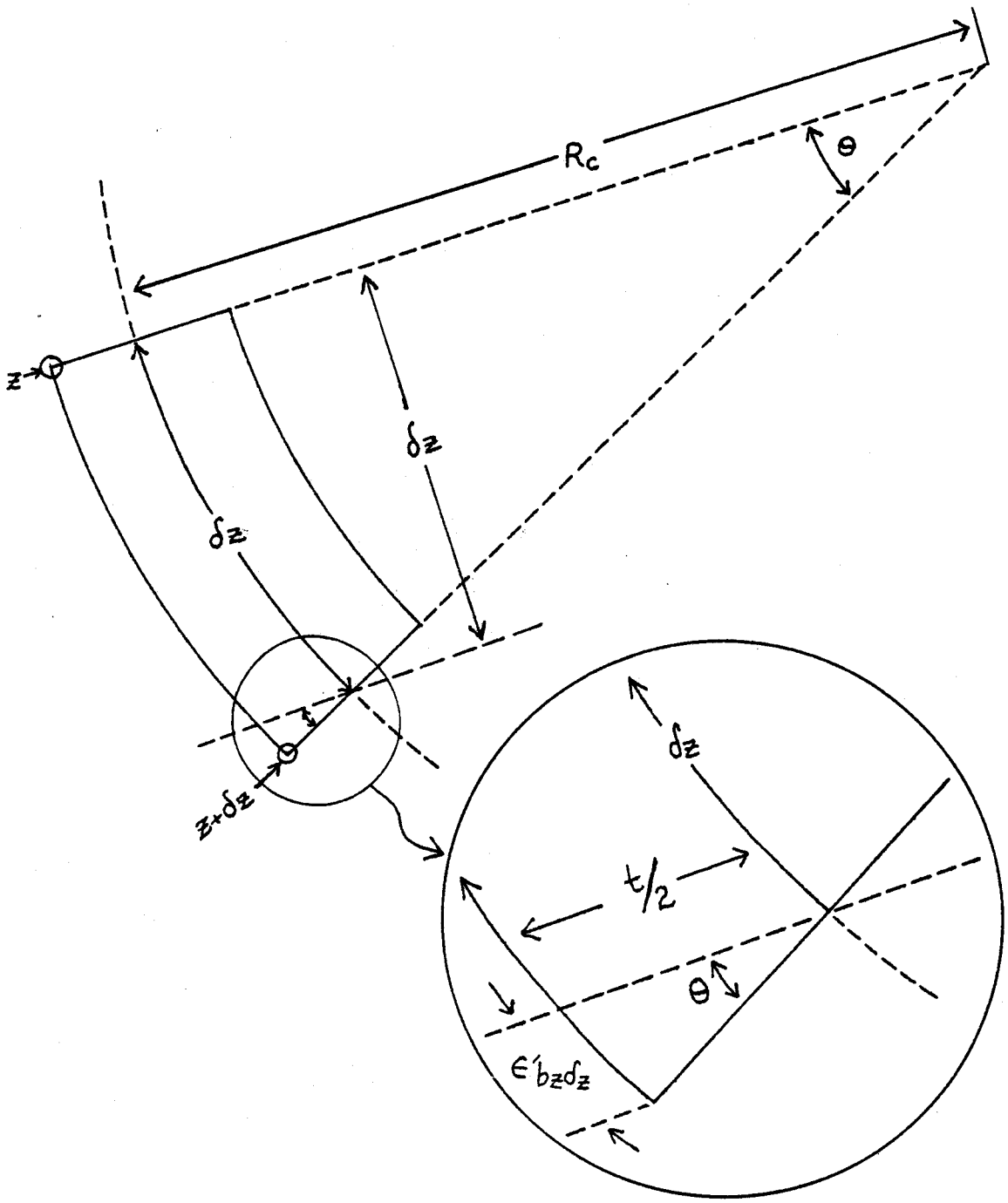

FIG. 3.3.3 Relation of Bending Strain to Radius of Curvature of Beam

Having obtained this expression for the axial strain, we return to equation 3.30 to obtain the z component of thermal stress for the three cases of interest.

Case 1, total axial restraint and no bending, is the easiest to apply and is obtained by setting $\epsilon_z = 0$. σ_z is then directly obtained as;

$$\sigma_z = \nu(\sigma_r + \sigma_\theta) - E\epsilon_T \qquad 3.40$$

In case 2, no axial restraints and no bending allowed, $\epsilon_z = \overline{\epsilon_z}$. The condition of no axial restraint is met by requiring

$$\int_A \sigma_z dA = 0 \qquad 3.41$$

where the integral is over the cross-sectional area, A, and $dA = rdrd\theta$. Equation 3.30 reduces for this case to;

$$\sigma_z = E(\overline{\epsilon_z} - \epsilon_T) + \nu(\sigma_r + \sigma_\theta) \qquad 3.42$$

Applying 3.41 to 3.42, we get an expression for $\overline{\epsilon_z}$ which can be substituted back into 3.42 to obtain σ_z. The integration and algebra is straight forward but lengthy. We include here only the results.

$$\overline{\epsilon_z} = \overline{\epsilon_T} - \frac{I}{\pi E(a^2 - b^2)} \qquad 3.43$$

$$\sigma_z = E(\overline{\epsilon_T} - \epsilon_T) + \nu(\sigma_r + \sigma_\theta) - \frac{I}{\pi(a^2 - b^2)} \qquad 3.44$$

where I is a complicated expression in terms of the rod geometry and heat loads resulting from multiple integrations over the rod temperature distribution;

$$I = \nu\pi\{(AA+B)(b^2-a^2)-(AA'+2B')(b^2 ln(\frac{b}{a})-\frac{(b^2-a^2)}{2})+\frac{AA'}{2b^2}(b^4-a^4)\} \qquad 3.45$$

where:

$$AA = \frac{q'''\alpha E b^2}{4k(1-\nu)}\left[\frac{2ln(\frac{b}{a})}{(1-\frac{a^2}{b^2})} - \frac{a^2}{2b^2} - \frac{3}{2}\right] \qquad 3.46$$

$$AA' = \frac{q'''\alpha E b^2}{4k(1-\nu)} \qquad 3.47$$

$$B = \frac{\alpha E T_o}{2(1-\nu)}\left[\frac{2b^2}{(b^2-a^2)} ln(\frac{b}{a}) - 1\right] \qquad 3.48$$

$$B' = \frac{\alpha E T_o}{2(1-\nu)} \qquad 3.49$$

and

$$T_o = \frac{bq''}{\pi k} \qquad 3.50$$

Finally, for case 3, no axial restraints and bending allowed, an additional restriction that the integrated moment over the tube cross section be zero is required;

$$\int_A \sigma_z x dA = 0 \tag{3.51}$$

Thus, with the following form for σ_z;

$$\sigma_z = E(\overline{\epsilon_z} - \epsilon_T - r\cos(\theta)\frac{\partial^2 w}{\partial z^2}) + \nu(\sigma_r + \sigma_\theta) \tag{3.52}$$

where $x = r\cos(\theta)$ has been substituted, equations 3.41 and 3.51 can be combined to solve for the unknowns σ_z and $\overline{\epsilon_z}$. The result for $\overline{\epsilon_z}$ is identical to 3.43, the result with no bending. σ_z is reduced relative to the no bending case by a bending factor as follows:

$$\sigma_z = E(\overline{\epsilon_T} - \epsilon_T) + \nu(\sigma_r + \sigma_\theta) - \frac{I}{\pi(a^2 - b^2)} - 2\nu C^{'} r\cos(\theta) \tag{3.53}$$

where

$$C^{'} = \frac{\alpha E C_1}{(a^2 - b^2)(1 - \nu)} \tag{3.54}$$

and C_1 is from equation 3.15. Note that this is no longer an exact solution to the equations of elasticity since it employs the "beam assumptions." For example. the transverse stresses caused by the bending are neglected.

Thus, using either equation 3.53, 3.44, or 3.40 (depending on the end condition) for the axial stresses and equations 3.27, 3.28 and 3.29 for the radial and theta stresses, we have the complete two dimensional thermal stress solution for the first wall.

Figure 3.4 is a plot of the thermal stresses at b versus theta for $q'' = 0.5\ MW/m^2$, $T_b = 320C$, $a = 5$ mm, and $b = 7$ mm. σ_r is small compared to σ_θ and σ_z. σ_z with no bending allowed is significantly larger than the bending allowed case. Note that calculations for first wall tubes with completely restrained ends (not shown here) indicate that the resulting axial stresses are unacceptably large (typically, factors of ≈ 3 higher than all others.) Each of these stresses can be plotted in the same format as figure 3.2 for all radii and theta as shown in figure 3.5 for σ_z, no bending allowed.

Also of interest is the amount of deflection experienced by the tube when it is completely free to bend. The deflection can be calculated by integrating $\frac{\partial^2 w}{\partial z^2}$ with respect to z. Using hinge supports at z = 0, L and assuming that the loads are uniform in z, the maximum deflection is:

$$w = \frac{\partial^2 w}{\partial z^2}\left(\frac{L^2}{8}\right) \qquad 3.55$$

The parameter $\frac{\partial^2 w}{\partial z^2}$ has already been obtained as part of the derivation of equation 3.50. The result is:

$$\frac{\partial^2 w}{\partial z^2} = \frac{2\nu C}{E} + \alpha(\bar{T})\left(\frac{2C_1}{a^2 + b^2} + D_1\right) \qquad 3.56$$

Using typical first-wall conditions, the deflection is found to be approximately 50 –

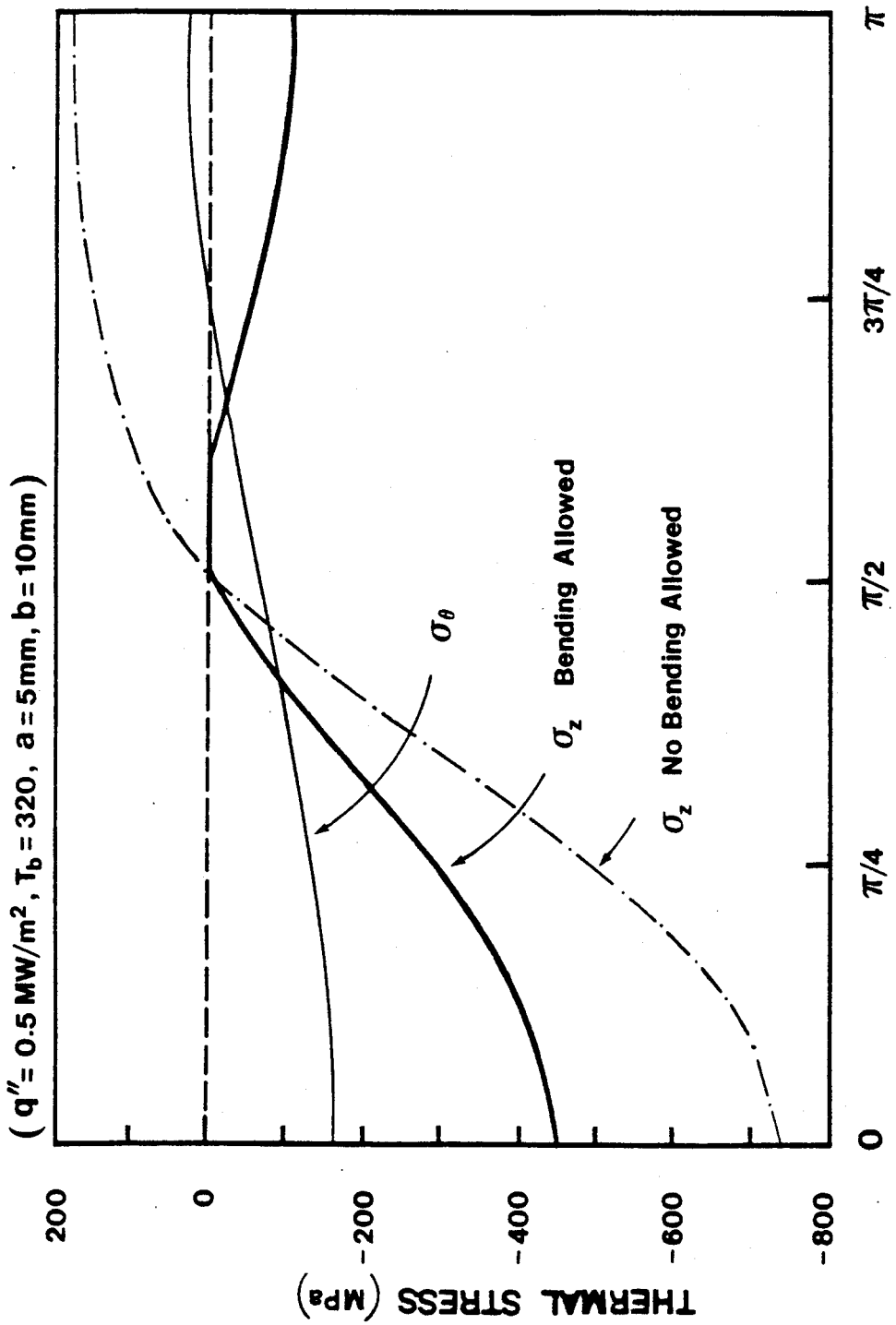

FIG. 3.4 Thermal Stresses versus Theta at Tube Outer Surface

FIG. 3.5 Axial Thermal Stress (Bending Allowed)
Contours in Stainless Steel at First Wall Tube

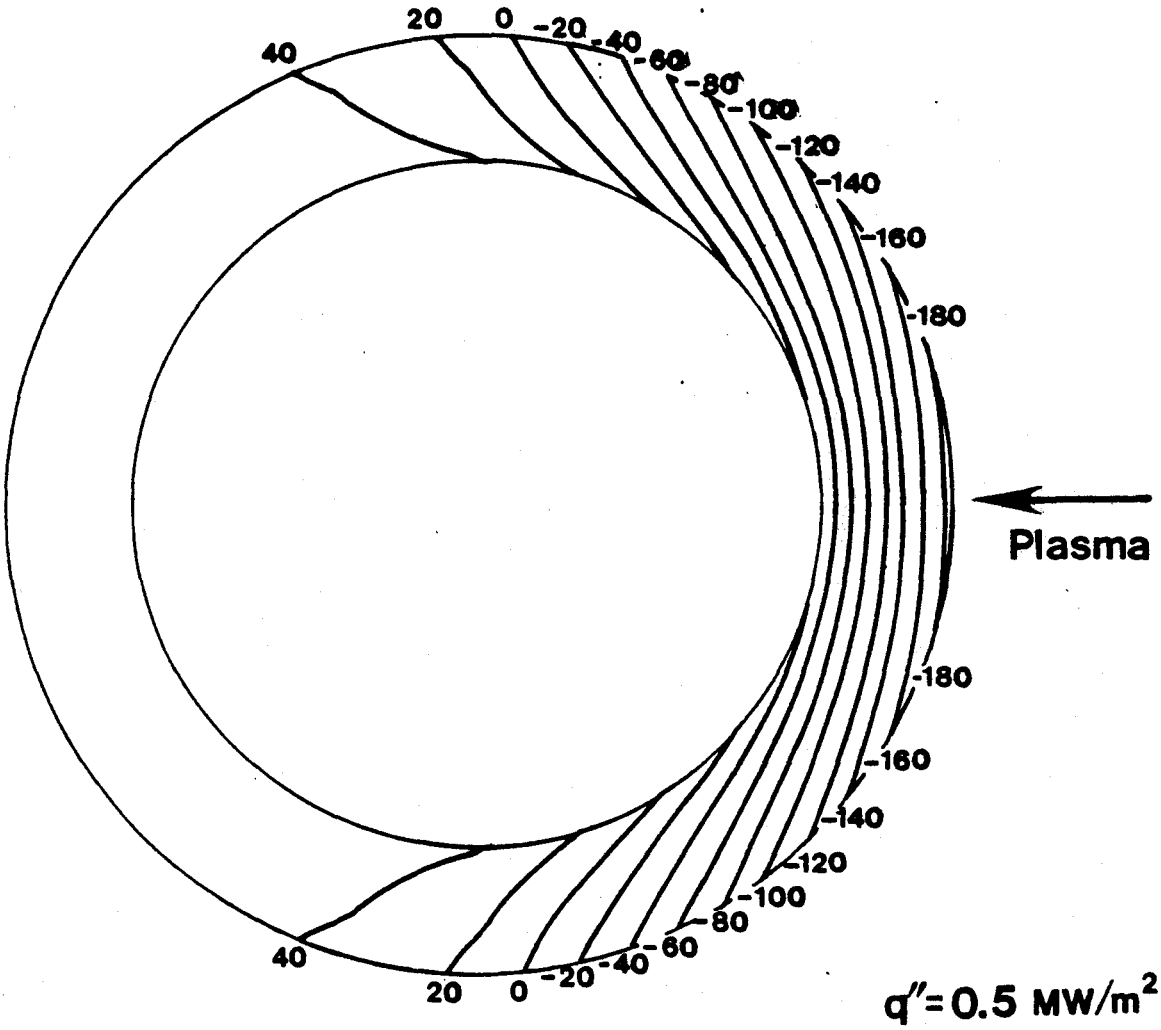

$q'' = 0.5$ MW/m^2
$T_b = 320°C$
a = 5mm
b = 7mm

100 mm. This amount of deflection is probably unacceptable since sections of the first wall tube may no longer have the protection of the scrape-off region created by the protrusion of the limiter. The result could be greatly increased erosion of the first wall tube leading to early failure. Thus, the axial stresses with no bending allowed, although higher compared to the bending allowed case, are probably more realistic. Therefore, the tube will have to be prevented from excessive bending by appropriate structural arrangement and σ_z, no bending allowed, will be the reference axial stress for the work that follows.

3.5 Fluid Heat Transfer

In order to base the analysis on a fixed bulk fluid temperature, a heat transfer coefficient for the fluid is needed. A relatively simple analysis is used here based on an energy balance for single phase and subcooled boiling heat transfer for water. Heat transfer with lithium is discussed below.

The subcooled boiling region is advantageous for high heat flux applications since good heat transfer is obtained while the surface temperature remains approximately constant. If a transition to two phase flow occurs, the heat transfer would be underestimated with the analysis to follow. A more detailed discussion of the heat transfer and pressure drop characteristics expected under typical first wall conditions can be found in reference [5].

The heat transfer coefficient, h, for turbulent, forced convection flow of water in tubes can be found with the correlation of McAdams [28]:

$$H = 0.023\left(\frac{k_f}{D}\right)\left(\frac{GD}{\mu_f}\right)^{0.8}\left(\frac{\mu_f c_{pf}}{k_f}\right)^{0.4}\left(\frac{\mu_f}{\mu_w}\right)^{0.14} \qquad 3.57$$

where G is the mass flux, D is the diameter, and μ_f, k_f, and c_{pf} are the fluid properties of viscosity, thermal conductivity, and heat capacity, respectively. μ_w is the viscosity evaluated at the wall temperature and all units are MKS.

The mass flux can be found using an energy balance on the coolant tube:

$$G = \frac{Q}{\pi a^2 c_p \Delta T_{rise}}; \qquad 3.58$$

where the energy deposited in the coolant is;

$$Q = \pi L\left[q'''(b^2 - a^2) + 2q''(a + h)\right]. \qquad 3.59$$

and ΔT_{rise} is the coolant temperature rise along the length of the tube.

The heat transfer coefficient for liquid sodium is taken from the Lyon - Martinelli [29] correlation for liquid metals under constant heat flux:

$$Nu = 7 + 0.025 Pe^{0.8} \qquad 3.60$$

where Pe is the Peclet number $\frac{Dv\rho c_p}{k}$ and Nu is the Nusselt number, $\frac{HD}{k}$. The velocity of the coolant is represented by v.

3.6 Summary

Procedures for calculating thermal and pressure stresses in a tubular first wall

geometry have been presented. The analysis includes the use of a thin shell treatment for one dimensional calculations and two dimensional calculations using the plane strain assumption. Asymmetric heat deposition and internal heat generation have been included in the two dimensional treatment.

Now the stress analysis can be used for calculating stresses and strains under typical first wall conditions for application to a fatigue analysis. Thus, all of the tools have been developed necessary for the generation of the design windows that follow.

4. DESIGN WINDOWS

4.1 Introduction

Although the intent of the present work is to examine each of the major engineering limits for a Tokamak first wall design and determine their relative importance, the emphasis has been placed on the thermal fatigue aspects of a pulsed design. This is due to the perceived importance of this issue in the fusion commumity. Severe lifetime limitations due to cyclic thermal fatigue could be a major liability to the Tokamak concept, especially without proof of principle for current drive in commercial size applications.

Section 4.2 combines the results of chapters two and three and presents tradeoffs of thermal fatigue versus the important geometric and thermal variables for a tubular first wall. Calculational procedure for thermal fatigue evaluations using a computer code developed for the purpose is given followed by a discussion on how to include some of the other important design limits in the presentation of the thermal fatigue results.

Design windows are obtained for two materials, Titanium modified 316 Stainless Steel and a Vanadium alloy. Insight is gained into the parameters and/or phenomena which will limit the first wall design.

Section 4.3 will be concerned with an entirely separate approach to developing design windows based on Bree diagrams. A large number of design limitations can be included in these diagrams in the context of the heat deposition, geometry, and lifetime of a tubular first wall.

4.2 Fatigue Calculations

A listing of the computer code ULTR used for the fatigue calculations is given in appendix C. Here, we summarize the fatigue evaluation by outlining the calculational procedure of the code, drawing on the content of chapters two and three.

The major input parameters required are;

- Inner radius of the first wall tube,
- A range of outer radii (code plots vs wall thickness),
- Bulk fluid temperature (choice of coolant),
- Surface heat deposition from plasma,
- Desired lifetime,
- Material (Steel and Vanadium presently available).

The heat transfer coefficient is calculated first using the heat balance as presented in 3.5. The calculation is made on the basis of a fixed coolant velocity or a fixed temperature rise over the length of the first wall channel (input choice).

The properties necessary for the stress calculations will be evaluated at the average temperature in the tube. Since the properties are temperature dependent, the code iterates between temperature and the property relations provided in the code (these are summarized in appendix A.)

Heat deposition, not neutron wall loading, is used to characterize the heat addition to the first wall. As a point of reference, we note that for a Deuterium - Tritium

fuel cycle, the neutron wall loading is roughly a factor of four higher than the heat deposition. However, this equvalency does not apply in general because the distribution of the surface load (alpha particles, etc.) is not necessarily the same as the neutron wall loading.

Using the results of chapter three, the temperature and stress distributions can now be calculated followed by the strain ranges and displacements. Each of these calculations is done for the three separate boundary conditions in the two dimensional plane strain solution and for the thin shell case.

Now, by entering the equivalent strain ranges into the fatigue design curves from the ASME code case N-47, an allowable number of cycles is obtained for each case and for each tube wall thickness. The design curves are temperature dependent and the peak temperature is used for entering the curves as recommended in the code case.

Thus, combined with the desired lifetime, a plot of thermal fatigue limited pulse length versus tube wall thickness is generated (recall section 2.4.) The fatigue design curves are incorporated into the code using a least squares fit.

We have chosen to plot the allowable pulse length for fatigue versus the wall thickness because the temperature gradient through the wall, which drives the fatigue, is a function of this thickness. In this way, the plot represents a range of allowable wall thicknesses for a given material, coolant, heat load, and inner radius.

Figure 4.1 is a fatigue curve comparing the different stress representations for 316 Stainless Steel, inner radius of 5 mm, bulk fluid temperature of $320C$, lifetime of 8 full power years, and heat deposition of $0.5MW/m^2$ (neutron wall loading of $2.0MW/m^2$). The vertical axis is the logarithm of pulse length in hours and the

FIG. 4.1 Fatigue Curves for Stainless Steel with Different Stress Representations

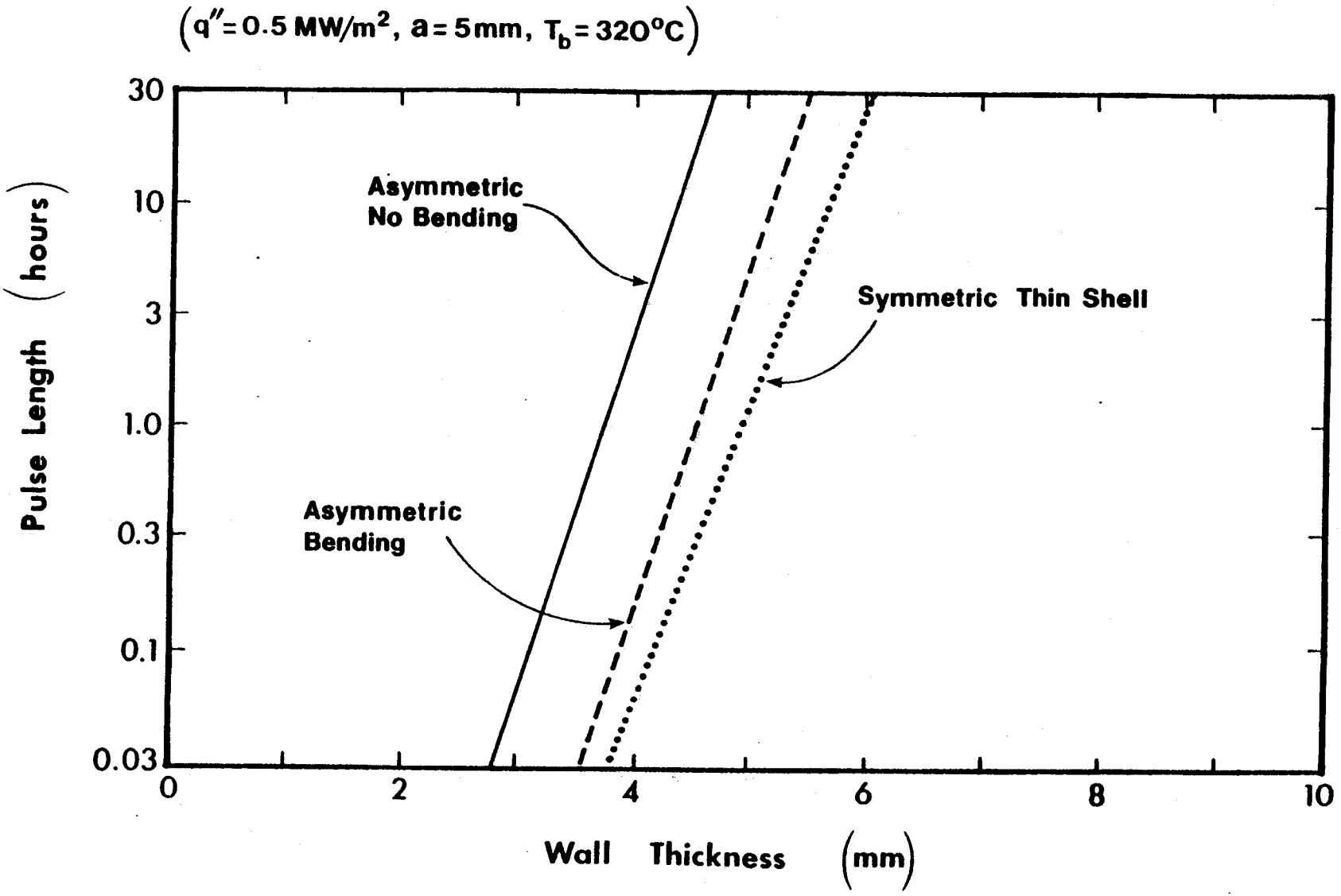

thickness on the horizontal axis is in mm.

The fatigue curve for asymmetric heat deposition, no tube bending allowed is the most conservative (and most realistic) model while the thin shell treatment is the least conservative. Note also that after $\frac{1}{2}$ to 2 hours, there is little gain in increasing the pulse length for fatigue. This suggests a smaller version of ULTR which would be less costly but still retain the same benefits in terms of first wall fatigue. Parameters for ULTR with a burn pulse of four hours is shown in table 4.1. Note that the major radius has been reduced from 9.7 m to 7.6 m.

However, fatigue is not the only phenomena limiting the wall thickness. As the wall is made thinner, there is a smaller ΔT across the wall and the fatigue improves, but there will eventually be a point where the tube can no longer safely contain its internal pressure.

Also, as the wall thickness increases, the peak temperature in the material increases (for a fixed bulk coolant temperature) and a limitation is reached due to excessive swelling and/or embrittlement. Therefore, it is convenient to create a design window with which the thickness is limited on the lower end by requirements of primary strength and on the upper end by irradiation effects and allowable pulse length for fatigue.

The minimum thickness required for containment of the coolant pressure is found by rearranging equation 3.4 for the primary stress in a thin shell;

$$h_{min} = \frac{pr}{S_{mt}},$$

where we have replaced the primary stress σ_p with the maximum allowable stress

Table 4.1

ULTR with Four Hour Pulse Length

Major Radius (m)	7.6
Minor Radius (m)	1.8
Plasma Elongation	1.5
Toroidal Beta	0.043
Magnetic Field on Axis (T)	6.2
Average Neutron Wall Loading (MW/m^2)	3.0
Fusion Power (MW)	3000
Superconductor	Nb_3Sn
Pulse Length(hours)	4

intensity, S_{mt}.

For simplicity, we limit the discussion of maximum thickness due to peak metal temperature to swelling effects. More data is available for swelling and the limits for swelling and embrittlement are generally quite similar for the cases of interest here.

Recall from section 2.5.2 that presently available swelling data for fluences to 60 dpa limit the peak temperature of PCA to less than $650C$. Since 60 dpa, or approximately $5MW \cdot yr/m^2$, is far below the fluence level expected in the first wall, a peak temperature limit based on available data of $500C$ is chosen conservatively for the stainless steel first wall. This is consistent with the approach of similar studies [6].

An alternative approach for expressing the swelling limit can be made using the swelling extrapolations introduced in section 2.5.2. Using these extrapolations, the variation of swelling with fluence can be estimated. Referring back to figure 2.6, the swelling remains at acceptable levels (less than 5 percent) until shortly after breakaway swelling occurs at 100 dpa (up to 120 dpa). This is applicable for peak metal temperature less than $550C$.

Since the fatigue curves at present are at fixed fluence (lifetime times wall loading), the extrapolated swelling approach is utilized by observing a peak temperature limit of $550C$ and ensuring that the product of neutron wall loading and wall lifetime does not exceed approximately $10 - 12MW \cdot yr/m^2$.

Presently available data for Vanadium with fluences to 35 dpa indicate no significant swelling. However, the extrapolated swelling curve indicates breakaway swelling above 175 dpa with the 5 percent limit reached above approximately 225 dpa. Thus, the product of lifetime and wall loading should not exceed $20-24MW \cdot$

yr/m^2 for satisfaction of the swelling limit.

No temperature limit is indicated for vanadium due to swelling. Turning to embrittlement data, a temperature limit from the available data of $900C$ is indicated as shown in chapter two. However, some studies [17] recommend a limit of $\frac{1}{2}T_m$ for materials with so little data available. This results in a limit of $750C$ with a margin of $50C$.

Figure 4.2 shows a comparison of fatigue curves for three different values of heat deposition with the primary stress and swelling/embrittlement limits included. The top chart is the same case as figure 4.1 with just the asymmetric, no bending allowed case shown. The minimum thickness due to primary stress is represented by the dotted line and the swelling/embrittlement limit for maximum thickness as the dashed segment.

Since one must operate to the left of the fatigue curve, the shaded sections of the chart are excluded from allowable design. Note that first wall thickness is an appropriate variable not only because it drives the peak temperature and fatigue limits but also because the design window clearly indicates tha amount of extra space, if any, that is available for a wall erosion allowance.

The second and third charts in figure 4.2 provide a comparison of the various limits for increased heat depositions of 1.0 and $1.5MW/m^2$, respectively. Note that fatigue becomes markedly more restrictive with increasing heat deposition as expected. At $1.0MW/m^2$, there still remains some space for design which all but disappears at $1.5MW/m^2$. The swelling/embrittlement limit (generated from available data) also moves in rapidly since the peak temperature is rising. However, this limit does not become more restrictive than fatigue.

It is important to note here that if the extrapolated swelling curves were invoked

FIG. 4.2 Fatigue Design Windows for Heat Deposition Comparison

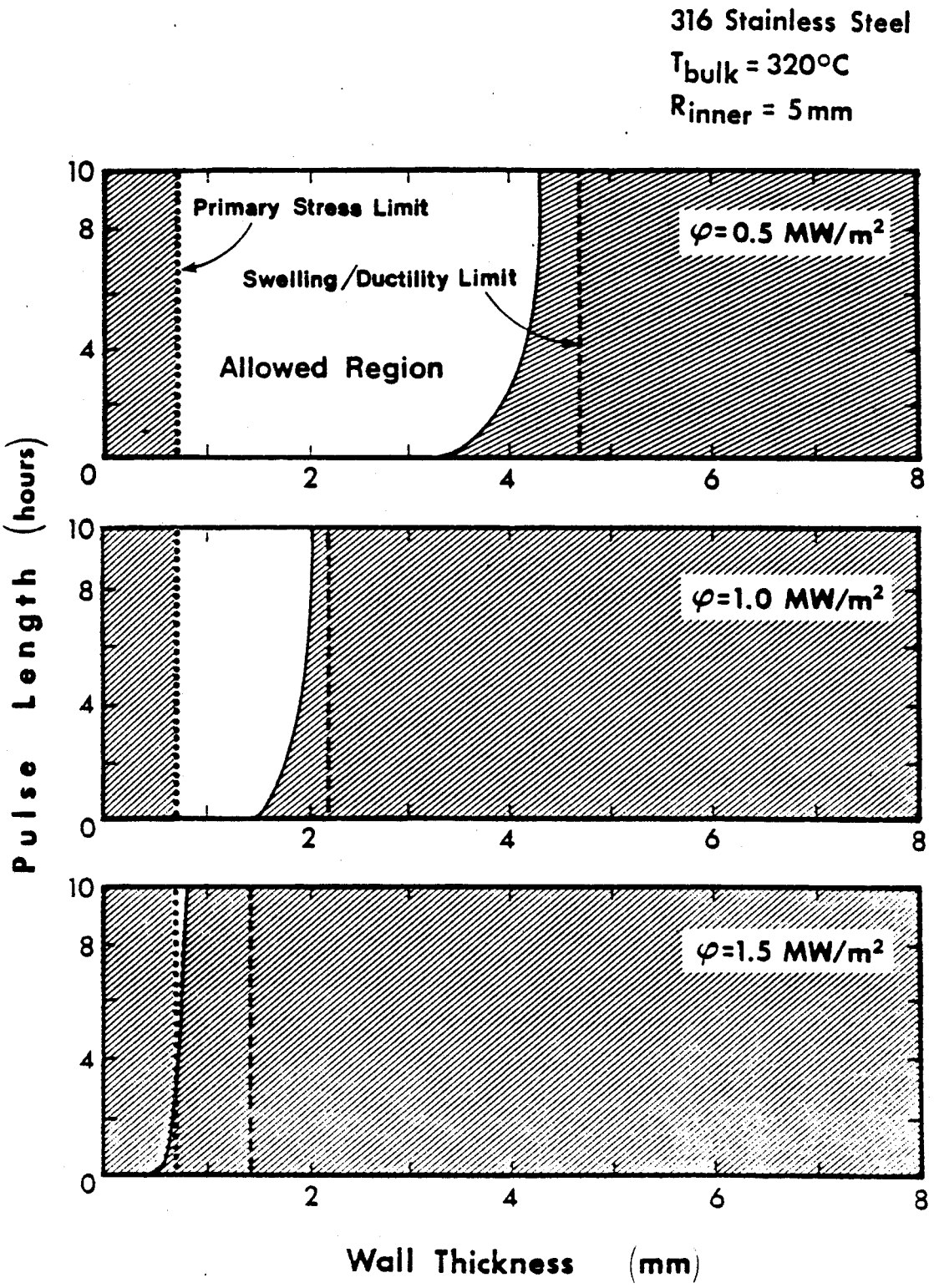

as the swelling limit in figure 4.2, these charts would not be allowable for any wall thicknesses. The first chart corresponds to a fluence of $16MW \cdot yr/m^2$ which exceeds the allowable from swelling according to the extrapolated curves. This failure is due partly to the relatively large lifetime selected as reference (8 full power years.)

As an illustration of the use of the fluence limit from swelling, we choose the case of the first chart in figure 4.2 ($q'' = 0.5MW/m^2$). Figure 4.3 shows this case for several different values of wall lifetime accomplished by scaling down the pulse length axis. Obviously, the fluence limit from swelling is reached at a 6 year lifetime. There is also an advantage for allowable fatigue pulse lengths with the shorter lifetimes. Note that the peak temperature limit from swelling still applies since temperatures above $550C$ are not allowed at any fluence.

The primary stress limit does not have a large impact in the heat deposition comparison but a separate examination of increases in the inner radius is shown in figure 4.4. Note for inner radii of $15 - 20$ mm or more, primary stresses exceed allowable for stainless steel.

A similar fatigue analysis for Vanadium is shown in figure 4.5. Here, fatigue curves for both 0.5 and $2.0MW/m^2$ are shown. Lithium coolant at a bulk fluid temperature of 550 C is used. Only the case of asymmetric heat deposition with no bending allowed is shown for $0.5MW/m^2$. Note, as expected from its superior thermo-physical properties, Vanadium is significantly more resistant to fatigue than Stainless Steel. The allowable thickness is on the order of twice that of Stainless Steel and even for a heat deposition of $2.0MW/m^2$, there is still significant design space. (Due to its high strength, the primary stress limit is less than 0.5 mm.) Note also the rather significant difference between the asymmetric, no bending allowed fatigue curve and the thin shell result.

FIG. 4.3 Fatigue Design Windows for Lifetime Comparison

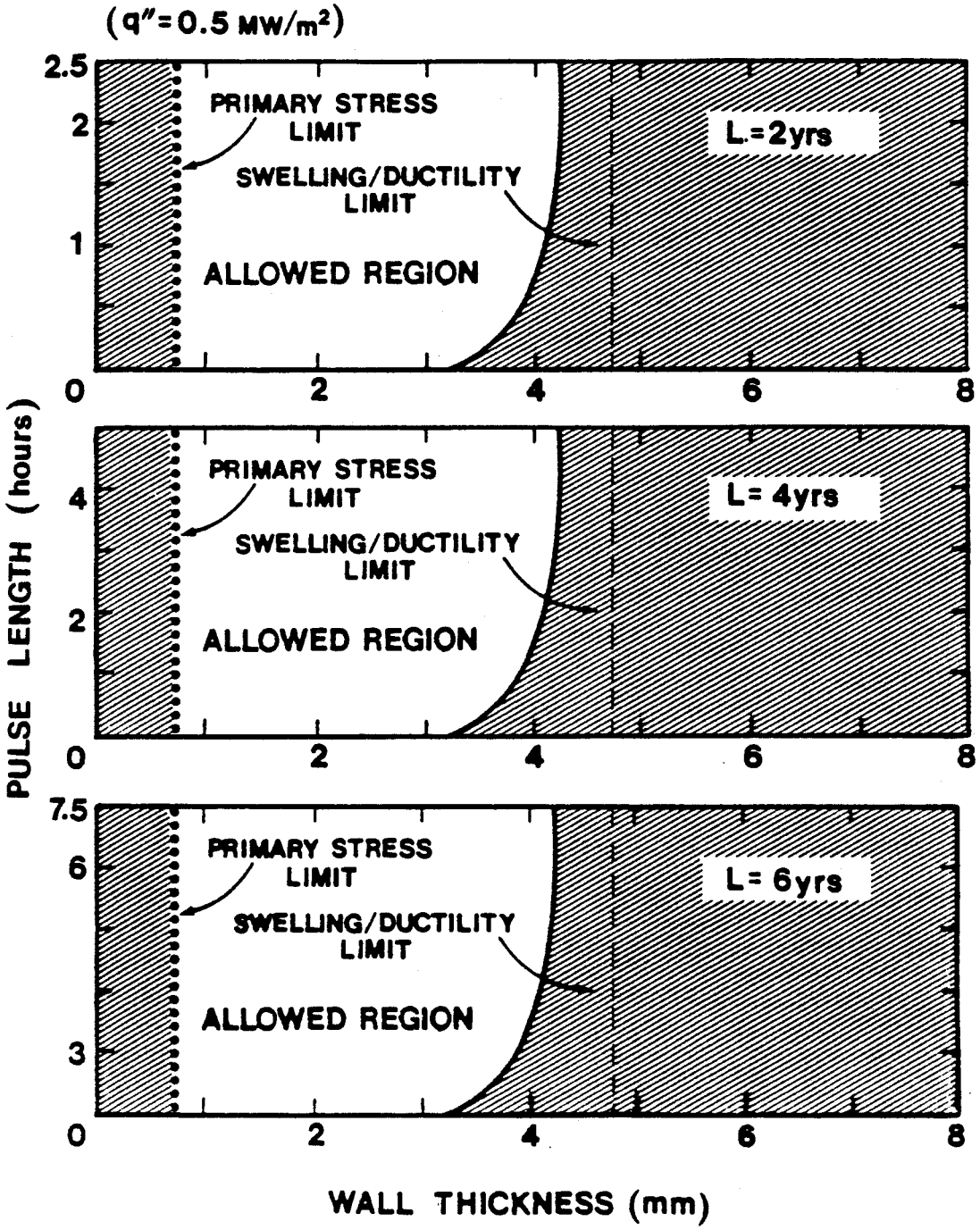

FIG. 4.4 Fatigue Design Window for Inner Radius Comparison

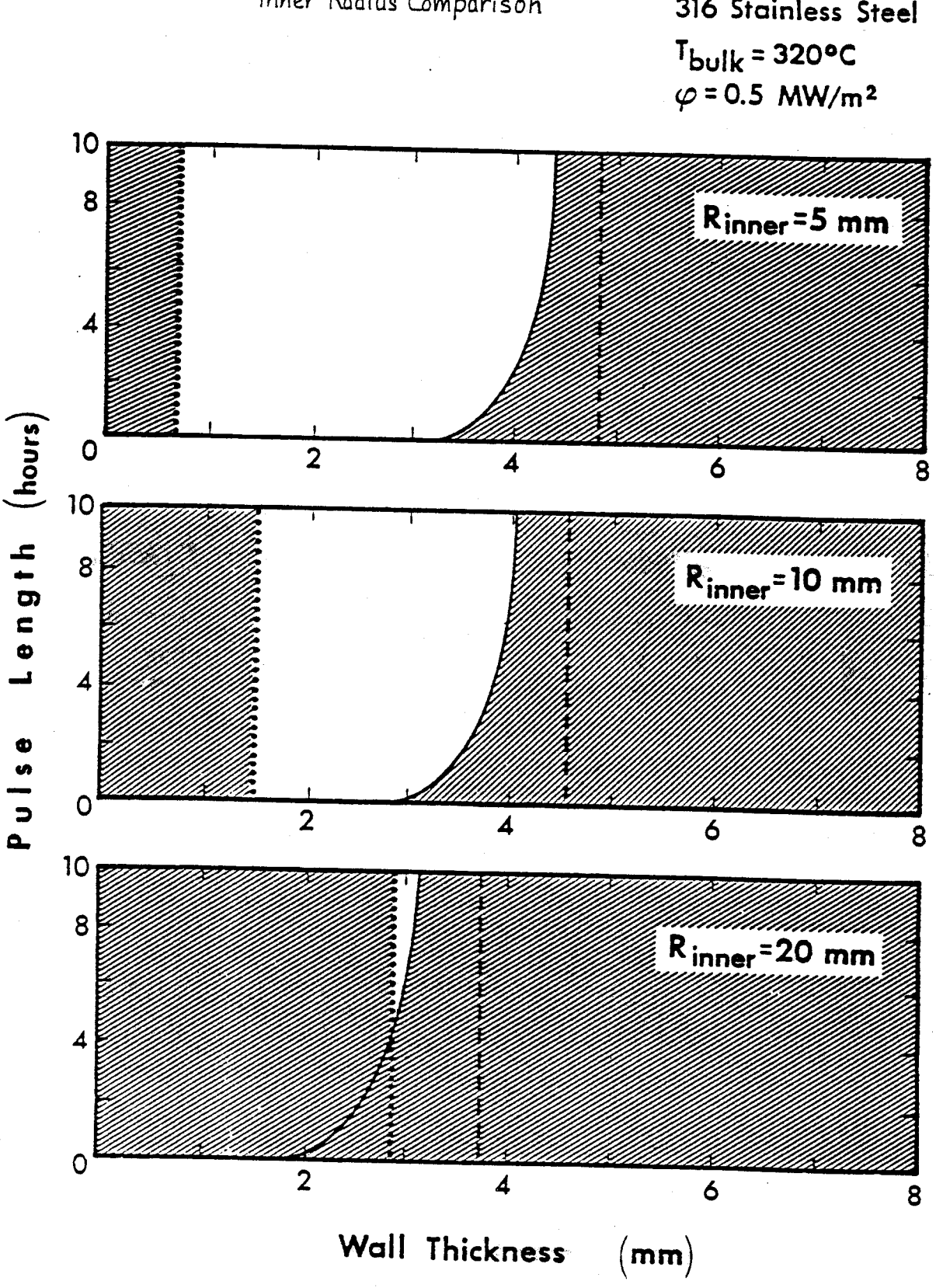

FIG. 4.5 Fatigue Curves for Vanadium

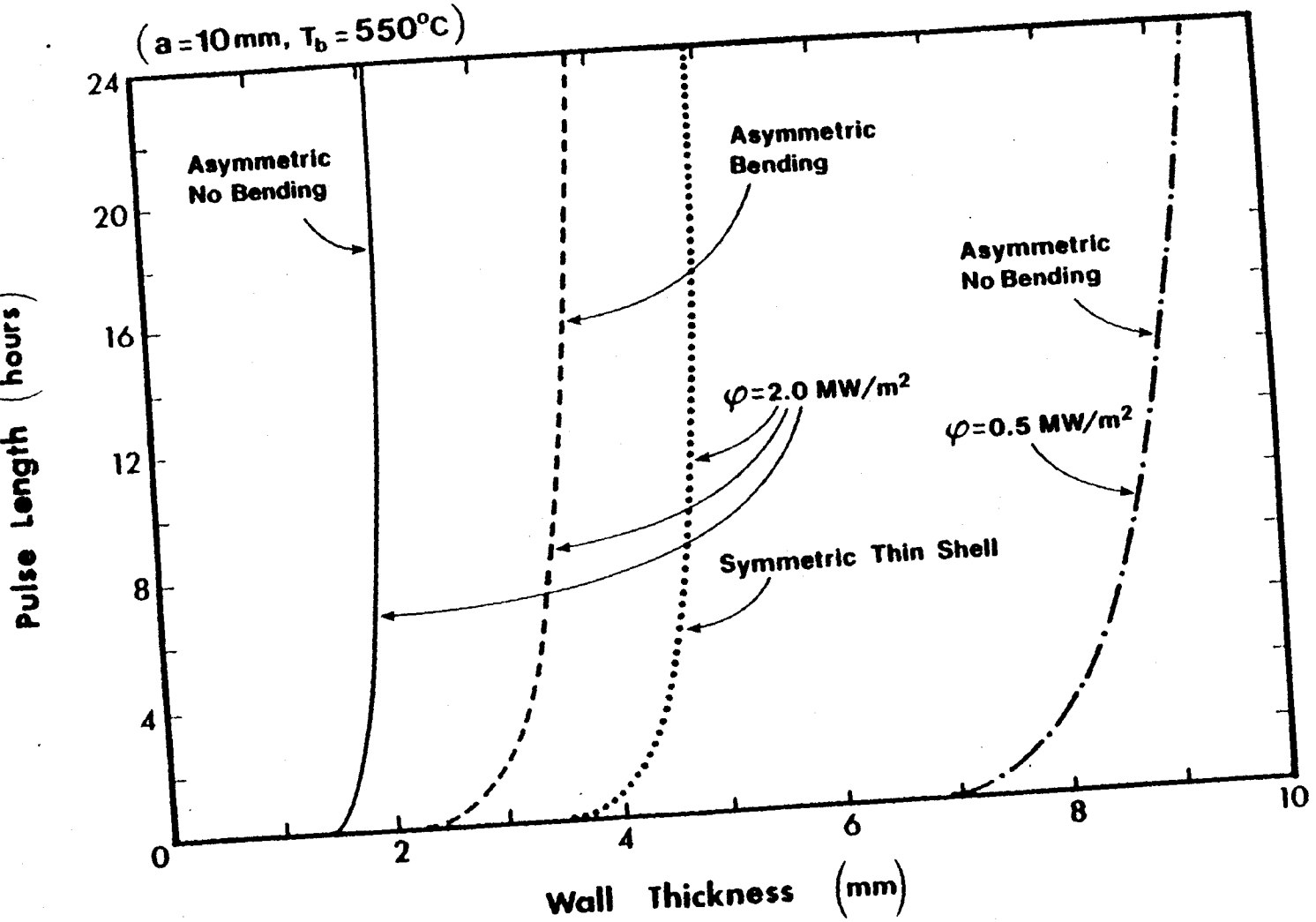

In summary, short pulse lengths ($\geq$ 100 s) can be tolerated in Tokamak operation based on the analysis outlined above. For Stainless Steel this is true for heat depositions up to $1MW/m^2$ while Vanadium can tolerate heat depositions as high as $2MW/m^2$. Long pulse operation can be used to modestly increase the allowable heat deposition or increase the useful wall thickness by 1 to 2 mm. Also, a two dimensional stress treatment with axisymmetric heat deposition can be significantly more conservative than a simple thin shell, symmetric heat deposition model.

Another interesting observation can be made by comparing fatigue and swelling using the extrapolated swelling curves as discussed above. Comparing the results of figure 4.2 for fatigue and figure 2.6 for swelling, it is apparent that even for relatively short pulse lengths, swelling is significantly more limiting than fatigue in terms of fluence. Stainless Steel is restricted to less than $12MW \cdot yr/m^2$ due to swelling but the fatigue limit is well above $24MW \cdot yr/m^2$ for pulse lengths of a few minutes or more.

4.3 Modified Bree Diagrams

A different set of design windows for use in first wall design can be derived using the Bree diagram approach. Two modifications to the Bree diagram are introduced now which combine many of the first wall design limits descussed in chapter two with the ratcheting information provided by the Bree diagram. A computer code MODBREE has been written in MACSYMA to calculate and plot these diagrams. A listing of the code is provided in appendix D.

In chapter two, the concept of the Bree diagram was introduced. This diagram is used to represent acceptable combinations of primary and secondary stresses in a material. The secondary - primary stress plane is divided into regions of elastic, shakedown, plastic, and ratchetting behavior with boundaries defined as [8]:

$$\sigma_p + \sigma_t = \sigma_y \qquad E - S \qquad 4.1$$

$$\sigma_p + \frac{\sigma_t}{4} = \sigma_y \qquad S - R \qquad 4.2$$

$$\sigma_t(\sigma_y - \sigma_p) = {\sigma_y}^2 \qquad S_1 - S_2 \qquad 4.3$$

$$\sigma_t = 2\sigma_y \qquad S - P \qquad 4.4$$

$$\sigma_p \sigma_t = {\sigma_y}^2 \qquad P - R \qquad 4.5$$

where equations 4.1 - 4.5 are, respectively, the boundaries between the elastic and shakedown (E - R), shakedown and ratchetting (S - R), subdivisions of the shakedown and ratchetting regions ($S_1 - S_2$), shakedown and plastic (S - P), and plastic and ratcheting (P - R) regions. The distinction between shakedown at high and low primary stress, regions S_1 and S_2, and ratchetting at high and low primary stress, regions R_1 and R_2, is made by equation 4.3. This distinction is only significant here for definition of the effective creep stress and will not be retained in the modified versions of the Bree diagram.

4.3.1 Mod1 Bree Diagram

The Bree diagram can be modified for use in first wall design by translating the axis of the diagram with parameters more readily dealt with from an engineering

standpoint for first wall investigations. This Mod1 Bree diagram takes advantage of the simple relations between heat flux and geometry and the stresses in a thin shell representation. By holding the product of coolant pressure and tube mean radius constant, a plot of heat flux versus first wall thickness is generated for a fixed design lifetime. All properties are evaluated at a single temperature which is chosen to be the hot side (peak) temperature in the tube. As an example, the elastic - shakedown stress boundary can be derived as follows:

$$\sigma_p + \sigma_t = \sigma_y \tag{4.1}$$

$$\frac{pR}{h} + \frac{\alpha E \Delta T}{2(1-\nu)} = \sigma_y \tag{4.6}$$

$$\frac{pR}{h} + \frac{\alpha E q'' h}{2k(1-\nu)} = \sigma_y \tag{4.7}$$

$$q'' = \frac{\sigma_y h - pR}{C_f h^2} \tag{4.8}$$

where:

$$C_f = \frac{\alpha E}{2k(1-\nu)} \tag{4.9}$$

and we have used the thin shell approximation for the pressure and thermal stresses as shown in chapter two.

Plotting equation 4.8 for heat flux, q'', versus first wall thickness, h, defines the elastic-shakedown region in this plane. Similarly, relations can be derived for each of the remaining boundaries;

$$q'' = \frac{{\sigma_y}^2}{C_f(\sigma_y h - pR)} \qquad S - R \qquad 4.10$$

$$q'' = \frac{2\sigma_y}{C_f h} \qquad S - P \qquad 4.11$$

$$q'' = \frac{{\sigma_y}^2}{C_f pR} \qquad P - R \qquad 4.12$$

where we have omitted the subdivisions within the shakedown and ratchetting regions.

Figure 4.6 is an illustration of the Mod1 Bree diagram for 316 Stainless Steel with hot side temperature $T_h = 540C$ and $pR = 0.25Mpa - m$. Ratchetting occurs at thin wall thicknesses and high heat fluxes. Recall that ratchetting is forbidden in design since it may lead to progressive deformation of the structure. Note also the relatively small region within which the material behaves elastically.

The design window that the ratchetting boundary represents can be further refined by imposing additional limits on this first wall representation. The work of O'Donnell and Porowski introduced in chapter two can be used to include creep effects in ratchetting. The effective creep stress is defined as;

$$\sigma_c = \sigma_t + \sigma_y - 2\sqrt{(\sigma_y - \sigma_p)\sigma_t} \qquad Region\ S_1 \qquad 4.13$$

FIG. 4.6 Mod 1 Bree Diagram for Stainless Steel
T_h = 500C, pR = 0.25 MPa-m

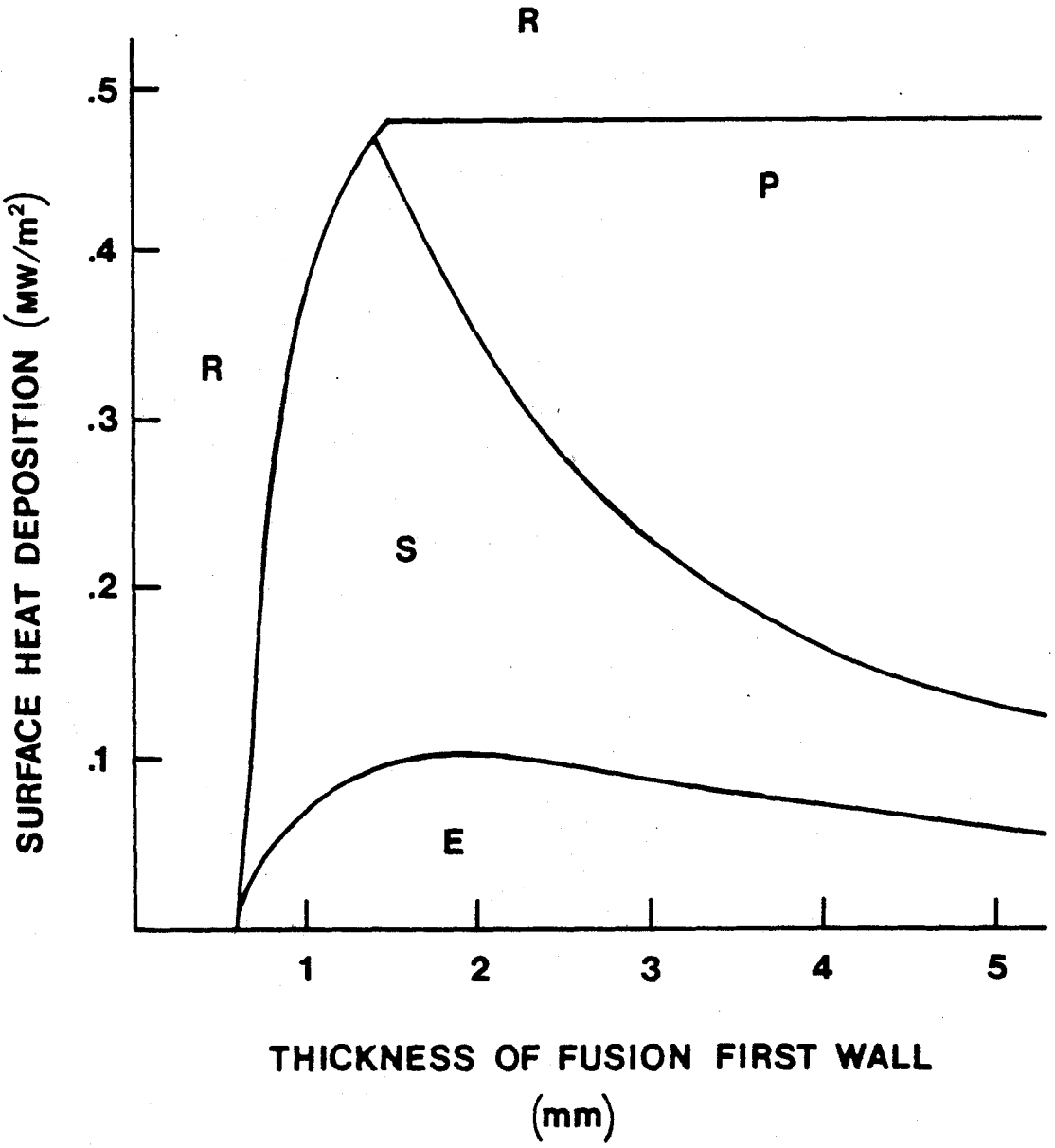

$$\sigma_c = \frac{\sigma_p \sigma_t}{\sigma_y} \qquad Regions\ S_2, P \qquad 4.14$$

in the indicated regions of the Bree diagram. When translated to the q'', h plane, these become;

$$q'' = \frac{1}{C_f h^2}[\sqrt{\sigma_y h - pR} + \sqrt{\sigma_c h - pR}]^2 \qquad Region\ S_1 \qquad 4.15$$

$$q'' = \frac{\sigma_c \sigma_y}{C_f pR}. \qquad Regions\ S_2, P \qquad 4.16$$

Entering equations 4.15 and 4.16 with the effective creep stress corrosponding to a one percent strain limit obtained from an isochronous stress-strain curve, the creep ratchetting limit can be added to the Mod1 Bree diagram.

A thin shell fatigue limit can be included in the diagram using;

$$\sigma_t = C_f q'' h = E\epsilon_t \qquad 4.17$$

or;

$$q'' = \frac{E\epsilon_t}{C_f h} \qquad 4.18$$

where ϵ_t is found from a fatigue design curve for a fixed number of burn cycles in

the first wall lifetime. Thus, equation 4.18 represents a restriction on the combination of q'' and h due to thermal fatigue.

Similarly, creep fatigue damage can be represented using equations 2.7, 2.8, and 2.9 to include creep effects in the fatigue q'', h restriction. σ_R, the reference stress for creep rupture is found from equations 2.8 and 2.9 and entered on a stress to rupture curve to obtain the time to rupture, T_d. The stress to rupture curve for Stainless Steel has been included in MODBREE for this calculation using a least squares fit.

Lastly, we include in the limits on the Mod1 Bree diagram a restriction on the thickness of the tube due to the internal coolant pressure. This is done in exactly the same manner as in the fatigue curves of section 4.2.

The result of the inclusion of these additional limits in the Bree diagram is shown in figure 4.7. Thinning of the first wall is limited by ratchetting (including creep) and strength requirements. Fatigue limits the thickness of the first wall depending on the heat flux but there is no absolute restriction on the thickness if the heat flux is very low or machine operation is steady state.

This illustrates one of the disadvantages of this diagram; the figure indicates no problem (except fatigue) in going to very thick first walls because the entire diagram is evaluated at one temperature. A more desirable approach should include a fixed cold side temperature and increasing hot side temperature with thickness so that restrictions associated with high metal temperatures such as swelling can be included. In its present form. the hot side temperature is fixed and the cold side temperature is decreasing with thickness which is not a very satisfying way to represent the first wall.

Returning to the discussion of the Mod1 Bree diagram, note that heat flux on the

FIG. 4.7 Mod 1 Bree Diagram Design Window for Stainless Steel

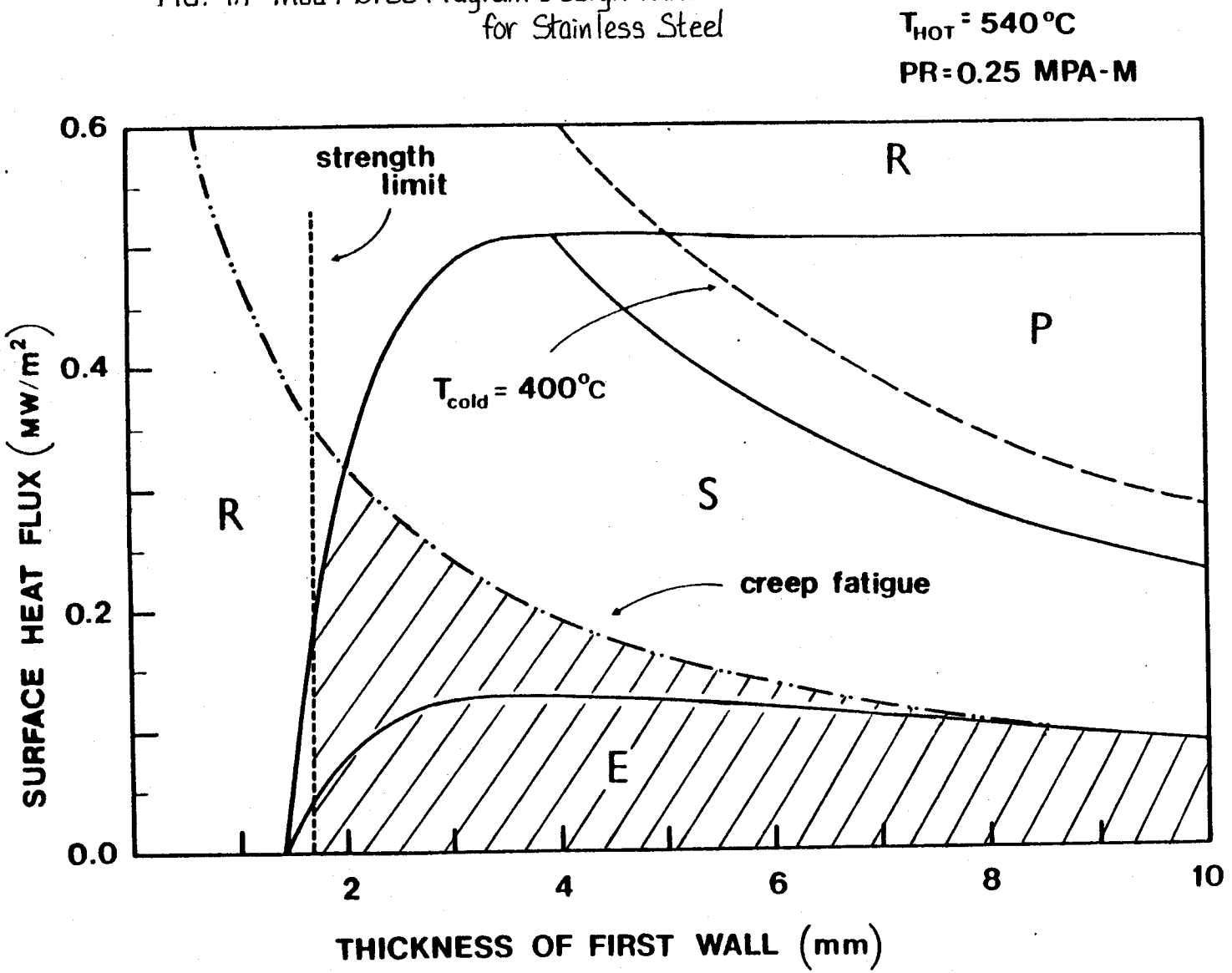

wall is restricted by a combination of fatigue and ratchetting limits. The simultaneous application of each of these limits defines a design window (shaded region) which illustrates the combinations of q'' and h allowable for the first wall corrosponding to the pR and lifetime indicated. This type of design window approach using the Bree diagram has been used in several studies [5],[6],[7] for parametric analysis of first walls by looking at several materials and varying the pR, T_h and lifetime parameters.

4.3.2 Mod2 Bree Diagram

As part of this work, a different modification of the Bree diagram was devised to improve the Mod1 Bree diagram in two important aspects. We will refer to this approach as the Mod2 Bree diagram. The first change attempts to improve on the single temperature approach of the Mod1 Bree diagram as discussed above by fixing the cold side temperature, T_c and allowing T_h to vary with wall thickness. This approach provides an improved physical picture of the actual situation and allows the inclusion of design limits which enter as a result of high peak metal temperature.

Secondly, pR represents something of an artificial parameter, not particularly suited to forming the basis of the diagrams. It is more desirable to restrict the input parameters and the plotting axis to parameters that represent clear physical first wall conditions. Examples are q'', p, T_c, and R, not pR.

Therefore, we choose to plot each of the boundaries in the Mod2 Bree diagram with mean radius versus wall thickness plotted and heat deposition, cold side temperature and lifetime as input parameters. Equations defining the different stress regimes can be derived analagously to equations 4.6 - 4.8. The result is:

$$R = \frac{\sigma_y h - q'' C_f h^2}{p} \qquad E - S \qquad 4.19$$

$$R = \frac{\sigma_y h - \frac{q'' C_f h^2}{4}}{p} \qquad S - R \qquad 4.20$$

$$h = \frac{2\sigma_y}{C_f q''} \qquad S - P \qquad 4.21$$

$$R = \frac{{\sigma_y}^2}{C_f q'' p} \qquad P - R \qquad 4.22$$

These equations are valid within the stress regimes as indicated. The requirement for strength becomes:

$$R = \frac{S_{mt} h}{p} \qquad 4.23$$

and the creep ratchetting limits are:

$$R = \frac{2C_f h q''(\sigma_y + \sigma_c) - (\sigma_y - \sigma_c)^2 - (c_f h q'')^2}{4C_f q'' p} \qquad Region\ S_1 \qquad 4.24$$

$$R = \frac{\sigma_c \sigma_y}{C_f q'' p} \qquad Regions\ S_2, P \qquad 4.25$$

An example of the Mod2 Bree diagram is shown in figure 4.8 for 316 Stainless Steel and $q'' = 0.5 MW/m^2$, $T_c = 350C$. and a lifetime of 8 full power years.

FIG. 4.8 Mod 2 Bree Diagram Design Window for Stainless Steel

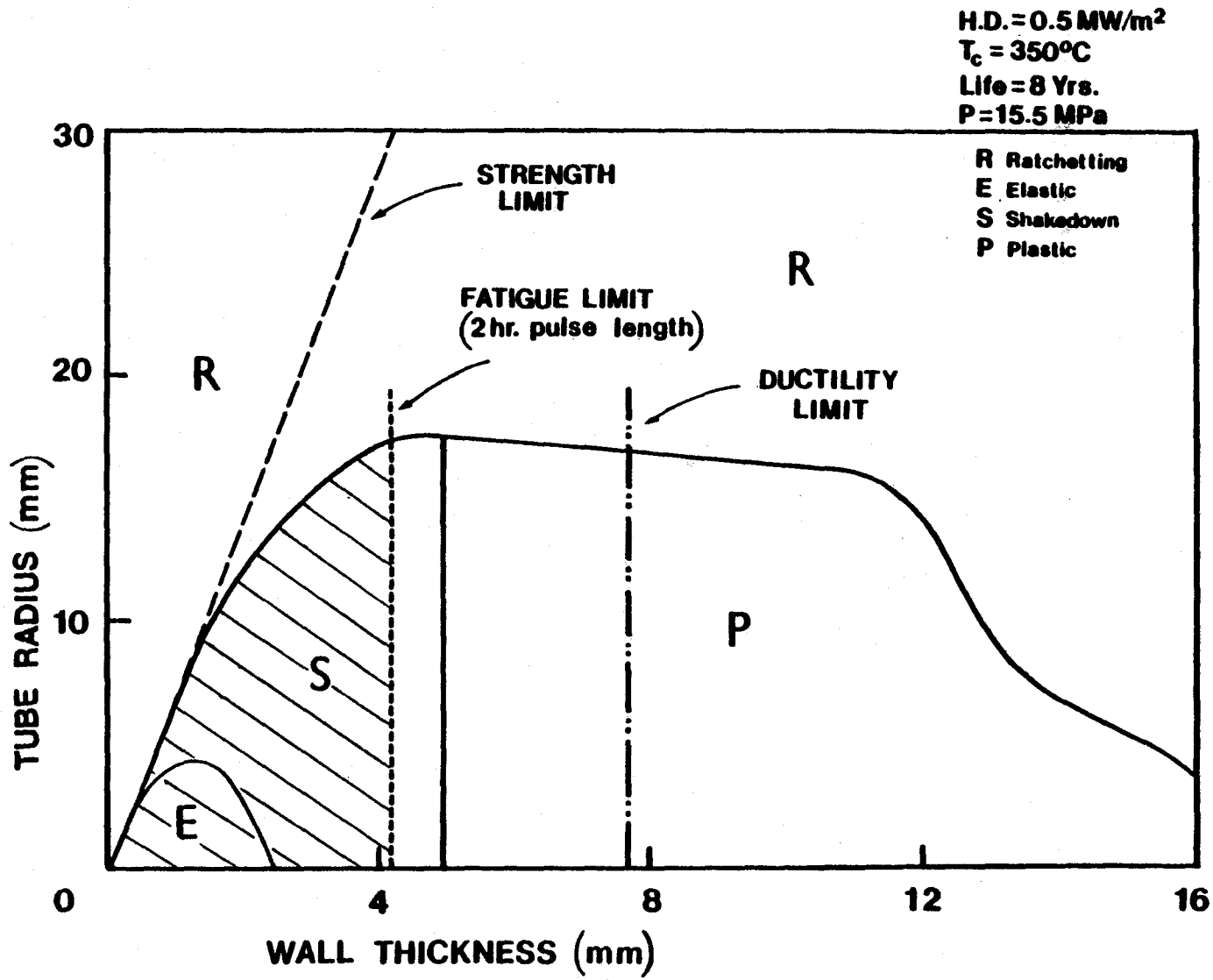

Here again, first wall thinning is limited by ratchetting and strength. Note that the strength limit is no longer vertical since the pressure stress is increasing with radius. Three limits restrict the thickness of the first wall. These are fatigue, creep ratchetting, and swelling or embrittlement, each of which are due to the increasing metal temperature with thickness. The fatigue limit is now a vertical line since heat deposition is fixed. The swelling limit was chosen to be $500C$ for this case.

The radius of the first wall tube, which did not show up explicitly in the Mod1 Bree diagram, is now seen to be restricted on the upper end by creep ratcheting. We could also imagine placing yet another limit on this diagram to restrict the tube radius from getting so small that sufficient coolant cannot pass to maintain the specified cold side temperature.

Thus. we can size the first wall tubes in the context of each of the design limits that has been covered and construct a design window, represented by the shaded section of figure 4.8. This Mod2 Bree diagram can be readily constructed using MODBREE for a number of materials and any combination of heat deposition and cold side temperature desired.

4.4 Summary

Two separate types of design windows for use in tubular fusion first wall design have been developed. Design windows based on modifications to the Bree diagram are relatively simple to construct and offer a good tool for parametric type analysis. Many of the design limits important in the first wall environment can be incorporated into these design windows.

A fatigue design window based on a more realistic two dimensional treatment of the stresses is introduced and used to evaluate thermal fatigue aspects of the ULTR design. It is found that pulse lengths of a few minutes or more can be tolerated

with Stainless steel for heat depositions up to 1 MW/m^2 and with Vanadium to 2 MW/m^2. Additional advantages can be obtained for pulse lengths up to a few hours in length in terms of increased allowance for heat deposition and wall thickness.

Even for pulse lengths of only a few minutes, swelling is significantly more limiting than fatigue for the cases of interest.

5. SUMMARY, CONCLUSIONS AND RECOMMENDATIONS

5.1 Summary and Conclusions

Fusion first wall design must consider a number of different phenomena which separately or in combination may compromise the integrity of the structure. Heat and particle deposition from charged particle, neutral particle, and electromagnetic radiations of the plasma lead to thermal stresses, creep, and erosion of the first wall material. Swelling and loss of ductility (embrittlement) will occur due to neutron radiation also emanating from the plasma. In addition, the first wall must contain the difference in pressure between the coolant removing the heat deposited in the wall and the near vacuum of the plasma chamber.

Most importantly, the first wall must operate in this hostile environment with a high degree of reliability. The slightest leakage of coolant through the first wall will probably result in immediate quench of the plasma burn and contamination of the vacuum vessel. Adequate evaluation of the loads and failure mechanisms relevant in the first wall environment is essential.

In this work, methods are developed for the analysis of a tokamak reactor first wall. In particular, a first wall design for the Ultra Long Pulse Tokamak Reactor (ULTR) is examined. This commercial reactor design (see table 5.1) is an alternative to tokamaks relying on current drive for steady state operation. The reliance of tokamaks on pulsed operation with conventional ohmic drive has been a concern due to fatigue effects in the first wall and toroidal field coils and the interuption of electric power to the grid. The ULTR design is capable of burn pulse lengths of up to 24 hours. Pulses of this length may alleviate some of the concerns associated with pulsed operation without reliance on current drive.

Table 5.1

ULTR Parameters

Major Radius (m)	9.7
Minor Radius (m)	2.0
Plasma Elongation	1.5
Toroidal Beta	0.036
Magnetic Field on Axis (T)	6.0
Plasma Current (MA)	9.7
Peak Electron Temperature (keV)	35
Average Neutron Wall Loading (MW/m^2)	2.3
Fusion Power (MW)	3200
Superconductor	Nb_3Sn
Voltsecond Capability of OH Transformer($V \cdot s$)	1100
Peak Field in OH Transformer(T)	10.5
Pulse Length(hours)	24

Thermal fatigue was a major focus of this study because of its perceived importance in the context of pulsed tokamak operation and the possibilities for alleviation of fatigue problems with the ULTR design. However, the results of one and two dimensional treatments of thermal fatigue for a tubular first wall configuration indicate significant design space even for pulse lengths of only a few minutes.

This work also indicates significant advantages for achieving pulse lengths of a few hours in length although the benefit saturates above this point. These advantages include moderate improvements in the allowed heat deposition for a given wall material and an increased wall thickness allowance which could be used to compensate for erosion of the wall surface due to plasma-wall interactions.

A survey of the present state-of-the-art along with a limited amount of calculations in the area of plasma-wall interactions has been done. Erosion of the first wall surface due to physical sputtering and disruption damage can be quite severe. There is still a great deal of uncertainty involved in these calculations but present results indicate that erosion rates of several mm/yr can be expected.

The posible benefits of achieving burn pulses of several hours suggests a scaled-down version of ULTR. If the first wall were the only fatigue concern, then an ULTR design of reduced size delivering pulses of a few hours would essentially be a steady state device. The parameters of such a device are shown in table 5.2. Certainly, first wall fatigue is not the only concern but the relative importance of each of the other effects of pulsed operation has not been determined.

Both Stainless Steel (with pressurized water coolant) and Vanadium (with liquid lithium coolant) are considered in the fatigue analysis. Thin shell and two dimensional 'plane strain' solutions are developed with allowances for end restraints, tube bending, and asymmetric heat deposition. The fatigue curves are plotted for fixed fluence (product of lifetime and heat deposition) as allowable pulse length

Table 5.2

ULTR with Four Hour Pulse Length

Major Radius (m)	7.6
Minor Radius (m)	1.8
Plasma Elongation	1.5
Toroidal Beta	0.043
Magnetic Field on Axis (T)	6.2
Average Neutron Wall Loading (MW/m^2)	3.0
Fusion Power (MW)	3000
Superconductor	Nb_3Sn
Pulse Length(hours)	4

versus tube wall thickness. The wall thickness is an important parameter because at fixed bulk fluid temperature, the peak metal temperature and the temperature change through the wall (which drives the fatigue) increases with increasing thickness.

A design window is established with these fatigue curves by placing a lower limit on the wall thickness from strength requirements and an upper limit due to peak temperature restrictions from swelling and/or embrittlement. The tube wall must be of some minimum thickness to avoid rupture from the internal pressure of the coolant. Irradiation swelling and embrittlement increase with peak temperature (and fluence) which places an upper limit on the first wall thickness. Requirements for the maximum stress intensity in a tube and a fatigue usage factor approach for evaluating fatigue damage limits are established in the ASME code case N-47-17.

An example of the fatigue design windows for three values of heat deposition (approximately equivalent to one fourth the neutron wall loading) for a Stainless Steel first wall is shown in figure 5.1. The allowable design space represented by the unshaded region of each chart becomes untenable at heat depositions exceeding 1 MW/m^2. The temperature limit from swelling and embrittlement, taken to be 500 C here, is always less limiting than fatigue for these cases. However, the fluence limit from swelling is a much stronger driver than temperature, at least with the presently available data and extrapolated data.

In fact, even for relatively short pulse lengths of a few minutes, swelling is significantly more limiting than fatigue in the first wall design. Adhering to the fluence limit of approximately $12 MW \cdot yr\ m^2$ due to swelling from extrapolated data [17], none of the charts in figure 5.1 exhibit any acceptable design space. This is true because the lifetime for these charts was chosen to be relatively long (8 full power years) and the lowest fluence represented in this figure is the top chart with $16 MW \cdot yr/m^2$. Fatigue design windows at reduced lifetime are shown in figure

FIG. 5.1 Fatigue Design Windows for Heat Deposition Comparison

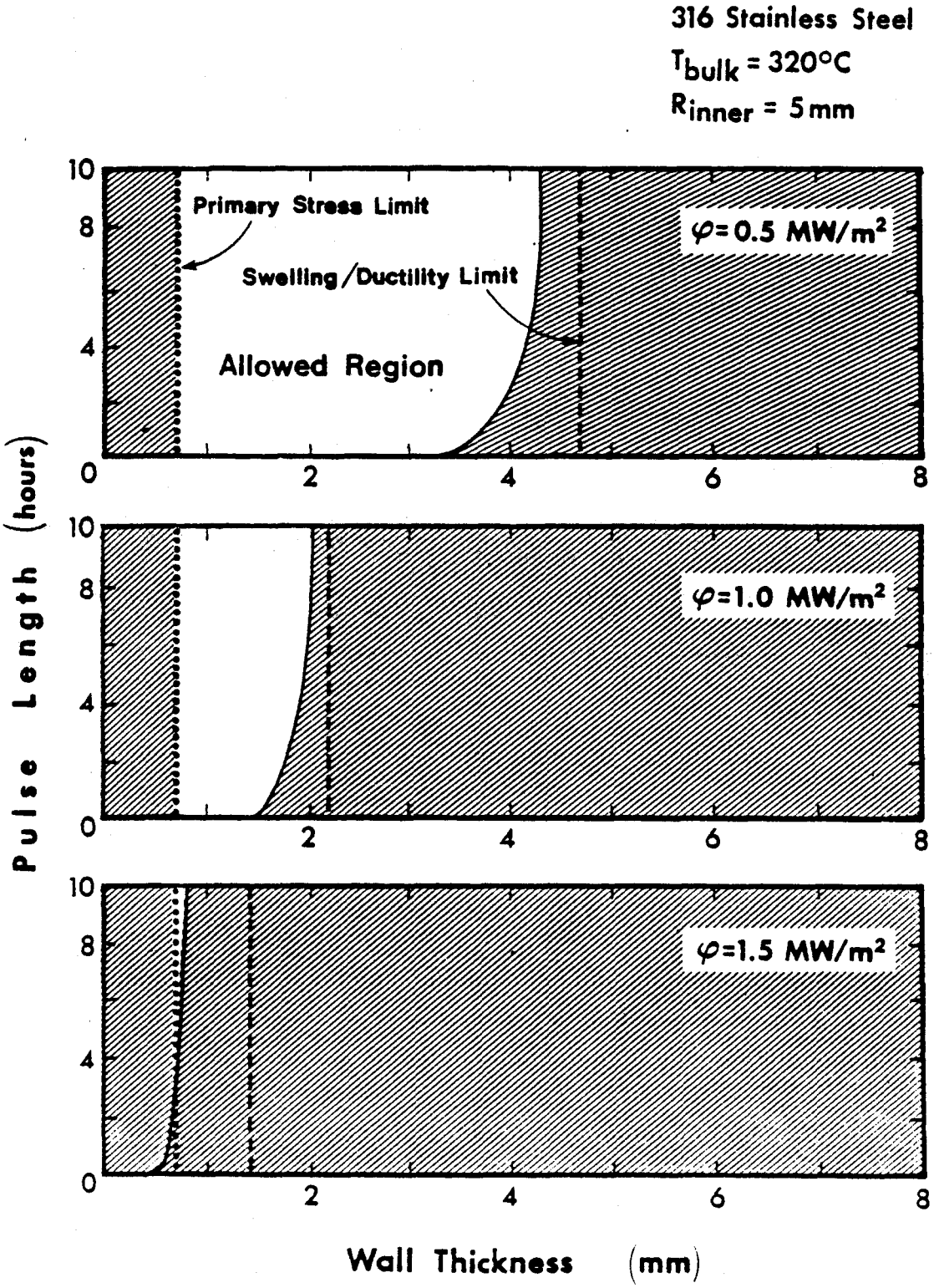

5.2. These charts fall within both the fatigue and swelling limits.

A separate design window approach has been develpoed based on Bree Diagrams [8]. The Bree diagram divides the stress state of a material into regions of elastic, shakedown, plastic, and ratcheting behavior. Modifications to the Bree diagram have been proposed [6] for use in first wall parametric analysis using a thin shell representation of a tubular geometry. A new modification of the Bree diagram is proposed here which permits a greater number of the design limits to be represented in a plot of tube mean radius versus wall thickness. An example of this approach for a Stainless Steel wall with $q'' = 0.5$ MW/m^2 is shown in figure 5.3.

The allowable operating regime in this Mod2 Bree diagram is represented by the shaded region. Operation in the ratcheting and creep ratcheting regime is prohibited since progressive deformation of the material can result. A minimum wall thickness is required for a given mean radius for coolant pressure containment while an upper limit on tube thickness is enforced by fatigue and peak temperature (swelling/embrittlement) considerations.

Note that the two dimensional treatment of fatigue gives more conservative results that the thin shell representation used in the Mod2 Bree diagram. Despite this, the Mod2 Bree diagram is a relatively simple analysis which lends itself easily to parametric type studies of tubular first wall designs. Once parameter space has been searched (including the material type), the more detailed analysis associated with the fatigue design curves is useful for further study.

5.2 Recommendations for Future Work

A study of the other possible liabilities associated with pulsed operation of tokamaks, including toroidal field coil fatigue, turbine rotor fatigue and the interuption

FIG. 5.2 Fatigue Design Windows for Lifetime Comparison

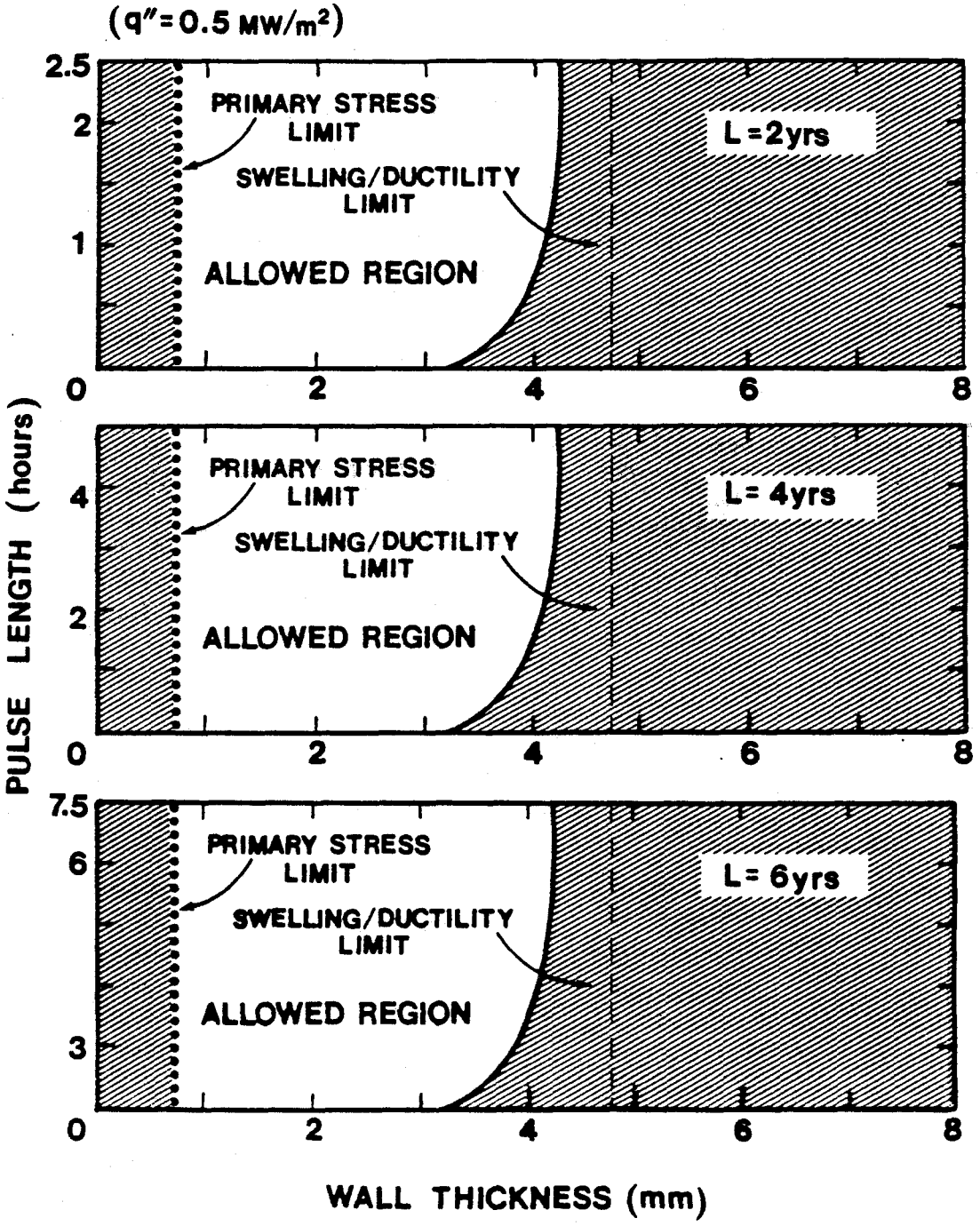

FIG. 5.3 Mod 2 Bree Diagram Design Window for Stainless Steel

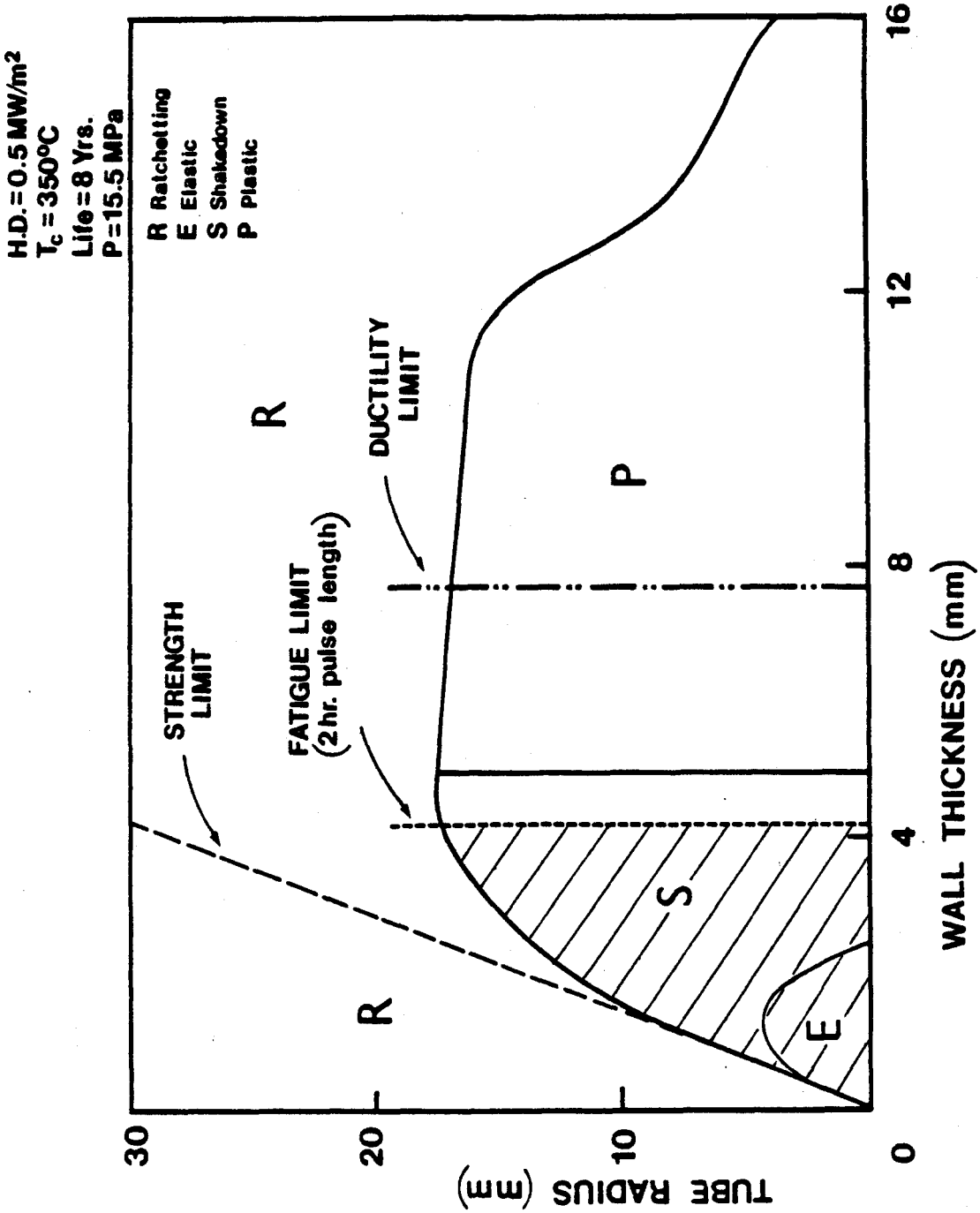

of electric power to the grid, must be done before the importance of long pulse operation can be properly evaluated. Some of this work is being done at MIT [2] and Argonne [30].

The first wall thermal fatigue evaluation here can be further refined by including stress concentration factors in the analysis and including a more complete treatment of the external restraints imposed at the ends and along the length of the first wall tube. Thermal fatigue studies of other first wall geometries would also be a valuable contribution. The data base should also be expanded to include other proposed first wall materials such as Ferritic Steels, Aluminum, and Copper.

Obtaining a more extensive data base for swelling, embrittlement, and plasma-wall interactions is crucial. These phenomena are potentially the most limiting design aspects of the first wall while the data barely affords an adequate analysis of their impact. This is especially true for materials other than Stainless Steel.

APPENDIX A

MATERIAL PROPERTIES

The property data used in this work for Stainless Steel and Vanadium is summarized. Temperature dependent material properties, fatigue data, isochronous stress-strain and creep rupture curves are included. All units are MKS with temperature (T) in celsius (except where noted.)

Stainless Steel

Thermal Expansion Coefficient:

$$\alpha = 10.28 \times 10^{-6}\ T^{0.093} \qquad A.1$$

Youngs Modulus:

$$465.0 \times 10^{9}\ T^{-0.18} \qquad A.2$$

Thermal Conductivity:

$$3.78\ T^{0.28} \qquad A.3$$

Yield Stress:

$$745.0 \times 10^{6}\ T^{-0.31} \qquad A.4$$

The poisson ratio is 0.27. The above property data is from reference [6]. Data for fatigue, stress to rupture, S_{mt}, and isochronous stress strain curves is available from the ASME code [4]. The fatigue design curve for Stainless Steel is found in figure A.1. The average isochronous stress-strain data is shown in table A.1. Stress to rupture data is shown in table A.2. Values of S_{mt} as a function of temperature and lifetime are given in table A.3.

Vanadium

Material properties for Vanadium are taken from references [5],[6].

Thermal Expansion Coefficient:

$$6.41 \times 10^{-6}\ T^{0.08} \qquad A.5$$

Youngs Modulus:

$$158.0 \times 10^{9}\ T^{-0.05} \qquad A.6$$

Thermal Conductivity:

$$13.5\ T^{0.14} \qquad A.7$$

The poisson ratio is 0.36. The fatigue data has been correlated with:

$$\epsilon_t = 4.12 \times 10^{-3} N_d{}^{-0.06} \qquad A.8$$

which includes a design scatter factor of four on fatigue lifetime. The data for S_{mt} is shown in table A.4.

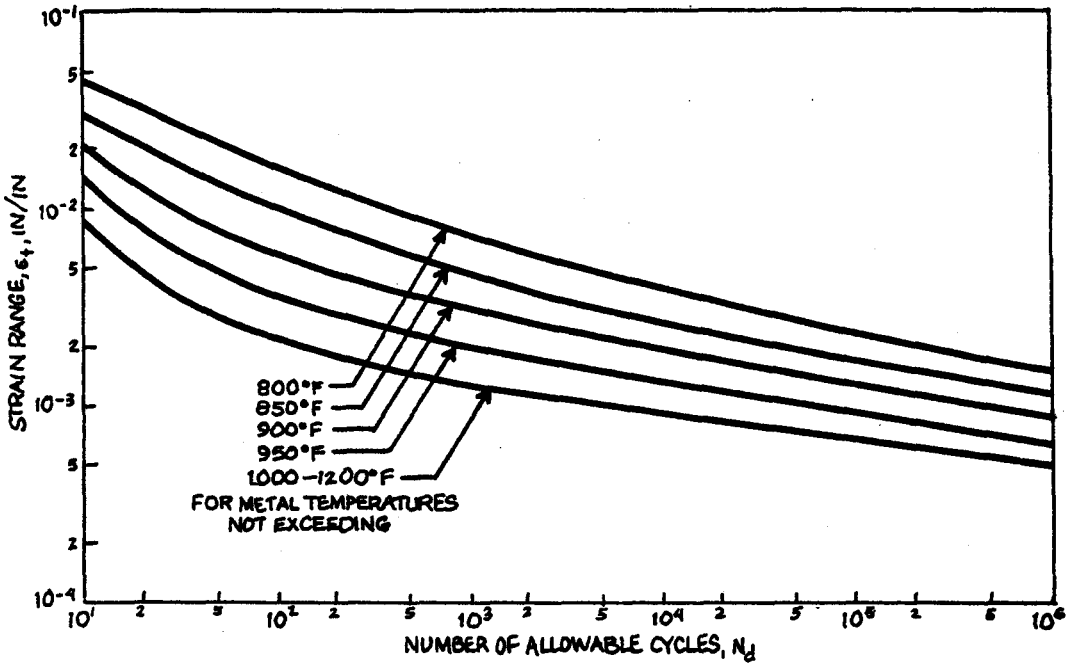

FIG. A.1 Fatigue Design Curve for Stainless Steel [4]

Table A.1

Stress for 1% Isochronous Strain (psi)

Stainless Steel

Temperature (°C)	Number of Cycles				
	10	**100**	**1000**	**10000**	**100000**
426.7	25900	25900	25900	25900	25900
454.4	25500	25500	25500	25500	25500
482.2	25200	25200	25200	25200	24700
510.0	24900	24900	24900	24400	22900
537.8	24500	24500	24200	22600	20300
565.6	23900	23100	21800	19800	16500
593.3	23600	22200	20800	18800	15800
621.1	22000	20500	17800	14300	11400
648.9	20900	17800	13300	10300	7500
676.7	18900	14300	10400	7800	5600

Table A.2

Minimum Rupture Stress, 316 Stainless Steel, psi

Temperature (°F)	Lifetime, hours				
	100	**1000**	**10000**	**100000**	**300000**
800	64500	64500	64500	64500	64500
850	63300	63300	63300	56000	52000
900	62200	62000	54100	42600	38000
950	60000	51600	42600	32400	28300
1000	51700	42100	33600	24600	21000
1050	43400	34400	26400	18800	16000
1100	36400	28100	20800	14300	11700
1150	30500	23000	16400	10900	8800
1200	25600	18800	12900	8300	6700

Table A.3

Stress Intensity for Stainless Steel, S_{mt}, (MPa)

Temperature (°C)	Lifetime, hours				
	100	**1000**	**10000**	**100000**	**300000**
300	109	109	109	109	109
400	109	109	109	109	109
500	107	107	107	107	107
600	102	102	91	61	51

Table A.4

Stress Intensity for Vanadium, S_{mt}, (MPa)

Temperature (°C)	Lifetime, hours				
	100	**1000**	**10000**	**100000**	**300000**
400	204	204	204	204	204
500	198	198	198	198	198
600	183	183	183	173	160
700	157	156	131	109	101
800	106	103	84	69	63

APPENDIX B

Interpreting Macsyma Programming

The three programs used in this work were written using the MACSYMA program on the PDP-10 "MC" at MIT. Provided here is the means to interpret the program listings included in these appendices for conversion to the FORTRAN language. The conversion is straight forward since the two languages are quite similar. MACSYMA has advantages over FORTRAN in the form of a completely interactive system and many readily available "canned" routines for plotting, integrating, etc.

The following syntax conversions are applicable:

- MACSYMA colon equivalent to FORTRAN equal sign
- MACSYMA square bracket for arrays equivalent to FORTRAN parenthesis
- MACSYMA carat ($\wedge$) or arrow ($\uparrow$) equivalent to FORTRAN double asterisk (**)
- MACSYMA breaks command lines with a comma
- Columns have no special significance in MACSYMA
- Comment statements begin with "/*" and end with "*/" in MACSYMA
- Variable and array names can be of any size in MACSYMA

A MACSYMA program essentially consists of subroutines which begin with "Function(Variable) := (" and end with ")$". The subroutine can be called by any other routine by specifying "Function(Variable)". No variable need be specified in the function statement. Variables are declared using the MODEDECLARE statement which designates variables as floating point (FLOAT) or integer (FIXNUM). The WRITEFILE and CLOSEFILE statements simply have the program output dumped into a file in the users directory and need not be translated for use in a FORTRAN program.

The equivalent of a do loop in MACSYMA is in the form " For n from k thru l do()" where n is the loop variable, k is the lower limit, l is the upper limit and the looped routines are enclosed in the parenthesis. MACSYMA conditional statements are in the form of "IF ... THEN ... ELSE" statements. There are no GO TO statements in MACSYMA.

Any other unrecognizable symbols or variables in the MACSYMA programs to follow are "canned" routines, the equivalent of which are available on most computer systems with FORTRAN compilers. Note that the intention here is not to teach MACSYMA programming. Following the rules above, however, the reader should be able to translate the enclosed programs into FORTRAN.

```
/* ******************  PROGRAM SPUT  ****************** */



TTYOFF : TRUE$

LOADFILE(SPUTNW,FASL,RENE)$

/* SUBSCRIPT 1 ..... INCIDENT PARTICLES
   SUBSCRIPT 2 ..... WALL PARTICLES    */

/* ***** FUNCTIONS TO CALCULATE ENERGY AND ANGULAR DEPENDENT
           SPUTTERING YIELDS FROM SMITH PAPER ***** */

F(E) := (MODEDECLARE([M1,M2,Z1,Z2,U0,ETH,B,A,S,MAXWELL,KT,E],FLOAT),
    ETH : (4.*M1 + M2)↑2*U0/(4.*M1*M2),
    B : 40./(Z1 + 40.),
    A : B - 0.2,
    S : CC*CPRIME/U0*Z1↑A*(Z2 - 1.8)↑2*((M1-1)/M2)↑1.5*
        (E - ETH)/(E - ETH + 50.*Z1↑B*Z2)↑2,
    MAXWELL : (4./3.1416)↑.5*(KT)↑(-1.5)*E↑.5*EXP(-E/KT),
                                    /* LEAVE N OUT.....IT CANCELS */
    S*MAXWELL )$

MAXWELL(E) := (MODEDECLARE([KT,E],FLOAT),
    (4./3.1416)↑.5*(KT)↑(-1.5)*E↑.5*EXP(-E/KT) )$

FTEST(E) := (MODEDECLARE([M1,M2,Z1,Z2,U0,ETH,
             B,A,S,MAXWELL,KT,QPHI,E],FLOAT),
    ETH : (4.*M1 + M2)↑2*U0/(4.*M1*M2),
    B : 40./(Z1 + 40.),
    A : B - 0.2,
    S : CC*CPRIME/U0*Z1↑A*(Z2 - 1.8)↑2*((M1-1)/M2)↑1.5*(E - ETH)/
      (E - ETH + 50.*Z1↑B*Z2)↑2,
    MAXWELL : (4./3.1416)↑.5*(KT)↑(-1.5)*(E-QPHI)↑.5*EXP(-(E-QPHI)/KT),
    S*MAXWELL )$

MAXWELLTEST(E) := (MODEDECLARE([KT,E,QPHI],FLOAT),
    (4./3.1416)↑.5*(KT)↑(-1.5)*(E-QPHI)↑.5*EXP(-(E-QPHI)/KT) )$

FTHETA(EE) := (MODEDECLARE([ETH,Z1,Z2,M1,M2,U0,
                BEGIN,F,MAXWELL2,EE,KT],FLOAT),
    ETH : (4.*M1 + M2)↑2*U0/(4.*M1*M2),
    BEGIN : 4. * ETH,
    F : 1./(20.*Z1)↑.5*(M2/M1)↑.25*(EE - 4.*ETH)↑.25,
    MAXWELL2 : (4./3.1416)↑.5*(KT)↑(-1.5)*EE↑.5*
         EXP(-EE/KT),    /* LEAVE N OUT.....IT CANCELS */
    F*MAXWELL2 )$

FTH(THETA):= (MODEDECLARE([BEG,END,FNEW,TERM2,THETA],FLOAT),
    FNEW : ROMBERG(FTHETA(EE),EE,BEG,END),
```

```
    COS(THETA)↑(-FNEW/TERM2*(1. - THETA/90.)↑0.5)    )$

FTOTAL(E) := (MODEDECLARE([F,Z1,M2,M1,Z2,ETH,E,THETADAT],FLOAT),
    F : 1./(20.*Z1)↑.5*(M2/M1)↑.25*(E - 4.*ETH)↑.25*
          (1. - THETADAT/90.)↑0.5,
    F(E)*COS(THETADAT*3.1415926/180.)↑(-F)    )$

FTOTALTEST(E) := (MODEDECLARE([F,Z1,M2,M1,Z2,ETH,E,THETADAT],FLOAT),
    F : 1./(20.*Z1)↑.5*(M2/M1)↑.25*(E - 4.*ETH)↑.25*
     (1. - THETADAT/90.)↑0.5,
    FTEST(E)*COS(THETADAT*3.1415926/180.)↑(-F)    )$

/* ESTABLISH ARRAYS */

(NN : 1,
 ARRAY(X,FLOAT,50),
 ARRAY(Y,FLOAT,50),
 ARRAY(A,FLOAT,11,11),
 ARRAY(B,FLOAT,11),
 ARRAY(CC,FLOAT,11),
 ARRAY(M1,FLOAT,4),
 ARRAY(Z1,FLOAT,4),
 ARRAY(S,FLOAT,4,50),
 ARRAY(F1,FLOAT,4,50),
 ARRAY(FF,FLOAT,4,50),
 ARRAY(P,FLOAT,10),
 ARRAY(THETA,FLOAT,50),
 ARRAY(E,FLOAT,50),
 ARRAY(THISISIT,FLOAT,4),
 ARRAY(P,FLOAT,20)  )$


FUNCS : [F,FTEST,FTHETA,FTH,MAXWELL,MAXWELLTEST,FTOTAL,FTOTALTEST,SPUT,
                        EQN,PLANGLE,PLENERGYLOG,PLENERGYLIN]$

/* MAIN ROUTINE. CALCULATES SPUTTERING YIELDS */

SPUT():= (

      MODEDECLARE([Z1,Z2,M1,M2,EDGEKT,CHARGESTATE,Q,
          DTENERGY,SELFSPUTENERGY,U0,
          EANGULAR,DENSITY,AVAIL,FLUXDT,CC,CPRIME,
          TERM1,TERM2,END,KT,
          ETH,BEG,FNEW,QPHI,B,A,THETADAT,STEPIT,BEGIN,
          MAXNEW,TOTYIELD,TOTALYIELD,
          TEMP,FACTOR,SUM,YLD,EROSIONDT,EROSIONHE,
          EROSIONSELF,EROSIONTOTAL],FLOAT,
          [M,IIIP1,EINTEGRAL,N,NUMBER,MX2,K,NM1,KP1,
             L,I,J,NN,III,JJJ,LL],FIXNUM),

CC : 1.,
Z1[1] : 1., Z1[2] : 1., Z1[3] : 2.,
M1[1] : 2., M1[2] : 3., M1[3] : 4.,

KT : READ("WHAT IS THE PLASMA EDGE TEMPERATURE IN EV?"),
Q : READ("WHAT IS THE AVERAGE CHARGE STATE OF THE SPUTTERED MATERIAL?"),
DTENERGY : 4.5*KT,
SELFSPUTENERGY : Q*3.*KT,
U0 : READ("WHAT IS THE BINDING ENERGY FOR THE WALL MATERIAL (IN EV)?"),
Z2 : READ("WHAT IS THE ATOMIC WEIGHT (Z) FOR THE
      WALL MATERIAL? (= 4 FOR BE)"),
M2 : READ("WHAT IS THE MASS (M) FOR THE WALL MATERIAL? (= 9 FOR BE)"),
EANGULAR : READ("WHAT ENERGY WOULD YOU LIKE TO PLOT
      THE ANGULAR YIELD DEPENDENCE FOR?"),
EINTEGRAL : READ("DO YOU WANT THE INTEGRALS CALCULATED? A 1 IS YES"),
DENSITY : READ("WHAT IS THE DENSITY OF WALL
```

```
      MATERIAL? (1.85 GM/CM↑3 FOR BE)"),
AVAIL : READ("WHAT IS THE AVAILABILITY TIMES THE DUTY CYCLE?"),
FLUXDT : READ("WHAT IS THE DT PARTICLE FLUX (PART/CM↑2/SEC)
         TO THE FIRST WALL?"),

Z1[4] : Z2,
M1[4] : M2,

/* YIELDS CALCULATED FOR DEUTERIUM, TRITIUM, HELIUM AND
            SELF SPUTTERING */

FOR I FROM 1 THRU 4 DO(
M1 : M1[I],
Z1 : Z1[I],
IF M1 > 1. THEN(CPRIME : 500.) ELSE(CPRIME : 2000.),
IF I = 4 THEN(QPHI : SELFSPUTENERGY)ELSE(QPHI : DTENERGY),
END : 4.*KT + QPHI,

/* AVERAGE THE ENERGY PART OF S OVER A MAXWELLIAN  */

IF EINTEGRAL = 1 THEN(

TERM2 : ROMBERG(MAXWELLTEST(E),E,QPHI,END),
TERM1 : ROMBERG(FTEST(E),E,QPHI,END)    ),

YIELD[I] : TERM1/TERM2,

PRINT("*********************************************************"),
PRINT("*********************************************************"),
PRINT("*********************************************************"),

PRINT("Z INCIDENT IS",Z1,"M INCIDENT IS",M1,
      "Z OF WALL IS",Z2,"M OF WALL IS",M2,
      "INTEGRAL OF S*MAXWELLIAN =",TERM1,"INTEGRAL
          OF MAXWELLIAN =",TERM2,
      "ENERGY DEPENDANT YIELD (NORMAL INCIDENCE) =",YIELD[I]),

/* CALCULATE FOR PLOTTING THE ANGULAR DEPENDANCE
          OF S FOR A GIVEN ENERGY */

        F1[I,NN] : 1./(20.*Z1)↑.5*(M2/M1)↑.25*
          (EANGULAR - 4.*ETH)↑.25*(1. - THETA[NN]/90.)↑0.5,
        FF[I,NN] : COS(THETA[NN]*3.1415926/180.)↑(-F1[I,NN]),

/* MULTIPLY TOGETHER THE ENERGY AND ANGULAR (WHICH
     IS ALSO A FUNCTION OF ENERGY) PARTS
     OF S AND AVERAGE THE RESULT OVER A MAXWELLIAN
     FOR A SERIES OF GIVEN THETA'S FROM
     0.0 TO 90.0.  FIT THE RESULTING CURVE WITH
     LEAST SQUARES AND AVERAGE THIS OVER
     SOME ASSUMED ANGULAR DISTRIBUTION OF THE PARTICLES
     (PROBABLY ISOTROPIC) TO GET A
     TOTAL YIELD (FOR EACH INCOMING SPECIES). */

THETADAT : -10.,
ETH : (4.*M1 + M2)↑2*U0/(4.*M1*M2),
B : 40./(Z1 + 40.),
A : B - 0.2,
IF I = 4 THEN( STEPIT : 10.*3./2.*SELFSPUTENERGY/50.)ELSE(
STEPIT : 10.*3./2.*ENERGYDT/50.),
BEGIN : 4.*ETH,

/* THIS USEFUL FOR PLOTTING THE ENERGY DEPENDANT
        YIELDS FOR NORMAL INCIDENT PARTICLES */

S[I,NN] : CC*CPRIME/U0*Z1↑A*(Z2 - 1.8)↑2*((M1-1)/M2)↑1.5*
```

```
                (E[NN] - ETH)/(E[NN] - ETH + 50.*Z1↑B*Z2)↑2,

IF EINTEGRAL = 1 THEN(
MAXNEW : ROMBERG(MAXWELLTEST(E),E,QPHI,END),
FOR J FROM 1 THRU 11 DO(
   IF THETADAT > 77.0 THEN (THETADAT : THETADAT + 5.)
         ELSE(THETADAT : THETADAT + 10.),
    TOTYIELD : ROMBERG(FTOTALTEST(E),E,QPHI,END),
    TOTALYIELD : TOTYIELD/MAXNEW,
    PRINT("TOTAL YIELD AVERAGED OVER A MAXWELLIAN FOR THETA OF",THETADAT,
       "DEGREES IS",TOTALYIELD),

/* PUT THE YIELD AND THETA IN Y AND X ARRAYS AND FIT TO A CURVE  */


/* M IS THE DEGREE OF THE POLYNOMIAL
   N = M + 1  = NUMBER OF EQUATIONS
   X,Y ARE THE DATA PAIRS
   NUMBER IS THE NUMBER OF DATA SETS  */


  X[J] : THETADAT,
  Y[J] : TOTALYIELD   ),

NUMBER : 10,
M : 3,
        MX2 : M * 2,
     FOR III FROM 1 THRU MX2 DO(
     P[III] : 0.0,
     FOR JJJ FROM 1 THRU NUMBER DO(
      P[III] : P[III] + X[JJJ]↑III )   ),
      N :  M + 1,
     FOR III FROM 1 THRU N DO(
     FOR JJJ FROM 1 THRU N DO(
      K : III + JJJ - 2,
      IF K > 0 THEN (A[III,JJJ] : P[K]) ELSE(
           A[1,1] : NUMBER*1./1.) )  ),
     B[1] : 0.0,
     FOR JJJ FROM 1 THRU NUMBER DO(
          B[1] : B[1] + Y[JJJ]  ),
     FOR III FROM 2 THRU N DO(
        B[III] : 0.0,
        FOR JJJ FROM 1 THRU NUMBER DO(
           B[III] : B[III] + Y[JJJ] * X[JJJ]↑(III - 1)  )   ),
     NM1 : N - 1,
      FOR K FROM 1 THRU NM1 DO(
        KP1 : K + 1,
        L : K,
      FOR III FROM KP1 THRU N DO(
         IF (ABS(A[III,K]) > ABS(A[L,K])) THEN (L : III)   ),
               IF L > K THEN(
                         FOR JJJ FROM K THRU N DO(
                         TEMP : A[K,JJJ],
                         A[K,JJJ] : A[L,JJJ],
                         A[L,JJJ] : TEMP ),
              TEMP : B[K],
              B[K] : B[L],
              B[L] : TEMP  ),
         FOR III FROM KP1 THRU N DO(
           FACTOR : A[III,K]/A[K,K],
           A[III,K] : 0.0,
         FOR JJJ FROM KP1 THRU N DO(
             A[III,JJJ] : A[III,JJJ] - FACTOR*A[K,JJJ]  ),
           B[III] : B[III] - FACTOR*B[K]  )  ),
         CC[N] : B[N]/A[N,N],
         III : NM1,
```

```
      FOR LL FROM 1 THRU N DO(
          IIIP1 : III + 1,
          SUM : 0.0,
          FOR JJJ FROM IIIP1 THRU N DO(
             SUM : SUM + A[III,JJJ]*CC[JJJ] ),
        CC[III] : (B[III] - SUM)/A[III,III],
        III : III - 1,
        IF III <= 0 THEN(
                 FOR III FROM 1 THRU N DO(
                  PRINT("CC[",III,"]= ", CC[III])  ),
                    LL : N,
                  PRINT("THE MULTIPLIER FOR THE VARIABLE TO THE POWER OF",
                    M,"IS C[",N,"] .... AND SO ON DOWN. ")
                                                          )   ),

      YLD : ROMBERG(EQN(ANGLE),ANGLE,0.,90.),
      THISISIT[I] : YLD*3.14159/180.,

      PRINT("TOTAL YIELD INTEGRATED OVER THE INCOMING
            PARTICLE ENERGY DISTRIBUTION
            WHICH IS MODIFIED FROM A MAXWELLIAN AT THE EDGE AND ISOTROPIC
                     ANGLE DISTR. IS",THISISIT[I]),

      PRINT("*********************************************") )  ),

          EROSIONDT : 3.1536E8*AVAIL*FLUXDT*(THISISIT[1]*0.5
                + THISISIT[2]*0.5)
                /(6.023E23*(1./M2)*DENSITY),
          EROSIONHE : 3.1536E8*AVAIL*0.05*FLUXDT*
                THISISIT[3]/(6.023E23*(1./M2)*DENSITY),
          EROSIONSELF : (EROSIONDT + EROSIONHE)*THISISIT[4]/
                (1. - THISISIT[4]),
          EROSIONTOTAL : EROSIONDT + EROSIONHE + EROSIONSELF,

               PRINT("************************************"),
               PRINT("************************************"),
               PRINT("DT EROSION RATE IN MM/YEAR IS",EROSIONDT),
               PRINT("HELIUM EROSION RATE IN MM/YEAR IS",EROSIONHE),
               PRINT("SELF-EROSION RATE IN MM/YEAR IS",EROSIONSELF),
               PRINT("TOTAL EROSION RATE IN MM/YEAR IS",EROSIONTOTAL),
               PRINT("************************************"),
               PRINT("************************************")    )$

EQN(ANGLE) := (
   (CC[4]*ANGLE↑3 + CC[3]*ANGLE↑2 + CC[2]*ANGLE + CC[1])*
        SIN(ANGLE*3.14159/180.)    )$

/* PLOTTING ROUTINES */

PLANGLE() :=  (
   FOR N FROM 1 THRU 46 DO(
          THETA[N] : -2. + 2.*N ),
  PARAMPLOT2(
     [THETA[NN]],
     [FF[1,NN],FF[2,NN],FF[3,NN],FF[4,NN]],
     NN, 1, 46, INTEGER,
     "ANGLE IN DEGREES", "YIELD","ANGULAR DEPENDENT
                YIELD AT FIXED ENERGY",
     [10, 20, 30, 40])   )$


PLENERGYLOG() :=  (
      FOR N FROM 1 THRU 51 DO(
        E[N] : -STEPIT + 20. + STEPIT*N ),
  PARAMPLOT2(
```

```
      [E[NN]],
      [S[1,NN],S[2,NN],S[3,NN],S[4,NN]],
      NN, 1, 51, INTEGER, LOGLOG,
      "ENERGY IN EV", "YIELD","ENERGY DEPENDENT YIELD AT NORMAL INCIDENCE",
      [10, 20, 30, 40])   )$

PLENERGYLIN() :=  (
       FOR N FROM 1 THRU 51 DO(
         E[N] : -STEPIT + 20. + STEPIT*N ),
  PARAMPLOT2(
      [E[NN]],
      [S[1,NN],S[2,NN],S[3,NN],S[4,NN]],
      NN, 1, 51, INTEGER,
      "ENERGY IN EV", "YIELD","ENERGY DEPENDENT YIELD AT NORMAL INCIDENCE",
      [10, 20, 30, 40])   )$
```

APPENDIX C

```
/*  ***************     PROGRAM ULTR     ************************** */


/* SUPPRESSES PRINTING WHILE PROGRAM IS BATCHING */

TTYOFF : TRUE


/* CALCULATES THE STRESSES AND FATIGUE STATE IN FIRST WALL TUBES WITH
AND WITHOUT BENDING WITH A "PLAIN STRAIN" ASSUMPTION. THE ENDS ARE
UNRESTRAINED. DOES THE TEMPERATURE, THERMAL, AND PREASURE STRESSES
ACCOUNTING FOR A COSINE SURFACE HEAT FLUX, INTERNAL
HEAT GENERATION, AND THICK SHELL. */

(
/* INITIALIZATIONS */

 CHAMBER : 2.4,
 MAJRADIUS : 9.7,
 DENSITYWATER : 720.,
 VELOCITYLIMIT : 5.,
 VELOCITYWANT : 0,
 TSTAR : 20.,
 TEMPRISE : 40.,
 SEGLENGTH : 3.0,
 NOPRINT : 0,
 REJTIME : 0.,  /* IN SECONDS */
 LAST : 1,
 LASTPLUS1 : LAST + 1,
 NNLAST : 50,
 NNLASTPLUS1 : NNLAST + 1,
 TEMPLAST : 50,
 TEMPLASTPLUS1 : TEMPLAST + 1,
 TTRYMAX : 800.,
 RIN : 1.E-2,     /* IN METERS */
 ROUTMIN : RIN,
 ROUTMAX : RIN + 10.E-3,
 MATNUM : 1,
 PWRLIFE : 8.*24.*365.,
 HEAT : 8.2E3, /* WATTS PER M↑2 -DEG K */
 PREAS : 15.5E6,  /* IN PA */
 PWRLIFE : 8.*365.*24.,
 Q2PRIME : 7.5E5, /* WATTS PER M↑2 */
 Q3PRIME : 10.E6, /* WATTS PER M↑3 */
 TBULK : 300.0    /* DEGREES C */ )

INPUT() := (
  RIN : READ("WHAT IS INNER RADIUS (M)?"),
  ROUTMIN : RIN,
  ROUTMAX : RIN + 10.E-3,
```

```
  TBULK : READ("WHAT IS TBULK?"),
  Q2PRIME : READ("WHAT IS SURFACE HEAT DEPOSITION"),
  Q3PRIME : Q2PRIME*40.,
  Q3WATER : Q3PRIME*1.,
  MATNUM : READ("WHAT MATERIAL WOULD YOU LIKE?"),
  IF MATNUM = 1 THEN(TBULKMIN : 200.,PREAS : 15.5E6,
       TEMPRISE : 40.,
       VELOCITYLIMIT : 5.),
  IF MATNUM = 2 THEN (TBULKMIN : 450.,PREAS : 1.E6,
      TEMPRISE : 150.,
      VELOCITYLIMIT : 0.5) )

/* ESTABLISH ARRAYS */

(
 ARRAY(BSQD,FLOAT,5),
 ARRAY(CC1PART,FLOAT,20),
 ARRAY(D1PART,FLOAT,20),
 ARRAY(SIGPMISESS2,FLOAT,2,51),
 ARRAY(SIGPRS2,FLOAT,2,51),
 ARRAY(SIGPTHS2,FLOAT,2,51),
 ARRAY(SIGPZS2,FLOAT,2,51),
 ARRAY(SIGPTHINS2,FLOAT,2,51),
 ARRAY(PULSETHINSHELL,FLOAT,51),
 ARRAY(TTRY,FLOAT,51),
 ARRAY(SMTSTRY,FLOAT,51),
 ARRAY(TCOLD,FLOAT,51),
 ARRAY(NCYEQUIVNOBEND,2,51),
 ARRAY(PULSEEQUIVNOBEND,FLOAT,2,51),
 ARRAY(NCYEQUIVBEND,2,51),
 ARRAY(PULSEEQUIVBEND,FLOAT,2,51),
 ARRAY(NCYTHINSHELL,51),
 ARRAY(SIGTHINTHERMAL,51),
 ARRAY(SIGTR,FLOAT,2,51),
 ARRAY(SIGTTH,FLOAT,2,51),
 ARRAY(SIGSHEAR,FLOAT,2,51),
 ARRAY(SIGTZNOBEND,FLOAT,2,51),
 ARRAY(SIGTZBEND,FLOAT,2,51),
 ARRAY(SIGTZREST,FLOAT,2,51),
 ARRAY(NCYEQUIVREST,FLOAT,2,51),
 ARRAY(PULSEEQUIVREST,FLOAT,2,51),
 ARRAY(TEMPDIFF,FLOAT,51),
 ARRAY(ROUTS2,FLOAT,51),
 ARRAY(TAVG,FLOAT,51),
 ARRAY(THICKS2,FLOAT,51),
 ARRAY(RADS2,FLOAT,2,51),
 ARRAY(TEMPPEAK,FLOAT,2,51),
 ARRAY(TAVGS2,FLOAT,51) )


/* SUBROUTINE TO CALCULATE MATERIAL PROPERTIES */

PROP(K) := (MODEDECLARE([LIFE,HMIN,AVAIL,PULSE,PWRLIFE,DEP,REJTIME,
                         CFCONST,SMT400,SMT500,SMT600,SMT700,SMT800,LNPWR,
                         Z1,Z2,Z3,ALPHA,YOUNG,TK,POISSON,YIELD,SMTSTRESS,
                         POWER,SIGISO,MULTIPLIER],FLOAT,[N,THATSENOUGH,K,
                         WANTREAD,NOPRINT,MATNUM],FIXNUM),


/* STAINLESS STEEL (316) PROPERTY DATA */

 IF MATNUM = 1 THEN(
   ALPHA : 10.28*TTRY[K]↑0.093*1.E-6,
   YOUNG : 465.*TTRY[K]↑(-0.18)*1.E9,    /* YOUNGS MODULUS */

   TK : 3.78*TTRY[K]↑0.28, /* THERMAL CONDUCTIVITY */
```

```
     POISSON : 0.27,
    Z1 : (6.5224E-3*TTRY[K]↑2-6.8764*TTRY[K]+1821.095)/1.E4,
    Z2 : -1.21448E-5*TTRY[K]↑2+0.01069*TTRY[K]-2.5663,
    Z3 : 5.4568E-5*TTRY[K]↑2-0.08336*TTRY[K]+48.1074,
    YIELD : 745.*TTRY[K]↑(-0.31)*1.E6,   /* YIELD STRESS */
    LNPWR : LOG(PWRLIFE),

 /* MAXIMUM STRESS INTENSITY FROM ASME CODE */

    SMT400 : 109.,
    SMT500 : 107.,
    SMT600 : 102.,
    IF PWRLIFE >= 3000. THEN(SMT600 :
        -0.8139765*LNPWR↑2+6.2849*LNPWR+99.147),
       IF TTRY[K] <= 400. THEN(SMTSTRESS : 109.) ELSE(
            IF TTRY[K] <= 500. THEN(SMTSTRESS :
           SMT400+(TTRY[K]-400.)/100.*
              (SMT500-SMT400))ELSE(
        IF TTRY[K] <= 600 THEN(SMTSTRESS:SMT500+
          (TTRY[K]-500.)/100.*(SMT600-SMT500))ELSE(
             SMTSTRESS : 25., IF NOPRINT = 0 THEN(
             PRINT("DATA FOR SMT STRESS FOR 316 ONLY
               RELIABLE UP TO 600 DEGREES C")),
             NOPRINT : 1 ) ) ),
    SMTSTRESS : SMTSTRESS*1.E6,
    CFCONST : 0.9,
    SIGISO : 15000.*6895. ),

 /* VANADIUM ALLOY PROPERTY DATA */

  IF MATNUM = 2 THEN(

    HMIN : .0001,
    ALPHA : (6.41*TTRY[K]↑(0.08))*1.E-6,
    YOUNG : 158.*TTRY[K]↑(-0.05)*1.E9,
    POISSON : 0.36,
    IF TTRY[K] <= 400. THEN(YIELD : 970.*TTRY[K]↑(-0.11)*1.E6) ELSE(
                          YIELD : 7000.*TTRY[K]↑(-0.44)*1.E6),

    TK : 13.5*TTRY[K]↑(0.14),
    RPLOTMAX : 2000.E-3,
    LNPWR : LOG(PWRLIFE),
    SMT400 : 204.,
    SMT500 : 198.,
    SMT600 : 183.,
    IF PWRLIFE >= 30000. THEN(SMT600 : -9.97478*LNPWR+286.47721),
    SMT700 : 157.,
    IF PWRLIFE >= 1000. THEN(SMT700 : 0.39723*LNPWR↑2-17.4297*LNPWR+257.4202),
    SMT800 : 106.,
    IF PWRLIFE >= 1000. THEN(SMT800 : 0.329*LNPWR↑2-13.3796*LNPWR+179.4854),
    IF TTRY[K] <= 400. THEN(SMTSTRESS : 204.E6) ELSE(
         IF TTRY[K] <= 500. THEN(SMTSTRESS
           : SMT400 + (SMT500-SMT400)*(TTRY[K]-400.)/100.)ELSE(
       IF TTRY[K] <= 600. THEN(SMTSTRESS:
           SMT500+(SMT600-SMT500)*(TTRY[K]-500.)/100.)ELSE(
        IF TTRY[K] <= 700. THEN(SMTSTRESS:
           SMT600+(SMT700-SMT600)*(TTRY[K]-600.)/100.)ELSE(
       IF TTRY[K] <= 800. THEN(SMTSTRESS:
           SMT700+(SMT800-SMT700)*(TTRY[K]-700.)/100.)ELSE(
          SMTSTRESS : 30.)  )   )    )       ),
    SMTSTRESS : SMTSTRESS*1.E6  ),

 /* HT-9 MATERIAL PROPERTIES */

  IF MATNUM = 3 THEN(
    ALPHA : 6.93*TTRY[K]↑(0.1)*1.E-6,
```

```
    YOUNG : 304.*TTRY[K]↑(-0.09),

    TK : 25.*TTRY[K]↑(0.02),
    POISSON : 0.27,
    IF TTRY[K] <= 400. THEN(YIELD : 808.*TTRY[K]↑(-0.13)) ELSE(
              YIELD : 1650000.*TTRY[K]↑(-1.41) ),
    IF TTRY[K] <= 300. THEN(SMTSTRESS : 199.E6) ELSE(
            IF TTRY[K] <= 400. THEN(SMTSTRESS : 197.E6) ELSE(
                WANTREAD : 1)  ),
    IF THATSENOUGH = 1 THEN WANTREAD : 0,
    IF WANTREAD = 1 THEN(SMTSTRESS : READ("WHAT IS THE SMT STRESS IN PA?") ),
    IF WANTREAD = 1 THEN THATSENOUGH : 1  )     )

/* SUBROUTINE TO CALCULATE COSINE TERMS IN TEMPERATURE FORMULATION */

COSINETERMS2(ANGLE) :=
    (MODEDECLARE([SUM,CC1,DD1,Q2PRIME,Q3PRIME,HEAT,TK,ALPHA,YOUNG,
    AOVERB,TBULK,ANSWER,RADOFS2,THEROUT,ANGLE],FLOAT,[N,NN,L,LL],FIXNUM),
     SUM : 0.0,
     CC1 : Q2PRIME*THEROUT↑2*RIN↑2/(2.*TK)*(TK-HEAT*RIN)
             /(TK*(THEROUT↑2-RIN↑2) +
            HEAT*RIN*(THEROUT↑2+RIN↑2)),
     DD1 : Q2PRIME*THEROUT↑2/(2.*TK)*(TK+HEAT*RIN)
            /(TK*(THEROUT↑2-RIN↑2) +
            HEAT*RIN*(THEROUT↑2+RIN↑2)),
     FOR L FROM 2 STEP 2 THRU 8 DO(
       M : L/2,
       AOVERB : THEROUT/RIN,
       CC1PART[L] : Q2PRIME*(-1)↑(M+1)/
         (3.1416*TK*M*(4.*M↑2 - 1.))*(THEROUT↑(2*M+1)*
              (2*M*TK-HEAT*RIN))/(2*M*TK*(AOVERB↑(4*M)-1.)
             +HEAT*RIN*(AOVERB↑(4*M)+1.)),
       D1PART[L] : 1./((RIN*10.)↑(4*M))*(CC1PART[L]*10↑(4.*M))
                          *(2*M*TK+HEAT*RIN)/(2*M*TK-HEAT*RIN) ),

     FOR LL FROM 2 STEP 2 THRU 8 DO(
       SUM : SUM + (CC1PART[LL]/RADOFS2↑LL +
         D1PART[LL]*RADOFS2↑LL)*COS(LL*ANGLE) ),
     ANSWER : (CC1/RADOFS2+DD1*RADOFS2)*COS(ANGLE) + SUM )


ULTR() := (MODEDECLARE([ALPHA,SIGTTH,SIGTR,SIGTZ,
             YOUNG,TK,Q3PRIME,Q2PRIME,POISSON,
            MINTEMPDIFF,RADOFS2,ROUTMIN,ROUTMAX,
            RAD2,RIN2,ROUT2,TTRYMIN,TTRYMAX,COSTERM,HEAT,
            STRAINMISES,STRAINTBAR,NCYMISES,TBULKMIN,NCYTBAR,
            SIGPTR,SIGPTTH,SIGPTZ,STRAINRHOT,
            TSAT,SEGLENGTH,SIGTRINTS2,SIGTTHINTS2,
            SIGTRSURF,SIGTTHSURF,SIGTHMISES,
            NCYTBAR,TEMPRISE,PULSETBAR,NCYMISES,
            PULSEMISES,SEGLENGTH,MAJRADIUS,CHAMBER,
            STRAINTHHOT,STRAINZHOT,STRAINRCOLD,TBULKINC,
            STRAINTHCOLD,STRAINZCOLD,DELTASTRAINR,
            DELTASTRAINTH,Q3WATER,DELTASTRAINZ,EQUIVSTRAIN,
            RIN,PWRLIFE,REJTIME,STRAINTHINSHELL,
            MASSFLUX,PREAS,THEROUT,THOT,THETAMIN,
            THETAMAX,CONST1,KKK,RHO,THEC,TBULK],FLOAT,
            [N,K,KK,THEK,J,LAST,LASTPLUS1,TEMPLAST,
            NNLASTPLUS1,NNLAST,TEMPLASTPLUS1,THETLAST,
            THETLASTPLUS1,NNN,NNNN,MATNUM,NN],FIXNUM),

WRITEFILE(RENE),

PRINT("*************************************************************"),
PRINT("*************************************************************"),
```

```
PRINT("****ROUTINE TO CALCULATE PREASURE, AND THERMAL STRESSES****"),
PRINT("****AND THE FATIGUE STATE OF A HOLLOW TUBE              ****"),
PRINT("****AS A FUNCTION OF RADIUS THROUGH THE TUBE THICKNESS ****"),
PRINT("****FOR A GIVEN INNER RADIUS WITH OUTER RADIUS VARYING.****"),
PRINT("****ONE SIDED HEAT FLUX AND INTERNAL HEAT GENERATION.  ****"),
PRINT("****PLANE STRAIN MODEL WITH NO RESTRAINTS ALONG LENGTH.****"),
PRINT("****BENDING IS ALLOWED IN ONE CASE.                    ****"),
PRINT("****ALL PROPERTIES EVALUATED AT AVERAGE TEMPERATURE,   ****"),
PRINT("****BUT FATIGUE DATA AVALUATED FOR THOT.               ****"),
PRINT("*************************************************************"),
PRINT("*** R INNER = ",RIN,"Q2PRIME = ",Q2PRIME,"Q3PRIME = ",Q3PRIME,"****"),
PRINT("****** MATERIAL NUMBER = ",MATNUM,"PREASURE =",PREAS,"******"),
PRINT("*** TBULK IS", TBULK, "FULL POWER LIFE (HRS) = ",PWRLIFE,"*********"),
PRINT("*****************************************************************"),
PRINT("*****************************************************************"),

/* LOOP FOR VARYING FIRST WALL THICKNESS */

FOR NN FROM 1 THRU NNLASTPLUS1 DO(

  ROUTS2[NN] : ROUTMIN + 0.0005 + (ROUTMAX-ROUTMIN-0.0005)*(NN-1)/NNLAST,
  THEROUT : ROUTS2[NN],
  THICKS2[NN] : ROUTS2[NN]-RIN,
  RIN2 : RIN↑2,
  ROUT2 : ROUTS2[NN]↑2,

/* CALCULATE HEAT TRANSFER COEFFICIENT */

MASSFLUX : ABS(3.14*SEGLENGTH*(Q3PRIME*(ROUTS2[NN]↑2-RIN↑2)
      +Q2PRIME*(RIN+THICKS2[NN])
      +Q3WATER*RIN↑2)/(4400.*TEMPRISE*3.14*RIN↑2)),
VELOC : MASSFLUX/DENSITYWATER,
IF MASSFLUX/DENSITYWATER > VELOCITYLIMIT THEN VELOCITYWANT : 1,
IF VELOCITYWANT = 1 THEN(MASSFLUX : VELOCITYLIMIT*DENSITYWATER,
     PRINT("HEAT TRANSFER
     COEFFICIENT BASED ON A FIXED VELOCITY OF ",
     VELOCITYLIMIT," M/S")) ELSE(
      PRINT("HEAT TRANSFER COEFFICIENT BASED ON
          A FIXED TEMP RISE UP THE SEGMENT
        OF ",TEMPRISE),PRINT("VELOCITY UP THE CHANNEL IS ",VELOC) ),
IF VELOCITYWANT = 1 THEN(TRISE : ABS(3.14*SEGLENGTH
   *(Q3PRIME*(ROUTS2[NN]↑2-RIN↑2) +
   Q2PRIME*(RIN+THICKS2[NN])+Q3WATER*RIN↑2)/(4400.*MASSFLUX*3.14*RIN↑2)),

PRINT("TEMPERATURE RISE UP THE CHANNEL IS NOW ",TRISE)  ),
HEAT : 0.023*(0.69/(2.*RIN))*(MASSFLUX*2.*RIN/1.61E-4)↑0.8*
    (1.61E-4*4400./0.69)↑0.4*
          (1.61E-4/1.39E-4)↑0.14,
IF MATNUM = 2 THEN (HEAT : 7.0*69./(2.*RIN)),

PRINT("R OUTER =", ROUTS2[NN]),
PRINT("THICKNESS OF TUBE =",THICKS2[NN]),
PRINT("MASSFLUX (KG/M↑2/SEC) = ", MASSFLUX,
    "HEAT TRANSFER COEFFICIENT (W/M↑2/C) = ", HEAT),
PRINT("LENGTH OF THE SEGMENT = ",SEGLENGTH),
PRINT("++++++++++++++++++++++++++++++++++++++++++++++++++++++++++++"),

  TEMPDIFF[0] : 100.,

/* ITERATE ON AVERAGE TEMPERATURE AND MATERIAL PROPERTIES */

FOR K FROM 1 THRU TEMPLASTPLUS1 DO(

   TTRY[K] : TBULK + (TTRYMAX-TBULK)*(K-1)/TEMPLAST,
   PROP(K),
   TAVGS2[K] : ROUTS2[NN]/TK*(ROUT2/(ROUT2-RIN2)*LOG(ROUTS2[NN]/RIN)-0.5)*
```

```
        (Q2PRIME/3.14+Q3PRIME*ROUTS2[NN]/2.) -
        (ROUT2-RIN2)/(8.*TK)*Q3PRIME + (3.14*(ROUT2-RIN2)*Q3PRIME
        + 2.*ROUTS2[NN]*Q2PRIME)/(2.*3.1416*RIN*HEAT) + TBULK,
    TEMPDIFF[K] : ABS(TAVGS2[K] - TTRY[K]) ),
    MINTEMPDIFF : APPLY(MIN,LISTARRAY(TEMPDIFF)),
      FOR KK FROM 1 THRU TEMPLASTPLUS1 DO(
        IF TEMPDIFF[KK] = MINTEMPDIFF THEN THEK : KK),
    TAVG[NN] : TAVGS2[THEK],
    PROP(THEK),

AVERAGESTRAIN : 9.41E-6*(TAVG[NN]↑1.093 - TSTAR↑1.093),

PRINT("THERMAL COND = ", TK,"ALPHA = ",ALPHA,"YOUNGMOD = ",
      YOUNG,"POIS = ",POISSON),

/* CONSTANTS FOR THERMAL STRESSES */

 BIGA : Q3PRIME*ALPHA*YOUNG/(1.-POISSON)*ROUT2/(4.*TK)*
          (2.*LOG(ROUTS2[NN]/RIN)/(1.- RIN2/ROUT2) - RIN2/(2.*ROUT2) - 1.5),
 APRIME : Q3PRIME*ALPHA*YOUNG/(1.-POISSON)*ROUT2/(4.*TK),
 BIGB : ALPHA*YOUNG*ROUTS2[NN]*Q2PRIME/(3.14*TK*2.*(1.-POISSON))*
          (2.*ROUT2/(ROUT2-RIN2)*LOG(ROUTS2[NN]/RIN) - 1.),
 BPRIME : ALPHA*YOUNG*ROUTS2[NN]*Q2PRIME/(3.14*TK*2.*(1.-POISSON)),
 CONST1 : Q2PRIME*ROUTS2[NN]↑2*RIN↑2/(2.*TK)*(TK-HEAT*RIN)/
          (TK*(ROUTS2[NN]↑2-RIN↑2) +
          HEAT*RIN*(ROUTS2[NN]↑2+RIN↑2)),
 DCONST1 : Q2PRIME*ROUT2/(2.*TK)*(TK+HEAT*RIN)/(TK*(ROUT2-RIN↑2) +
          HEAT*RIN*(ROUT2+RIN↑2)),
 CSTAR : ALPHA*YOUNG*CONST1/((ROUT2+RIN2)*(1.-POISSON)),
 BIGI : POISSON*3.14*((BIGA+BIGB)*(ROUT2-RIN2)-(APRIME+2.*BPRIME)*
        (ROUT2*LOG(ROUTS2[NN]/RIN)-(ROUT2-RIN2)/2.) +
        APRIME/(2.*ROUT2)*(ROUT2↑2-RIN2↑2)),
 WDOUBLEPRIME : -2.*POISSON*CSTAR/YOUNG - (1.028E-5*TAVG[NN]↑0.093)*
      (2.*CONST1/(ROUT2+RIN2) + DCONST1),
 DEFLECTION : WDOUBLEPRIME*(SEGLENGTH/2.)↑2/2.,
 INERTIA : 3.14*(ROUT2↑2-RIN2↑2)/2.,
 MOMENT : (-POISSON*CSTAR*(ROUT2+RIN2)/2. - YOUNG*
          (1.028E-5*TAVG[NN]↑0.093)*(CONST1/2.+
           DCONST1*(ROUT2+RIN2)/4.))*(ROUT2-RIN2)*3.14,

 RADOFS2 : RIN,
 COSTERMTCOLD : COSINETERMS2(0.0),
 TCOLD[NN] : (3.1416*(ROUT2-RIN2)*Q3PRIME
      + 2.*ROUTS2[NN]*Q2PRIME)/(2.*3.1416*RIN*HEAT) + COSTERMTCOLD + TBULK,

/* ITERATE THROUGH FIRST WALL RADII */

FOR N FROM 1 THRU LASTPLUS1 DO(

  RADS2[N,NN] : RIN + 0.0005 + (ROUTS2[NN]-RIN-0.0005)*(N-1)/LAST,
  RADOFS2 : RADS2[N,NN],
  RAD2 : RADS2[N,NN]↑2,

/* CALCULATE PRESSURE STRESSES */

  SIGPRS2[N,NN] : -PREAS*(RIN2/(ROUT2-RIN2))*(ROUT2/RAD2 - 1.),
  SIGPTHS2[N,NN] : PREAS*(RIN2/(ROUT2-RIN2))*(ROUT2/RAD2 + 1.),
  SIGPZS2[N,NN] : PREAS*(RIN2/(ROUT2-RIN2)),
  SIGPTHINS2[N,NN] : PREAS*(ROUTS2[NN]+RIN)/(2.*THICKS2[NN]),
  SIGPMISESS2[N,NN] : SQRT(0.5*((SIGPRS2[N,NN]-
       SIGPTHS2[N,NN])↑2 + (SIGPTHS2[N,NN]-
       SIGPZS2[N,NN])↑2 + (SIGPZS2[N,NN]-SIGPRS2[N,NN])↑2)),

  COSTERM : COSINETERMS2(0.),

 TEMPPEAK[N,NN] : ROUTS2[NN]/TK*(Q2PRIME/3.1416+Q3PRIME*
```

```
        ROUTS2[NN]/2.)*LOG(RADS2[N,NN]/RIN) -
        Q3PRIME/(4.*TK)*(RAD2-RIN2) + (3.1416*(ROUT2-RIN2)*Q3PRIME
        + 2.*ROUTS2[NN]*Q2PRIME)/(2.*3.1416*RIN*HEAT) + COSTERM + TBULK,

/* THERMAL STRESS COMPONENTS FROM SURFACE HEAT FLUX */

 SIGTRSURF : ALPHA*YOUNG*ROUTS2[NN]*Q2PRIME/(3.1416*TK*2.*(1.-POISSON))*
      ((ROUTS2[NN]/RADS2[N,NN])↑2*(RAD2-RIN2)/
      (ROUT2-RIN2)*LOG(ROUTS2[NN]/RIN) -
      LOG(RADS2[N,NN]/RIN)) + ALPHA*YOUNG*RADS2[N,NN]/(2.*(ROUT2+RIN2)
      *(1.-POISSON))*(1.-RIN2/RAD2)*(1.-ROUT2/RAD2)*CONST1*COS(0.0),
 SIGTTHSURF : ALPHA*YOUNG*ROUTS2[NN]*Q2PRIME/(3.1416*TK*2.*(1.-POISSON))*
      ((ROUTS2[NN]/RADS2[N,NN])↑2*(RAD2+RIN2)/
      (ROUT2-RIN2)*LOG(ROUTS2[NN]/RIN) -
      LOG(RADS2[N,NN]/RIN)-1.)
      + ALPHA*YOUNG*RADS2[N,NN]/(2.*(ROUT2+RIN2)*(1.-POISSON))*
      (3.-(ROUT2+RIN2)/RAD2-ROUT2*RIN2/RAD2↑2)*CONST1*COS(0.0),
  SIGSHEAR[N,NN] : ALPHA*YOUNG*RADS2[N,NN]/(2.*(ROUT2+RIN2))*
          (1.- ROUT2/RAD2)*(1.- RIN2/RAD2)*CONST1*SIN(0.0),
  SHEARSTRAIN : SIGSHEAR[N,NN]/YOUNG*(2.+2.*POISSON),

/* THERMAL STRESS COMPONENTS FROM INTERNAL HEAT GENERATION */

  RHO : RADS2[N,NN]/RIN,
  KKK : ALPHA*YOUNG/(1.-POISSON),
  THEC : ROUTS2[NN]/RIN,
  SIGTRINTS2 : Q3PRIME*KKK*ROUT2/(4.*TK)*((1.-1./RHO↑2)*
      (LOG(THEC)/(1.-1./THEC↑2) -
       1./(4.*THEC↑2) - 0.75) - LOG(RHO) +
       0.5 - 1./(2.*RHO↑2) + 1./(4.*THEC↑2)*
      (RHO↑2-1./RHO↑2)),
  SIGTTHINTS2 : Q3PRIME*KKK*ROUT2/(4.*TK)*
      ((1.+1./RHO↑2)*(LOG(THEC)/(1.-1./THEC↑2) -
      1./(4.*THEC↑2) - 0.75) - 0.5 + 1./(2.*RHO↑2) + 1./(4.*THEC↑2)*
      (3.*RHO↑2+1./RHO↑2)),

/* TOTAL THERMAL STRESSES */

  SIGTR[N,NN] : SIGTRSURF + SIGTRINTS2,
  SIGTTH[N,NN] : SIGTTHSURF + SIGTTHINTS2,
  SIGTZREST[N,NN] : POISSON*(SIGTR[N,NN]+SIGTTH[N,NN])
        - YOUNG*(AVERAGESTRAIN +
        1.028E-5*TAVG[NN]↑0.093*(TEMPPEAK[N,NN]-TAVG[NN])),
  SIGTZNOBEND[N,NN] : POISSON*(SIGTR[N,NN]+SIGTTH[N,NN])
        - BIGI/(3.14*(ROUT2-RIN2)) -
        YOUNG*(1.028E-5*TAVG[NN]↑0.093*(TEMPPEAK[N,NN]-TAVG[NN])),
  SIGTZBEND[N,NN] : SIGTZNOBEND[N,NN] + (2.*POISSON*CSTAR +
       (1.028E-5*TAVG[NN]↑0.093)*YOUNG*(2.*CONST1/
       (ROUT2+RIN2) + DCONST1))*RADS2[N,NN]*COS(0.0),

/* CALCULATE STRAINS */

  STRAINZREST : 0.0,
  STRAINZNOBEND : AVERAGESTRAIN - BIGI/(3.14*YOUNG*(ROUT2-RIN2)),
  STRAINZBEND : STRAINZNOBEND - RADS2[N,NN]*COS(0.)*WDOUBLEPRIME,
  DISPLNOBEND : STRAINZNOBEND*SEGLENGTH,
  DISPLBEND : DISPLNOBEND,

  THOT : TEMPPEAK[N,NN],
  SIGPTR : SIGTR[N,NN] + SIGPRS2[N,NN],
  SIGPTTH : SIGTTH[N,NN] + SIGPTHS2[N,NN],
  SIGPTZREST : SIGTZREST[N,NN] + SIGPZS2[N,NN],
  SIGPTZNOBEND : SIGTZNOBEND[N,NN] + SIGPZS2[N,NN],
  SIGPTZBEND : SIGTZBEND[N,NN] + SIGPZS2[N,NN],
  STRAINRHOTREST : 1./YOUNG*(SIGPTR-POISSON*(SIGPTTH+SIGPTZREST)),
  STRAINTHHOTREST : 1./YOUNG*(SIGPTTH-POISSON*(SIGPTR+SIGPTZREST)),
```

```
  STRAINZHOTREST : 1./YOUNG*(SIGPTZREST-POISSON*(SIGPTR+SIGPTTH)),
  STRAINRHOTNOBEND : 1./YOUNG*(SIGPTR-POISSON*(SIGPTTH+SIGPTZNOBEND)),
  STRAINTHHOTNOBEND : 1./YOUNG*(SIGPTTH-POISSON*(SIGPTR+SIGPTZNOBEND)),
  STRAINZHOTNOBEND : 1./YOUNG*(SIGPTZNOBEND-POISSON*(SIGPTR+SIGPTTH)),
  STRAINRHOTBEND : 1./YOUNG*(SIGPTR-POISSON*(SIGPTTH+SIGPTZBEND)),
  STRAINTHHOTBEND : 1./YOUNG*(SIGPTTH-POISSON*(SIGPTR+SIGPTZBEND)),
  STRAINZHOTBEND : 1./YOUNG*(SIGPTZBEND-POISSON*(SIGPTR+SIGPTTH)),
  STRAINRCOLD : 1./YOUNG*(SIGPRS2[N,NN]-POISSON*
      (SIGPTHS2[N,NN]+SIGPZS2[N,NN])),
  STRAINTHCOLD : 1./YOUNG*(SIGPTHS2[N,NN]-POISSON*
      (SIGPRS2[N,NN]+SIGPZS2[N,NN])),
  STRAINZCOLD : 1./YOUNG*(SIGPZS2[N,NN]-POISSON*
      (SIGPRS2[N,NN]+SIGPTHS2[N,NN])),

/* CALCULATE STRAIN RANGES */

DELTASTRAINRREST :(STRAINRHOTREST-STRAINRCOLD),
  DELTASTRAINTHREST :(STRAINTHHOTREST-STRAINTHCOLD),
  DELTASTRAINZREST : (STRAINZHOTREST-STRAINZCOLD),
  DELTASTRAINRNOBEND :(STRAINRHOTNOBEND-STRAINRCOLD),
  DELTASTRAINTHNOBEND :(STRAINTHHOTNOBEND-STRAINTHCOLD),
  DELTASTRAINZNOBEND : (STRAINZHOTNOBEND-STRAINZCOLD),
  DELTASTRAINRBEND : (STRAINRHOTBEND-STRAINRCOLD),
  DELTASTRAINTHBEND :(STRAINTHHOTBEND-STRAINTHCOLD),
  DELTASTRAINZBEND : (STRAINZHOTBEND-STRAINZCOLD),

/* CALCULATE VON MISES EQUIVELENT STRAIN RANGE */

  EQUIVSTRAINREST : SQRT(2.)/3.*SQRT(((DELTASTRAINRREST-DELTASTRAINTHREST)↑2
     +(DELTASTRAINTHREST-DELTASTRAINZREST)↑2
     +(DELTASTRAINZREST-DELTASTRAINRREST)↑2 + 3./2.*SHEARSTRAIN↑2)),
  EQUIVSTRAINNOBENDNOSHEAR : SQRT(2.)/3.*
     SQRT(((DELTASTRAINRNOBEND-DELTASTRAINTHNOBEND)↑2
     +(DELTASTRAINTHNOBEND-DELTASTRAINZNOBEND)↑2
     +(DELTASTRAINZNOBEND-DELTASTRAINRNOBEND)↑2)),
  EQUIVSTRAINNOBEND : SQRT(2.)/3.*
     SQRT(((DELTASTRAINRNOBEND-DELTASTRAINTHNOBEND)↑2
     +(DELTASTRAINTHNOBEND-DELTASTRAINZNOBEND)↑2
     +(DELTASTRAINZNOBEND-DELTASTRAINRNOBEND)↑2 + 3./2.*SHEARSTRAIN↑2)),
  EQUIVSTRAINBEND : SQRT(2.)/3.*
     SQRT(((DELTASTRAINRBEND-DELTASTRAINTHBEND)↑2
     +(DELTASTRAINTHBEND-DELTASTRAINZBEND)↑2
     +(DELTASTRAINZBEND-DELTASTRAINRBEND)↑2 + 3./2.*SHEARSTRAIN↑2)),

/* FIND ALLOWABLE CYCLES BY CALLING ASME DATA ("FINDCYCLES) */

  NCYEQUIVREST[N,NN] : FINDCYCLES(EQUIVSTRAINREST),
  PULSEEQUIVREST[N,NN] : PWRLIFE/NCYEQUIVREST[N,NN]-REJTIME/3600.,
  NCYEQUIVNOBEND[N,NN] : FINDCYCLES(EQUIVSTRAINNOBEND),
  PULSEEQUIVNOBEND[N,NN] : PWRLIFE/NCYEQUIVNOBEND[N,NN]-REJTIME/3600.,
  NCYEQUIVBEND[N,NN] : FINDCYCLES(EQUIVSTRAINBEND),
  PULSEEQUIVBEND[N,NN] : PWRLIFE/NCYEQUIVBEND[N,NN]-REJTIME/3600.,


PRINT("RADIUS[",N,",",NN,"] = ",RADS2[N,NN]),
PRINT("TEMPPEAK = ",TEMPPEAK[N,NN],"TAVG = ",TAVG[NN],
          "TCOLD = ",TCOLD[NN]),
PRINT("SIGPRS2 = ",SIGPRS2[N,NN],"SIGPTHS2 = ",
    SIGPTHS2[N,NN],"SIGPZS2 = ",SIGPZS2[N,NN]),
PRINT("SIGPTHINS2 = ",SIGPTHINS2[N,NN],"SIGPMISESS2 = ",SIGPMISESS2[N,NN]),
PRINT("SIGTRSURF = ",SIGTRSURF,"SIGTTHSURF = ",SIGTTHSURF),
PRINT("SIGTRINTS2 = ",SIGTRINTS2,"SIGTTHINTS2 = ",SIGTTHINTS2),
PRINT("SIGTR = ",SIGTR[N,NN],"SIGTTH = ",SIGTTH[N,NN]),
PRINT("SIGPTR = ",SIGPTR,"SIGPTTH = ",SIGPTTH),
PRINT("SIGSHEAR = ",SIGSHEAR[N,NN],"SHEARSTRAIN =",SHEARSTRAIN),
PRINT("SIGTZNOBEND = ",SIGTZNOBEND[N,NN],"SIGTZBEND = ",SIGTZBEND[N,NN],
```

```
        "STRAINTHERMAL = ",STRAINTHERMAL),
PRINT("SIGTZREST = ", SIGTZREST[N,NN],"STRAINZREST = ",STRAINZREST),
PRINT("STRAINZNOBEND = ",STRAINZNOBEND,"STRAINZBEND = ",
        STRAINZBEND,"DISPLNOBEND = ",
        DISPLNOBEND,"DISPLBEND = ",DISPLBEND),
PRINT("EQUIVSTRAINNOBENDNOSHEAR = ",EQUIVSTRAINNOBENDNOSHEAR,
       "EQUIVSTRAINNOBEND = ",  EQUIVSTRAINNOBEND),
PRINT("EQUIVSTRAINBEND = ",EQUIVSTRAINBEND,
       "NCYEQUIVNOBEND = ",NCYEQUIVNOBEND[N,NN]),
PRINT("NCYEQUIVBEND = ",NCYEQUIVBEND[N,NN],
       "PULSEEQUIVNOBEND = ",PULSEEQUIVNOBEND[N,NN],
         "PULSEEQUIVBEND = ",PULSEEQUIVBEND[N,NN]),
PRINT("EQUIVSTRAINREST = ",EQUIVSTRAINREST,"NCYEQUIVREST = ",
       NCYEQUIVREST[N,NN],
         "PULSEEQUIVREST = ",PULSEEQUIVREST[N,NN]),
PRINT("-------------------------------------------------------")  ),

TCO : (Q3PRIME*THICKS2[NN]↑2/2.+Q2PRIME*THICKS2[NN])/
       (THICKS2[NN]*HEAT) + TBULK,
THOT : TCO + Q2PRIME*THICKS2[NN]/TK + Q3PRIME*THICKS2[NN]↑2/(2.*TK),
SIGTHINTHERMAL[NN] : ALPHA*YOUNG/(2.*(1.-POISSON))*
          (THOT - TCO),
PRINT("SIGTHINTHERMAL = ",SIGTHINTHERMAL[NN]),

/* THIN SHELL CALCULATIONS */

STRAINTHIN : ALPHA*(THOT-TCO)/(2.*(1.-POISSON)),
STRAINTHINSHELL : STRAINTHIN*2./3.*(POISSON + 1.),
PRINT("THOT FOR THIN SHELL = ",THOT),
PRINT("TCOLD FOR THIN SHELL = ",TCO),
NCYTHINSHELL[NN] : FINDCYCLES(STRAINTHINSHELL),
PULSETHINSHELL[NN] : PWRLIFE/NCYTHINSHELL[NN] - REJTIME/3600.,
PRINT("STRAINTHINSHELL = ",STRAINTHINSHELL,
      "NCYTHINSHELL = ",NCYTHINSHELL[NN],
        "PULSETHINSHELL = ", PULSETHINSHELL[NN]),
PRINT("WDOUBLEPRIME = ",WDOUBLEPRIME,"DEFLECTION = ",
     DEFLECTION,"MOMENT =",MOMENT),
PRINT("*******************************************************"),
PRINT("*******************************************************")  ),
CLOSEFILE(STRS2,>,RENE)     )

/* SUBROUTINE TO LOCATE TEMPERATURE LIMIT FOR
     SWELLING AND STRENGTH LIMIT */

FINDLIMITS() := (MODEDECLARE([M,SIGNALT,SIGNALP,
        NNLASTPLUS1,LASTPLUS1],FIXNUM),

  SIGNALT : 0,
  SIGNALP : 0,
  FOR M FROM 1 THRU NNLASTPLUS1 DO(
  TTRY[M] : TAVG[M],
  IF TEMPPEAK[LASTPLUS1,M] > 500. THEN(IF SIGNALT = 0 THEN(
                          PRINT("PEAK TEMPERATURE EXCEEDS 500"),
                          PRINT("PEAK TEMP IS ",TTRY[M]),
                          PRINT("THICKNESS = ",(ROUTS2[M]-RIN)),
                          SIGNALT : 1)  ),
  PROP(M),
  SMT[M] : SMTSTRESS,
  IF SIGPTHS2[LASTPLUS1,M] > SMT[M] THEN( IF SIGNALP = 0 THEN(
     PRINT("VON MISES PRIMARY STRESS EXCEEDS SMT LIMIT"),
     PRINT("SMTSTRESS = ",SMT[M],"TRESCA STRESS = ",SIGPTHS2[2,M]),
     PRINT("THICKNESS = ",(ROUTS2[M]-RIN)),
                            SIGNALP : 1)  ),

  IF SIGNALT + SIGNALP = 2 THEN(M : NNLASTPLUS1)    )     )
```

```
/* SUBROUTINE THAT CALCULATES ALLOWABLE NUMBER OF CYCLES
      FROM FIT OF ASME FATIGUE DESIGN CURVE */

FINDCYCLES(STRAIN) := (MODEDECLARE([STRAIN,LOGOFN426,
                        LOGOFN454,LOGOFN482,
                        LOGOFN510,ENDSTRAIN,NCYCLES,LOGOFN,
                        LOGOFN649,THOT,LNN],FLOAT,[MATNUM,N],FIXNUM),

LOGSTRAIN : LOG(STRAIN),

IF MATNUM = 1 THEN(

 LOGOFN426 : (LOGSTRAIN+3.7587178)/(-0.198105441),
 LOGOFN454 : (LOGSTRAIN+4.2563621)/(-0.183711238),
 LOGOFN482 : (LOGSTRAIN+4.6637048)/(-.17626645),
 LOGOFN510 : (LOGSTRAIN+5.1613625)/(-0.16112635),
 LOGOFN649 : (LOGSTRAIN+5.691763)/(-0.14084195),

BSQD[1] : 8.763E-3↑2-4.*4.548E-4*(0.046-STRAIN),
BSQD[2] : 4.941E-3↑2-4.*2.525E-4*(0.02675-STRAIN),
BSQD[3] : 2.537E-3↑2-4.*1.2564E-4*(0.01459-STRAIN),
BSQD[4] : 1.133E-3↑2-4.*5.199E-5*(7.3355E-3-STRAIN),
BSQD[5] : 6.558E-4↑2-4.*3.09E-5*(4.3448E-3-STRAIN),
FOR PP FROM 1 THRU 5 DO(
   IF BSQD[PP] < 0.0 THEN BSQD[PP] : 0.0),

 IF STRAIN > 0.00376 THEN(
                LOGOFN426:(8.763E-3-SQRT(BSQD[1]))/(2.*4.548E-4)),

 IF STRAIN > 0.00261 THEN(
              LOGOFN454:(4.941E-3-SQRT(BSQD[2]))/(2.*2.525E-4)),
 IF STRAIN > 0.00186 THEN(
              LOGOFN482:(2.537E-3-SQRT(BSQD[3]))/(2.*1.2564E-4)),
 IF STRAIN > 0.0013 THEN(
              LOGOFN510:(1.133E-3-SQRT(BSQD[4]))/(2.*5.199E-5)),
 IF STRAIN > 0.000922 THEN(
              LOGOFN649:(6.558E-4-SQRT(BSQD[5]))/(2.*3.09E-5)),

 IF THOT > 538. THEN THOT:538,
 IF THOT > 649. THEN(PRINT("FATIGUE DATA NO GOOD FOR THOT > 649.")),
 IF THOT <= 426. THEN(
   LOGOFN : LOGOFN426) ELSE(
 IF THOT <= 454. THEN(
   LOGOFN : LOGOFN426 + (THOT-426.)/(454.-426.)*
    (LOGOFN454-LOGOFN426))ELSE(
 IF THOT <= 482. THEN(
   LOGOFN : LOGOFN454 + (THOT-454.)/(482.-454.)*
     (LOGOFN482-LOGOFN454))ELSE(
 IF THOT <= 510. THEN(
   LOGOFN : LOGOFN482 + (THOT-482.)/(510.-482.)*
     (LOGOFN510-LOGOFN482))ELSE(
   LOGOFN : LOGOFN510+(THOT-510.)/(538.-510.)*
      (LOGOFN649-LOGOFN510) ) ) ) ) ),


    IF MATNUM = 2 THEN(
          IF STRAIN < 4.12E-5 THEN STRAIN : 4.12E-5,
          LOGOFN : LOG((STRAIN/4.12E-3)↑(-1./0.06))    ),

   IF LOGOFN > 15. THEN LOGOFN : 15.,
   NCYCLES : EXP(LOGOFN)    )

TTYOFF : FALSE
```

APPENDIX D

```
/* ************************  PROGRAM MODBREE ***************** */



 TTYOFF : TRUE$

/* INITIALIZATIONS */

( YMIN : 0.0,
  XMIN : 0.0,
  YMAX : 30.0,
  XMAX : 15.0,
  HMIN : 0.0001,
  HMAX : 0.015,
  STOPR : 10,
  STOPRPLUS1 : STOPR + 1,
  RPLOTMIN : 0.0,
  RPLOTMAX : 25.0E-3,
  WANTREAD : 0,
  STOPH : 50,
  STOPHPLUS1 : STOPH + 1,
  SEGLENGTH : 1.0,
  CHAMBER : 2.0,
  MAJRADIUS : 9.0,
  REJTIME : 100.0, /* REJUVENATION TIME IN SECONDS */
  THOT[1] : 400.0  /* PLASMA SIDE TEMPERATURE IN DEGREEES CELSIUS OF FIRST
                      WALL FOR MATERIAL PROPERTY EVALUATION */
                    )$

FUNCS : [BREE,FATIGUE,SOLFAT,INPUTPROPERTIES,ISOSIG,FATSTRAIN]$


READIT() := (

   MATNUM : READ("WHAT MATERIAL DO YOU WANT? IF IT IS STAINLESS STEEL THEN
            ENTER A 1, IF IT IS VANADIUM ALLOY, ENTER A 2,
            IF IT IS HT-9 THEN ENTER A 3"),
   LIFE : READ("WHAT IS THE FULL CALENDAR LIFE IN YEARS?"),
   AVAIL : READ("WHAT IS THE AVAILABILITY?"),
   PWRLIFE : LIFE*AVAIL,
   PRINT("WALL LIFETIME IN FULL POWER YEARS IS",PWRLIFE),
   DEP : READ("WHAT IS THE SURFACE HEAT FLUX IN MW/M↑2?"),
   DEP : DEP*1.E6,
   PRES : READ("WHAT IS THE PREASURE IN MEGAPASCALS?"),
   PRES : PRES*1.E6,
   TCOLD : READ("WHAT IS THE COLD SIDE TEMPERATURE (IN DEGREES C)??")  )$


INPUTPROPERTIES(N) := (MODEDECLARE([LIFE,HMIN,AVAIL,PULSE,PWRLIFE,
               DEP,TCOLD,REJTIME,
               CFCONST,SMT400,SMT500,SMT600,SMT700,SMT800,LNPWR,
               Z1,Z2,Z3,ALPHA,YOUNGMOD,THERMALCOND,
```

```
                POISSON,YIELDSTRESS,SMTSTRESS,
                POWER,SIGISO,MULTIPLIER],FLOAT,[N,
                THATSENOUGH,WANTREAD,MATNUM],FIXNUM),

/* STAINLESS STEEL (316) PROPERTY DATA */

 IF MATNUM = 1 THEN(
   ALPHA : 10.28*THOT[N]↑0.093*1.E-6,
   YOUNGMOD : 465.*THOT[N]↑(-0.18)*1.E9,

   THERMALCOND : 3.78*THOT[N]↑0.28,
   MULTIPLIER : 3.78/1.28,
   POWER : 1.+.28,

   POISSON : 0.27,
   Z1 : (6.5224e-3*THOT[N]↑2-6.8764*THOT[N]+1821.095)/1.E4,
   Z2 : -1.21448E-5*THOT[N]↑2+0.01069*THOT[N]-2.5663,
   Z3 : 5.4568E-5*THOT[N]↑2-0.08336*THOT[N]+48.1074,
   YIELDSTRESS : 745.*THOT[N]↑(-0.31)*1.E6,
   LNPWR : LOG(PWRLIFE),
   SMT400 : 109.,
   SMT500 : 107.,
   SMT600 : 102.,
   IF PWRLIFE >= 3000. THEN(SMT600 : -0.8139765*
         LNPWR↑2+6.2849*LNPWR+99.147),
      IF THOT[N] <= 400. THEN(SMTSTRESS : 109.) ELSE(
           IF THOT[N] <= 500. THEN(SMTSTRESS : SMT400+(THOT[N]-400.)/100.*
                (SMT500-SMT400))ELSE(
       IF THOT[N] <= 600 THEN(SMTSTRESS:SMT500+
          (THOT[N]-500.)/100.*(SMT600-SMT500))ELSE(
            SMTSTRESS : 25.,
            PRINT("DATA FOR SMT STRESS FOR 316 ONLY
            RELIABLE UP TO 600 DEGREES C") ) ) ),
   SMTSTRESS : SMTSTRESS*1.E6,
   CFCONST : 0.9,
   SIGISO : 15000.*6895. ),


/* VANADIUM ALLOY PROPERTY DATA */

 IF MATNUM = 2 THEN(
   HMIN : .0001,
   ALPHA : (6.41*THOT[N]↑(0.08))*1.E-6,
   YOUNGMOD : 158.*THOT[N]↑(-0.05)*1.E9,
   POISSON : 0.36,
   IF THOT[N] <= 400. THEN(YIELDSTRESS : 970.*THOT[N]↑(-0.11)*1.E6) ELSE(
                        YIELDSTRESS : 7000.*THOT[N]↑(-0.44)*1.E6),

   THERMALCOND : 13.5*THOT[N]↑(0.14),
   MULTIPLIER : 13.5/1.14,
   POWER : 1.+.14,
   RPLOTMAX : 2000.E-3,
   LNPWR : LOG(PWRLIFE),
   SMT400 : 204.,
   SMT500 : 198.,
   SMT600 : 183.,
   IF PWRLIFE >= 30000. THEN(SMT600 : -9.97478*LNPWR+286.47721),
   SMT700 : 157.,
   IF PWRLIFE >= 1000. THEN(SMT700 :
        0.39723*LNPWR↑2-17.4297*LNPWR+257.4202),
   SMT800 : 106.,
   IF PWRLIFE >= 1000. THEN(SMT800 :
        0.329*LNPWR↑2-13.3796*LNPWR+179.4854),
   IF THOT[N] <= 400. THEN(SMTSTRESS : 204.E6) ELSE(
        IF THOT[N] <= 500. THEN(SMTSTRESS :
```

```
        SMT400 + (SMT500-SMT400)*(THOT[N]-400.)/100.)ELSE(
      IF THOT[N] <= 600. THEN(SMTSTRESS:SMT500+
         (SMT600-SMT500)*(THOT[N]-500.)/100.)ELSE(
       IF THOT[N] <= 700. THEN(SMTSTRESS:
         SMT600+(SMT700-SMT600)*(THOT[N]-600.)/100.)ELSE(
      IF THOT[N] <= 800. THEN(SMTSTRESS:
         SMT700+(SMT800-SMT700)*(THOT[N]-700.)/100.)ELSE(
         SMTSTRESS : 30.)  )   )    )       ),
   SMTSTRESS : SMTSTRESS*1.E6  ),

/* HT-9 MATERIAL PROPERTIES */

 IF MATNUM = 3 THEN(
   ALPHA : 6.93*THOT[N]↑(0.1)*1.E-6,
   YOUNGMOD : 304.*THOT[N]↑(-0.09),

   THERMALCOND : 25.*THOT[N]↑(0.02),
   MULTIPLIER : 25./1.02,
   POWER : 1.02,

   POISSON : 0.27,
   IF THOT[N] <= 400. THEN(YIELDSTRESS : 808.*THOT[N]↑(-0.13)) ELSE(
             YIELDSTRESS : 1650000.*THOT[N]↑(-1.41) ),
   IF THOT[N] <= 300. THEN(SMTSTRESS : 199.E6) ELSE(
          IF THOT[N] <= 400. THEN(SMTSTRESS : 197.E6) ELSE(
             WANTREAD : 1)  ),
   IF THATSENOUGH = 1 THEN WANTREAD : 0,
   IF WANTREAD = 1 THEN(SMTSTRESS : READ("WHAT IS
        THE SMT STRESS IN PA?") ),
   IF WANTREAD = 1 THEN THATSENOUGH : 1  )    )$

   /* Subroutine to find isochronous stress with fit to ASME data */

ISOSIG() := (MODEDECLARE([THOT,PWRLIFE,LOGLIFE,SIG426,SIG454,SIG482,
                  SIG510,TEMPHOT,SIG538,SIG566,SIG593,SIG621,SIG649,
                              SIG816,SIGISO],FLOAT),

  LOGLIFE : LOG(PWRLIFE),
    SIG426 : 25.9,
    SIG454 : 25.4,
    SIG482 : 25.1,
      IF PWRLIFE > 3.E4/(365.*24.) THEN( SIG482 : -0.20706*
        LOGLIFE↑2+4.26763*LOGLIFE+23.11098),
    SIG510 : 24.8,
      IF PWRLIFE > 3.E3/(365.*24.)
        THEN( SIG510 : -0.0788467*LOGLIFE↑2+1.0188069*LOGLIFE+21.69797),
    SIG538 : 24.2,
      IF PWRLIFE > 1.E3/(365.*24.)
        THEN( SIG538 : -.150847*LOGLIFE↑2+1.892527*LOGLIFE+18.209254),
    SIG566 : 23.2,
      IF PWRLIFE > 1.E2/(365.*24.)
        THEN( SIG566 : -0.093397*LOGLIFE↑2+.545305*LOGLIFE+22.586297),
    SIG593 : -0.06551679*LOGLIFE↑2+0.1186688*LOGLIFE+23.183697,
    SIG621 : -0.02484417*LOGLIFE↑2-0.889941*LOGLIFE+25.056534,
    SIG649 : 8.,
    SIG816 : 1.0,
  IF TEMPHOT < 426. THEN SIGISO : 25.9,
  IF TEMPHOT < 454. AND TEMPHOT >= 426. THEN(
       SIGISO : SIG426 + (TEMPHOT-426.)/(454.-426.)*(SIG454-SIG426) ),
  IF TEMPHOT < 482. AND TEMPHOT >= 454. THEN(
       SIGISO : SIG454 + (TEMPHOT-454.)/(482.-454.)*(SIG482-SIG454) ),
  IF TEMPHOT < 510. AND TEMPHOT >= 482. THEN(
       SIGISO : SIG482 + (TEMPHOT-482.)/(510.-482.)*(SIG510-SIG482) ),
  IF TEMPHOT < 538. AND TEMPHOT >= 510. THEN(
       SIGISO : SIG510 + (TEMPHOT-510.)/(538.-510.)*(SIG538-SIG510) ),
  IF TEMPHOT < 566. AND TEMPHOT >= 538. THEN(
```

```
      SIGISO : SIG538 + (TEMPHOT-538.)/(566.-538.)*(SIG566-SIG538) ),
  IF TEMPHOT < 593. AND TEMPHOT >= 566. THEN(
      SIGISO : SIG566 + (TEMPHOT-566.)/(593.-566.)*(SIG593-SIG566) ),
  IF TEMPHOT < 621. AND TEMPHOT >= 593. THEN(
      SIGISO : SIG593 + (TEMPHOT-593.)/(621.-593.)*(SIG621-SIG593) ),
  IF TEMPHOT < 649. AND TEMPHOT >= 621. THEN(
      SIGISO : SIG621 + (TEMPHOT-621.)/(649.-621.)*(SIG649-SIG621) ),
  IF TEMPHOT < 816. AND TEMPHOT >= 649. THEN(
      SIGISO : SIG649 + (TEMPHOT-649.)/(816.-649.)*(SIG816-SIG649) ),
  IF TEMPHOT >= 816 THEN SIGISO : 0.0  )$

/* SUBROUTINE TO FIND STRAIN FROM CYCLES USING ASME FATIGUE DATA */

FATSTRAIN(NCY) := (MODEDECLARE([THSTRAIN,THSTRAIN426,
      THSTRAIN454,THSTRAIN482,
      THSTRAIN510,THSTRAIN649,THOTGUESS,LNN,NCY,THOT],FLOAT),

   THOT : THOTGUESS,
   LNN : LOG(NCY),
   IF LNN >= 9.21 THEN(
     THSTRAIN426 : -4.775E-4*(LNN) + 7.908E-3,
     THSTRAIN454 : -3.184E-4*(LNN) + 5.413E-3,
     THSTRAIN482 : -2.238E-4*(LNN) + 3.8529E-3,
     THSTRAIN510 : -1.484E-4*(LNN) + 2.6358E-3,
     THSTRAIN649 : -9.668E-5*(LNN) + 1.795E-3) ELSE(
THSTRAIN426 : 4.548E-4*LNN↑2-8.763E-3*LNN+0.046,
THSTRAIN454 : 2.525E-4*LNN↑2-4.941E-3*LNN+.02675,
THSTRAIN482 : 1.2564E-4*LNN↑2-2.537E-3*LNN+.01459,
THSTRAIN510 : 5.199E-5*LNN↑2-1.133E-3*LNN+7.3355E-3,
THSTRAIN649 : 3.09E-5*LNN↑2-6.558E-4*LNN+4.3448E-3    ),

     IF THOT <= 426. THEN (THSTRAIN : THSTRAIN426) ELSE(
       IF THOT <= 454. THEN(THSTRAIN :
          THSTRAIN426+(THOT-426.)/(454.-426.)*
                (THSTRAIN454-THSTRAIN426)) ELSE(
     IF THOT <= 482. THEN(THSTRAIN :
          THSTRAIN454+(THOT-454.)/(482.-454.)*
                (THSTRAIN482-THSTRAIN454)) ELSE(
     IF THOT <= 510. THEN(THSTRAIN :
          THSTRAIN482+(THOT-482.)/(510.-482.)*
                (THSTRAIN510-THSTRAIN482)) ELSE(
     THSTRAIN : THSTRAIN510+(THOT-510.)/
          (649.-510.)*(THSTRAIN649-THSTRAIN510)
                              ) ) )  )    )$


SOLFAT() := (MODEDECLARE([N24,N12,N2HR,PWRLIFE,THOT,
            TCOLD,THOTGUESS,CONSTANT,ALPHA,YOUNGMOD,
            THERMALCOND,POISSON,STRAIN24,STRAIN12,STRAIN2HR,
            DEP,NCY,HFATIG24,HFATIG12,HFATIG2,THOT24,
            THOT12,THOT2,HFATIGFINAL24,
            HFATIGFINAL12,MIN24,MIN12,MIN2HR,HFATIGFINAL2],FLOAT,[K,KK,
            STOPHPLUS1,MATNUM],FIXNUM),

/* CALCULATE H LIMIT FROM DIFFERENT PULSE LENGTHS DUE TO FATIGUE */

   N24 : PWRLIFE*365.*24./24.,
   N12 : PWRLIFE*365.*24./12.,
   N2HR  : PWRLIFE*365.*24./2.,
   FINDMIN24[0] : 100., FINDMIN12[0] : 100., FINDMIN2HR[0] : 100.,
   THOTGUESS : TCOLD,
   FOR K : 1 STEP 1 THRU STOPHPLUS1 DO(
    THOTGUESS : THOTGUESS + 10.,
    THOT[0] : THOTGUESS,
    INPUTPROPERTIES(0),
```

```
    CONSTANT : ALPHA*YOUNGMOD/(2.*THERMALCOND*(1.-POISSON)),
   NCY : N24,
   IF MATNUM = 1 THEN(STRAIN24 : FATSTRAIN(NCY)),
   IF MATNUM = 2 THEN(STRAIN24 : NCY↑(-0.06)*4.12E-3),
   NCY : N12,
   IF MATNUM = 1 THEN(STRAIN12 : FATSTRAIN(NCY)),
   IF MATNUM = 2 THEN(STRAIN12 : NCY↑(-0.06)*4.12E-3),
   NCY : N2HR,
   IF MATNUM = 1 THEN(STRAIN2HR : FATSTRAIN(NCY)),
   IF MATNUM = 2 THEN(STRAIN2HR : NCY↑(-0.06)*4.12E-3),
   HFATIG24[K] : STRAIN24*YOUNGMOD/(CONSTANT*DEP),
   HFATIG12[K] : STRAIN12*YOUNGMOD/(CONSTANT*DEP),
   HFATIG2[K] : STRAIN2HR*YOUNGMOD/(CONSTANT*DEP),
   THOT24 : (1./MULTIPLIER*(DEP*HFATIG24[K] +
        MULTIPLIER*TCOLD↑(POWER)))↑(1./POWER),
   THOT12 : (1./MULTIPLIER*(DEP*HFATIG12[K] +
        MULTIPLIER*TCOLD↑(POWER)))↑(1./POWER),
   THOT2 : (1./MULTIPLIER*(DEP*HFATIG2[K] +
        MULTIPLIER*TCOLD↑(POWER)))↑(1./POWER),
   FINDMIN24[K] : ABS(THOT24-THOTGUESS),
   FINDMIN12[K] : ABS(THOT12-THOTGUESS),
   FINDMIN2HR[K] : ABS(THOT2-THOTGUESS)    ),
   MIN24 : APPLY(MIN,LISTARRAY(FINDMIN24)),
   MIN12 : APPLY(MIN,LISTARRAY(FINDMIN12)),
   MIN2HR : APPLY(MIN,LISTARRAY(FINDMIN2HR)),
  FOR KK : 1 STEP 1 THRU STOPHPLUS1 DO(
   IF FINDMIN24[KK] = MIN24 THEN(KK24 : KK),
   IF FINDMIN12[KK] = MIN12 THEN(KK12 : KK),
   IF FINDMIN2HR[KK] = MIN2HR THEN(KK2 : KK) ),

   HFATIGFINAL24 : HFATIG24[KK24],
   HFATIGFINAL12 : HFATIG12[KK12],
   HFATIGFINAL2 : HFATIG2[KK2]        )$

/* Main routine. Finds boundaries for Mod2 Bree diagram */

BREE() := (MODEDECLARE([CONSTANT,HMIN,HMAX,PRES,RADIUS,SIGMAC,
            ALPHA,YOUNGMOD,THERMALCOND,POISSON,YIELDSTRESS,SMTSTRESS,
            LNN,MAJRADIUS,SEGLENGTH,CHAMBER,MULTIPLIER,
            POWER,DEP,NUMBERCYCLES,REJTIME,
            CFCONST,SIGMAREFKPSI,TAU,
            INTPOLERROR,SIGTHERMAL,SIGMAREF,TRYSIGMA,
            TSUBD,SIGMAMIN,NSUBD,PWRLIFE,LIFE,AVAIL,PULSE,
            TCOLD,THOT],FLOAT,[MATNUM,N,STOPHPLUS1,STOPH],FIXNUM),

THOT[1] : 400.,
INTPOLERROR : 0.0,
INPUTPROPERTIES(1),

FOR N : 1 STEP 1 THRU STOPHPLUS1 DO(

  /* INCREMENT THICKNESS OF FIRST WALL */

  H[N] : HMIN+(HMAX-HMIN)*(N-1)/STOPH,

    THOT[N] : (1./MULTIPLIER*(DEP*H[N] +
       MULTIPLIER*TCOLD↑(POWER)))↑(1./POWER),
    INPUTPROPERTIES(N),
    CONSTANT : ALPHA*YOUNGMOD/(2.*THERMALCOND
                *(1. - POISSON)),

/* LOOP FOR FIRST WALL MEAN RADIUS */

  FOR M : 1 STEP 1 THRU STOPRPLUS1 DO(

   RTUBES[M] : 0.001 + (RPLOTMAX - 0.001)*(M-1)/STOPR,
```

```
   NTUBES[N,M] : 3.1416*CHAMBER/(RTUBES[M]+H[N])*2.*
        3.1416*MAJRADIUS/SEGLENGTH  ),


/* CALCULATE SMT LIMIT */

    RTOPLOT[N] : (RPLOTMAX - RPLOTMIN)*(N-1)/STOPH,
    RPRIMARY[N] : SMTSTRESS*H[N]/PRES,

/* DEMARCATE THE E, S, P, AND R REGIONS OF THE BREE DIAGRAM */

    RELASTIC[N] : (YIELDSTRESS*H[N] - CONSTANT*DEP*H[N]↑2)/PRES,

    RRATCHET[N] : H[N]*YIELDSTRESS/PRES - CONSTANT*DEP*H[N]↑2/(4.*PRES),
      IF H[N] > 2.*YIELDSTRESS/(DEP*CONSTANT) THEN(
           RRATCHET[N] : YIELDSTRESS↑2/(PRES*CONSTANT*DEP) ),

    HPLASTIC[N] : 2.*YIELDSTRESS/(CONSTANT*DEP),


/* CALCULATE THE CREEP - RATCHETING CURVE */

IF MATNUM = 1 THEN(
  TEMPHOT : THOT[N],
  ISOSIG(),
  SIGMAC : SIGISO*1000.*6895./1.25,
      RCUTOFF : (YIELDSTRESS - YIELDSTRESS↑2/
        (CONSTANT*DEP*H[N]))*H[N]/PRES,
      IF RCUTOFF < 0.0 THEN RCUTOFF : 0.0,
         RCREEPRATCHET[N] : SIGMAC*YIELDSTRESS/(CONSTANT*
                  PRES*DEP),
      IF RCREEPRATCHET[N] > RCUTOFF THEN(
            RCREEPRATCHET[N] : (2.*CONSTANT*H[N]*
               DEP*(YIELDSTRESS+SIGMAC)-CONSTANT↑2*
       H[N]↑2*DEP↑2 - YIELDSTRESS↑2 +2.*SIGMAC*YIELDSTRESS-SIGMAC↑2)/
            (4.*CONSTANT*PRES*DEP)  ),
       if rcreepratchet[n] > rratchet[n] then
             rcreepratchet[n] : rratchet[n]
                                                    )    )   )$


FATIGUE() :=(MODEDECLARE([CONSTANT,HMIN,HMAX,PRES,RADIUS,SIGMAC,
            ALPHA,YOUNGMOD,THERMALCOND,POISSON,YIELDSTRESS,SMTSTRESS,
            LNN,MULTIPLIER,POWER,DEP,NUMBERCYCLES,REJTIME,
            CFCONST,SIGMAREFKPSI,TAU,
            INTPOLERROR,SIGTHERMAL,SIGMAREF,TRYSIGMA,
            TSUBD,SIGMAMIN,NSUBD,PWRLIFE,LIFE,AVAIL,PULSE,
            TCOLD,THOT],FLOAT,[MATNUM,N,STOPHPLUS1,STOPH],FIXNUM),

/* CALCULATE PULSE LENGTH VERSUS WALL THICKNESS FOR ASME FATIGUE DATA */

   RADIUSGUESS : READ("WHAT RADIUS DO YOU WANT
      THE CREEP RUPTURE STRESS EVALUATED AT?"),

FOR N : 1 STEP 1 THRU STOPHPLUS1 DO(

  /* INCREMENT THICKNESS OF FIRST WALL */

  H[N] : HMIN+(HMAX-HMIN)*(N-1)/STOPH,

    THOT[N] : (1./MULTIPLIER*(DEP*H[N] + MULTIPLIER*
      TCOLD↑(POWER)))↑(1./POWER),
    THETHOT : THOT[N],
    INPUTPROPERTIES(N),
    CONSTANT : ALPHA*YOUNGMOD/(2.*THERMALCOND
                *(1. - POISSON)),
```

```
   THESTRAIN[N] : CONSTANT*DEP*H[N]/YOUNGMOD,

   NCYCLES[N] : findcycles(thestrain[n]),
   TRYTIME : PWRLIFE*365.*24./NCYCLES[N],
   REJTIME : 10. + (TRYTIME-0.083)/(24.-0.083)*90.,
   IF TRYTIME <= 0.083 THEN REJTIME : 10.,

   TPULSE[N] : PWRLIFE*365.*24.*3600./NCYCLES[N] - REJTIME,
   TPULSE[N] : TPULSE[N]/3600.,

/* CALCULATE THE CREEP - FATIGUE CURVE */

IF MATNUM = 1 THEN(

   SIGTHERMAL : CONSTANT*H[N]*DEP,
   SIGMAREF : (PRES*RADIUSGUESS/H[N] + SIGTHERMAL)/CFCONST,
   TRYSIGMA : 1.25*YIELDSTRESS/CFCONST,
   IF TRYSIGMA < SIGMAREF THEN( SIGMAREF : TRYSIGMA),
   SIGMAREFKPSI : SIGMAREF/1000./6895.,
   TSUBD : EXP( Z1*SIGMAREFKPSI↑2+Z2*SIGMAREFKPSI+Z3 ),
   IF THOT[N] <= 450. THEN(TSUBD : 500000.,
       IF SIGMAREFKPSI > 52. THEN(
              PRINT("N=",N,"....HELP!!!!!!!...")) ),
   IF THOT[N] > 450. AND THOT[N] <= 538. THEN
        (IF SIGMAREFKPSI > 28.3 THEN(
         PRINT("N=",N,"....HELP!!!!!!!...")) ELSE(TSUBD:300000.)),
   PULSECREEP[N] : PWRLIFE*365.*24./((1.-PWRLIFE*
        365.*24./TSUBD)*NCYCLES[N])
                                        )     )       )$


FINDCYCLES(STRAIN) := (MODEDECLARE([STRAIN,LOGOFN426,LOGOFN454,LOGOFN482,
            LOGOFN510,ENDSTRAIN,NCYCLES,LOGOFN,LOGOFN649,
            THETHOT,LNN],FLOAT,[MATNUM,N],FIXNUM),

IF MATNUM = 1 THEN(

 LOGOFN426 : (STRAIN-7.908E-3)/(-4.775E-4),
 LOGOFN454 : (STRAIN-5.413E-3)/(-3.184E-4),
 LOGOFN482 : (STRAIN-3.8529E-3)/(-2.238E-4),
 LOGOFN510 : (STRAIN-2.6358E-3)/(-1.484E-4),
 LOGOFN649 : (STRAIN-1.795E-3)/(-9.668E-5),

BSQD[1] : 8.763E-3↑2-4.*4.548E-4*(0.046-STRAIN),
BSQD[2] : 4.941E-3↑2-4.*2.525E-4*(0.02675-STRAIN),
BSQD[3] : 2.537E-3↑2-4.*1.2564E-4*(0.01459-STRAIN),
BSQD[4] : 1.133E-3↑2-4.*5.199E-5*(7.3355E-3-STRAIN),
BSQD[5] : 6.558E-4↑2-4.*3.09E-5*(4.3448E-3-STRAIN),
FOR PP FROM 1 THRU 5 DO(
   IF BSQD[PP] < 0.0 THEN BSQD[PP] : 0.0),

 IF STRAIN > 0.00376 THEN(
                 LOGOFN426:(8.763E-3-SQRT(BSQD[1]))/(2.*4.548E-4)),

 IF STRAIN > 0.00261 THEN(
                LOGOFN454:(4.941E-3-SQRT(BSQD[2]))/(2.*2.525E-4)),
 IF STRAIN > 0.00186 THEN(
                 LOGOFN482:(2.537E-3-SQRT(BSQD[3]))/(2.*1.2564E-4)),
 IF STRAIN > 0.0013 THEN(
              LOGOFN510:(1.133E-3-SQRT(BSQD[4]))/(2.*5.199E-5)),
 IF STRAIN > 0.000922 THEN(
              LOGOFN649:(6.558E-4-SQRT(BSQD[5]))/(2.*3.09E-5)),
 IF THETHOT <= 426. THEN(
   LOGOFN : LOGOFN426) ELSE(
 IF THETHOT <= 454. THEN(
```

```
   LOGOFN : LOGOFN426 + (THETHOT-426.)/(454.-426.)*
        (LOGOFN454-LOGOFN426))ELSE(
 IF THETHOT <= 482. THEN(
   LOGOFN : LOGOFN454 + (THETHOT-454.)/(482.-454.)*
     (LOGOFN482-LOGOFN454))ELSE(
 IF THETHOT <= 510. THEN(
   LOGOFN : LOGOFN482 + (THETHOT-482.)/(510.-482.)*
     (LOGOFN510-LOGOFN482))ELSE(
      LOGOFN : LOGOFN510+(THETHOT-510.)/
             (649.-510.)*(LOGOFN649-LOGOFN510) ) ) ) ) )  ,


    IF MATNUM = 2 THEN(
         IF STRAIN < 4.12E-5 THEN STRAIN : 4.12E-5,
         LOGOFN : LOG((STRAIN/4.12E-3)↑(-1./0.06))    ),

   IF LOGOFN > 15. THEN LOGOFN : 15.,
   NCYCLES : EXP(LOGOFN)   )$

/* PLOTTING ROUTINES */

PLOTBREE() := (
       PARAMPLOT2([H[N]*1000.,H[N]*1000.,HPLASTIC[N]
              *1000.,H[N]*1000.,H[N]*1000.],
              [RPRIMARY[N]*1000.,RELASTIC[N]*1000.,RTOPLOT[N]*1000.,
              RRATCHET[N]*1000.,RCREEPRATCHET[N]*1000.],
              N,1,STOPHPLUS1,INTEGER,
              LABEL("THICKNESS OF FIRST WALL, MILLIMETERS"),
              LABEL("RADIUS OF FIRST WALL, MILLIMETERS"),
              LABEL("MODIFIED MODIFIED BREE DIAGRAM"),
              [0,1,2,3,4]
                                          )  )$

PLOTBREEVAN() := (
       PARAMPLOT2([H[N]*1000.,H[N]*1000.,HPLASTIC[N]*1000.,H[N]*1000.,
              HFATIGFINAL24*1000.,HFATIGFINAL12
                 *1000.,HFATIGFINAL2*1000.],
              [RPRIMARY[N]*1000.,RELASTIC[N]*1000.,RTOPLOT[N]*1000.,
              RRATCHET[N]*1000.,RTOPLOT[N]*1000.,
              RTOPLOT[N]*1000.,RTOPLOT[N]*1000.],
              N,1,STOPHPLUS1,INTEGER,
              LABEL("THICKNESS OF FIRST WALL, MILLIMETERS"),
              LABEL("RADIUS OF FIRST WALL, MILLIMETERS"),
              LABEL("MODIFIED MODIFIED BREE DIAGRAM"),
              [0,1,2,3,49,59,69]
                                          )  )$


PLOTFATIGUEVAN() := (
       PARAMPLOT2([H[N]*1000.],
              [TPULSE[N]],
              N,1,STOPHPLUS1,INTEGER,
              LABEL("THICKNESS OF FIRST WALL, MILLIMETERS"),
              LABEL("PULSE LENGTH IN HOURS"),
              LABEL("MODIFIED MODIFIED BREE DIAGRAM",DEP),
              [5]
                                          )  )$


PLOTTHOT() := (
       PARAMPLOT2(H[N]*1000.,THOT[N],N,1,STOPHPLUS1,INTEGER,
              LABEL("THICKNESS OF FIRST WALL, MILLIMETERS"),
              LABEL("HOT SIDE TEMPERATURE IN DEGREES CELSIUS"),
              LABEL("HOT SIDE TEMPERATURE IN DEGREES CELSIUS")  )  )$
```

```
(
  ARRAY(BSQD,FLOAT,5),
  ARRAY(H,FLOAT,51),
  ARRAY(RELASTIC,FLOAT,51),
  ARRAY(RCREEPRATCHET,FLOAT,51),
  ARRAY(HFATIG24,FLOAT,51),
  ARRAY(HFATIG12,FLOAT,51),
  ARRAY(HFATIG2,FLOAT,51),
  ARRAY(FINDMIN24,FLOAT,51),
  ARRAY(FINDMIN12,FLOAT,51),
  ARRAY(FINDMIN2HR,FLOAT,51),
  ARRAY(HPLASTIC,FLOAT,51),
  ARRAY(RRATCHET,FLOAT,51),
  ARRAY(THOT,FLOAT,51),
  ARRAY(RTUBES,FLOAT,51),
  ARRAY(NTUBES,FLOAT,51,51),
  ARRAY(RPRIMARY,FLOAT,51),
  ARRAY(THESTRAIN,FLOAT,51),
  ARRAY(NCYCLES,FLOAT,51),
  ARRAY(TPULSE,FLOAT,51),
  ARRAY(PULSECREEP,FLOAT,51),
  ARRAY(PULSECREEPMIN,FLOAT,51)
                                    )$

TTYOFF : FALSE$
```

REFERENCES

[1] D.R. Cohn, J.E.C. Williams, and L. Bromberg, "The Low Beta Pulsed Tokamak as a Modular Commercial Reactor with Very Long Pulses," PFC/JA-82-13, July 1982.

[2] R.J. LeClaire, J.E. Meyer, L. Bromberg, D.R. Cohn, J.E. Williams, "Aspects of Long Pulse Commercial Tokamak Reactor Design", PFC/CP-83-15, December, 1983.

[3] J.E. Meyer, "Structural Advantages of Steady State Fusion Power Reactors," PFC/TR-78-3, March 1978.

[4] "Class 1 Components in Elevated Temperature Service", Cases of ASME Boiler and Pressure Vessel Code Case N-47-17, 1979.

[5] Y-N Chan, "Design Window Methodology: Applications to the Parametric First-Wall, Divertor and Limiter of a Tokamak Fusion Reactor,"S.M. thesis, MIT, 1982.

[6] D. L. Smith, et al., "Fusion Reactor Blanket/Shield Design Study", ANL/FPP-79-1, July, 1979.

[7] G-P Yu. "Relationship of Material Properties to the Design of a Fusion Reactor First-Wall,"PhD thesis, MIT, 1981.

[8] J. Bree. "Elastic/Plastic Behavior of Thin Tubes Subjected to Internal Pressure and Intermittent High-Heat Fluxes with Application to Fast-Nuclear- Reactor Fuel Elements", Journal of Strain Analysis, Vol. 2, No. 3, 1967.

[9] W.J. O'Donnell and J. Porowski, "Upper Bounds for Accumulated Strain due to Creep Ratcheting", Welding Research Council Bulletin, No. 195, June 1974.

[10] M.A. Abdou et al., "Impurity Control and First Wall Engineering," U.S. Contribu-

tion to the International Tokamak Reactor Workshop, FED INTOR/ICFW/82-17, 1982.

[11] Steven J. Piet, "Potential Consequences Of Tokamak Fusion Reactor Accidents: The Materials Impact", PhD Thesis, MIT, May, 1982.

[12] H. Yamanovchi, Y. Asada, and Y. Wakamatsu, Unpublished Test Data Mentioned in Author's Closure to "Ratchetting Under Cyclic Axial Strain with Torsional Stress", *Fatigue at Elevated Temperatures*, ASTM STP 520, Am. Soc. Testing and Materials. 1973.

[13] T.W. Pickel et al., "Studies of Shakedown and Ratchetting of Structures" in "High-Temperature Structural Design Methods for LMFBR Components", Quarterly Progress Report for Period Ending June 30, 1973, USAEC Report ORNL-TM-4356, December, 1973.

[14] R.E. Gold. et al, "Materials Technology for Fusion: Current Status and Future Requirements". Nuclear Technology/Fusion Vol. 1, Apr., 1981.

[15] J.T.A. Roberts, *Structural Materials in Nuclear Power Systems*, Plenum Press, New York and London, 1981.

[16] Tenth Symposium on Fusion Engineering Proceedings, Philadelphia, PA, December 5-9, 1983.

[17] M.A. Abdou et al., "Blanket Comparison and Selection Study," ANL/FPP/TM-177, Argonne National Laboratory, 1983.

[18] C.C. Baker et al., "STARFIRE. A Commercial Tokamak Power Plant Study," ANL/FPP/82-1, Argonne National laboratory, 1982.

[19] D.R. Olander, "Fundamental Aspects of Nuclear Reactor Fuel Elements," Technical Information Center, ERDA, TID-26711-P1, 1976.

[20] G.M. McCracken, P.E. Stott, "Plasma Surface Interactions in Tokamaks," *Nuclear Fusion*, Vol. 19, No. 7, 1979.

[21] D.L. Smith, "Physical Sputtering Model for Fusion Reactor First-Wall Materials", *Journal of Nuclear Materials*, No. 75, 1978.

[22] D.L. Smith, J.N. Brooks et al., "DSPUT: A Physical Sputtering Code for Fusion Applications," ANL/FPP/TM-157, 1982.

[23] B.J. Merrill, "Intor First Wall Erosion During Plasma Disruption", Ninth Symposium on Fusion Engineering, Chicago, October, 1981.

[24] J.H. Rust, *Nuclear Power Plant Engineering*, Haralson Publishing Co., Buchanan, Georgia, 1979.

[25] Thomas J. McManamy, "Fusion Reactor Blanket Heat Removal Using Helium and Flibe," PhD Thesis, MIT, February, 1979.

[26] B.A. Boley and J.H. Weiner, *Theory of Thermal Stresses*, John Wiley and Sons, 1960.

[27] S. Timoshenko, *Elements of Strength of Materials*, D. Van Nostrand Co., New York, NY, 1949.

[28] W.M. Rohsenhow and Choi, *Heat, Mass and Momentum Transfer*, Prentice-Hall, 1961.

[29] M.M. El-Wakil. *Nuclear Heat Transport*, American Nuclear Society, La Grange Park, Illinois, 1978.

[30] D.A. Ehst, et al., "Tokamak Burn Cycle Study: A Data Base for Comparing Long Pulse and Steady State Power Reactors."ANL/FPP/TM-178, Argonne National Laboratory, November, 1983.